

For Reference

NOT TO BE TAKEN FROM THIS ROOM

Ex libris
UNIVERSITATIS
ALBERTAENSIS



BRUCE PEEL SPECIAL COLLECTIONS LIBRARY
UNIVERSITY OF ALBERTA LIBRARY

REQUEST FOR DUPLICATION

I wish a photocopy of the thesis by

FLINT, D.W. (author)

entitled ESTIMATION OF COAL RESOURCE
QUANTITIES

The copy is for the sole purpose of private scholarly or scientific study and research. I will not reproduce, sell or distribute the copy I request, and I will not copy any substantial part of it in my own work without permission of the copyright owner. I understand that the Library performs the service of copying at my request, and I assume all copyright responsibility for the item requested.

THE UNIVERSITY OF ALBERTA

Estimation of Coal Resource Quantities
by Statistical Methods

by



David Warren Flint

A THESIS

SUBMITTED TO THE FACULTY OF GRADUATE STUDIES AND RESEARCH
IN PARTIAL FULFILMENT OF THE REQUIREMENTS FOR THE DEGREE
OF MASTER OF SCIENCE

DEPARTMENT OF GEOLOGY

EDMONTON, ALBERTA

SPRING, 1978

ABSTRACT

Undisturbed coal-bearing strata of the Interior Plains region are commonly covered to a varying depth by pre-glacial and glacial deposits which obscure the coal zones from direct observation. Indirect methods such as use of exploration boreholes result in a fragmented view of the coal deposit and hence uncertainty in the estimate of distribution and quantity of coal resource.

Statistical methods provide quantitative statements of geologic assurance for estimators. Kriging and the arithmetic average are unbiased estimators of the coal zone average thickness over areas sampled irregularly and systematically respectively. Subjective probability methods and an approximation formula provide uncertainty estimates for the area underlain by coal.

Application of these methods to data from three coal zones in the Tertiary Ravenscrag Formation of southern Saskatchewan results in estimates classified as measured and indicated according to traditional resource classification schemes. In all cases examined, over two-thirds of the uncertainty in estimates of volume is contributed by the area estimate whereas uncertainty in the average thickness of the coal zone accounts for less than one-third.

Local structure in the bedrock of glaciotectionic

glacial action or salt collapse origin impairs prediction of the coal subcrop location. The irregular nature of lithologic boundaries between coal and penecontemporaneous clastic facies forms the other major component of uncertainty in the area.

The precision of average thickness estimates is controlled by the variability of the selected net coal thickness, the size of the area estimated and the average spacing of observations. For this reason classification methods based only on arbitrary minimum observation spacing fail to classify accurately resource estimates of different coal zones and different sizes of areas. A systematic sampling scheme on a square grid is recommended as the most efficient form of exploration for resource evaluation of undisturbed coal-bearing strata in southern Saskatchewan.

ACKNOWLEDGEMENTS

The impetus for this study came from Mr B.A. Latour of the Institute of Sedimentary and Petroleum Geology, Calgary which subsequently provided data and financial support. Mr J.A. Irvine, also of that institution, discussed the coal geology of the Estevan area with the author and provided interpretive expertise in the subjective probability aspect of this study.

Messers M. David, M. Guarascio and C. Huijbreghts kindly provided support for the author to attend a NATO Advanced Study Institute on Geostatistics in Italy while the Presidents' special research fund contributed to travelling expenses. Aquitaine Company of Canada Ltd. kindly permitted access to their proprietary software package KRIGPACC and provided free computing time for estimating surfaces. Claude Ribordy of Aquitaine facilitated the use of the package.

Special thanks are due to Tom Lam and Dave Proudfoot who aided many times in the computer aspects of this study, and Susan Shaw who swiftly and accurately compiled data for the small scale area.

Thanks are also due to my advisor, Dr Gordon Williams who provided the environment in which this study was allowed to grow unhindered by logistical limitations. And finally, thanks to Judy, who patiently endured months of near widow

status so that this thesis could be completed.

TABLE OF CONTENTS

		Page
CHAPTER 1	INTRODUCTION	1
1.1	Resource Estimation Terminology	3
1.2	Objectives	9
CHAPTER 2	GEOLOGY OF SELECTED COAL ZONES	11
2.1	Previous Work	11
2.2	Regional Geology	14
2.3	Geology of the Ravenscrag Formation	16
2.4	Coal Geology	17
2.5	Data Compilation	19
2.6	Estevan Area	25
2.7	Estevan Zone	28
2.8	Boundary Zone	33
2.9	Small Scale Area	38
CHAPTER 3	STATISTICAL METHODS	48
3.1	Stationary Stochastic Processes	51
3.2	Intrinsic Random Functions	55
3.3	Structural Analysis	56
3.4	Kriging	64
3.5	Non-stationary Phenomena	67
3.6	Areal Methods	71
CHAPTER 4	APPLICATIONS TO IRREGULAR SAMPLING PATTERNS: ESTEVAN AREA	76
4.1	Location of Coal Subcrop	76
4.2	Subjective Probability of the Area Underlain by Coal	102
4.3	Average Thickness of Net Coal	107
4.4	Tonnage Estimates	111
CHAPTER 5	APPLICATIONS TO SYSTEMATIC SAMPLING PATTERNS: SMALL SCALE AREA	118
5.1	Precision of Area Estimates	120
5.2	Structural Analysis of Exploration Data	123
5.3	Precision of Thickness Estimates	139
5.4	Precision of Volume Estimates	148
CHAPTER 6	SUMMARY AND CONCLUSIONS	152
6.1	Conclusions on the Spatial Continuity of Coal Zones	152
6.2	Conclusions on Statistical Methods	153
6.3	Conclusions on Geologic Assurance of Coal Resource Estimates	155
6.4	Recommendations	158

	Page
Selected Bibliography	159

LIST OF TABLES

Table	Description	Page
1	Coal resource/reserve classifications according to the maximum distance in metres between observations.	6
2	Residual sum of squares at data points estimated by kriging.	81
3	Area estimates of the coal zones, Estevan coalfield.	103
4	Parameters of estimated coal resource quantity distributions and component variables.	114
5	Components of the estimation variance, tonnage distributions.	116
6	Precision of area estimates using Matheron's approximation formula for relative estimation variance.	122
7	Sample mean and variance of net coal thickness observations at three drill spacings. Data from three square miles only.	126
8	Sample mean and variance of net coal thickness observations at three drill spacings. All observations in the small scale area.	127
9	Variance of the error made in extending the value of a central borehole to the square L metres by L metres.	142
10	Precision of average net coal thickness estimates in the small scale area.	144
11	Precision of coal volume estimates and components of the variance at three drill spacings.	149

LIST OF FIGURES

Figure	Description	Page
1	Resource/reserve classification diagram.	4
2	Index map locating the area of study.	12
3	Seam nomenclature applied to a hypothetical coal zone.	21
4	Diagrammatic explanation of coal thickness terms.	22
5	Distribution of boreholes in the Estevan coalfield.	26
6	Surface topography of the Estevan coalfield.	27
7	Bedrock topography of the Estevan coalfield.	29
8	Distribution of boreholes intersecting the Estevan zone.	30
9	Structure contours on the top of the Estevan zone.	32
10	Isopach of net coal thickness, Estevan zone.	34
11	Distribution of boreholes intersecting the Boundary zone.	35
12	Structure contours on the top of the Boundary zone.	37
13	Isopach of net coal thickness in the Boundary zone.	39
14	Distribution of boreholes in the small scale area.	40
15	Surface topography of the small scale area.	41
16	Bedrock topography of the small scale area.	42
17	Structure contours on the base of the coal zone, small scale area.	44

Figure	Description	Page
18	Sand channel and erosional areas in the coal zone, small scale area.	46
19	Isopach of net coal thickness in the coal zone, small scale area.	47
20	Distance and angular criteria used to select pairs of points for experimental variograms.	59
21	Characteristics of variograms.	60
22	Bedrock surface, variograms and model.	82
23	Standard deviation of the estimation error, bedrock surface.	84
24	Estevan zone surface, variograms and model.	85
25	Standard deviation of the estimation error, Estevan zone surface.	87
26	Isopach of the interval between the bedrock surface and Estevan zone surface.	88
27	Standard deviation of the estimation error, isopach between the bedrock and the Estevan zone surfaces.	90
28	Estimated lines of subcrop of the Estevan zone at four levels of probability.	91
29	Boundary zone surface, variograms and model.	93
30	Standard deviation of the estimation error, Boundary zone surface.	95
31	Isopach of the interval between the bedrock surface and the Boundary zone surface.	96
32	Standard deviation of the estimation error, interval between the bedrock and Boundary zone surfaces.	97
33	Estimated lines of subcrop of the Boundary zone at four levels of probability.	99

Figure	Description	Page
34	Maximum, minimum and modal estimates of the areal extent of the Estevan zone.	104
35	Maximum, minimum and modal estimates of the areal extent of the Boundary zone.	105
36	Cumulative probability distributions of the areal extent of coal.	106
37	Variograms and model, Estevan net coal thickness.	108
38	Variograms and model, Boundary net coal thickness.	110
39	Cumulative probability distribution of estimated tonnages, Estevan coalfield.	113
40	Precision of the estimated areal extent of coal as a function of the number of observations.	124
41	Average variogram of net coal thickness, selected samples:year 1.	129
42	Average variogram of net coal thickness, all samples:year 1.	130
43	Experimental variograms of net coal thickness, selected samples:year 2.	131
44	Experimental variograms of net coal thickness, all samples:year 2.	132
45	Experimental variograms of net coal thickness, selected samples:year 3.	134
46	Experimental variograms of net coal thickness, selected samples:year 4.	135
47	Experimental variograms of net coal thickness, all samples:year 3.	136
48	Average variogram of net coal thickness, samples from the eroded areas.	137
49	Average variogram and model of net coal thickness for all samples:year 3.	140

Figure	Description	Page
50	Precision of the average net coal thickness estimate as a function of the number of observations.	145
51	Precision of the volume estimate of coal as a function of the number of observations.	150

CHAPTER 1

1. Introduction

Decision makers in industry and government require estimates of the quantities of coal resources available in a region or country as basic information for making choices among various energy alternatives. Furthermore, such estimates should include some quantitative statement of assurance that the resource is actually available.

The quantity of coal resource contained in a coal bed is simply the product of the area underlain by the coal bed, the average thickness of the bed and a tonnage factor. If the boundaries of such a coal bed were exposed in outcrop and the bed was of uniform thickness and quality, then single area, thickness and quality measurements would suffice for a resource quantity estimate. In practice however, there is significant uncertainty about the actual values of the area, thickness and quality of coal beds.

The area underlain by a coal bed is not known with certainty because erosional boundaries and lateral facies transitions are commonly obscured by more recent deposits. Using lithologic logs and geophysical logs from rotary boreholes, the geologist creates structural models of the seam surfaces and of the erosional unconformities affecting the seams. Using these structural interpretations, the

subcrop boundaries of the seam can be estimated. Commonly without the hard sedimentological information found in outcrop or continuous cores, the geologist interprets the available data to produce a generalized facies model outlining areas of coal non-deposition.

The thickness of coal in a succession of beds varies locally. Rock partings and high-ash coal lenses which separate beds of clean combustible coal result from local depositional conditions which are difficult to predict given the usual scale of sample availability in a regional resource evaluation program. Furthermore, control points are irregularly spaced and clustered in locations of complex geology, resulting in a sample set which may not be representative of the whole area.

Coal quality parameters such as specific gravity, heating value, ash, volatile and sulfur content must be measured and used in the selection of local potentially mineable areas. Specific gravity is used in calculating a tonnage factor for the regional resource evaluation.

Uncertainty in the geological interpretation of exploration data is compounded by errors in measurement of coal thickness from geophysical logs, errors in determining location and elevation of boreholes or other sample locations from topographic maps and analytical errors in the determination of specific gravity and other quality data.

How is the exploration geologist to provide an estimate with some quantitative statement of geological assurance?

Estimation methods have been developed which permit one to make statistical inferences about the values of population parameters. Some methods, although intuitively simple, are mathematically complex and require large numbers of calculations; until the advent of high speed computers the cost of using such methods was prohibitive. Advanced estimation methods in combination with a computer exploration data base can now provide coal resource quantity estimates more rapidly and economically than previous manual methods.

This thesis deals with the application of several statistical methods to the problem of coal resource quantity estimation in the undisturbed coal-bearing Tertiary strata of southern Saskatchewan.

1.1 Resource Estimation Terminology

McKelvey (1976) has classified the resource base of a mineral commodity along two axes (Figure 1). He restricts the use of reserve to (p.2):

"...that portion of the identified resource from which a usable mineral or energy commodity can be economically and legally extracted at the time of determination."

This study is not concerned with the economics of coal extraction, but rather it focuses on the other axis, the

TOTAL RESOURCES

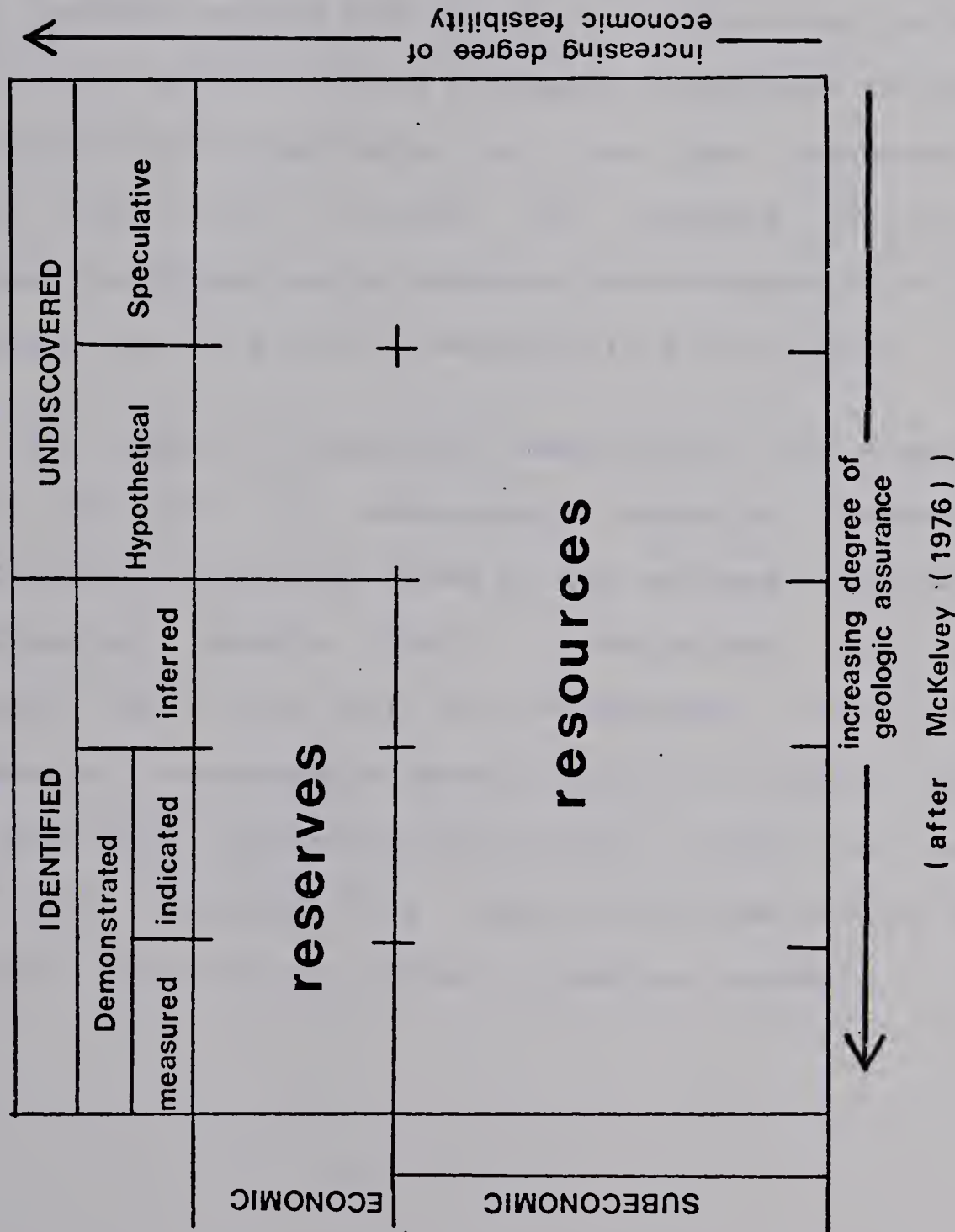


Figure 1. Resource/reserve classification

(after McKelvey (1976))

"degree of geologic assurance". Therefore the quantities estimated are termed resources rather than reserves.

The degree of geologic assurance or "assurance of existence" is composed of two separate problems: (1) does the resource exist? and (2) if it exists, what is its size? The former question is of paramount importance in estimating the volume of undiscovered oil and gas resources (Haun, 1976; EMR, 1977), whereas the presence of coal in the Ravenscrag Formation of southern Saskatchewan is well known and only the size of the resource is in question.

The degree of geologic assurance of coal resources has been reported by government agencies according to classification schemes based on the maximum distance between observation points. Table 1 summarizes these distance cutoffs in metres for the "Measured", "Indicated" and "Inferred" resources/reserves classes of Canada, USA, India and the USSR. The distances in Table 1 apply to horizontal or gently dipping beds under conditions similar to those found in the Interior Plains of western Canada.

<u>COUNTRY</u>	<u>RESOURCES</u>		
	<u>Measured</u>	<u>Indicated</u>	<u>Inferred</u>
Canada (Plains)	<800	800-1600	>1600
USA	<800	800-2400	2400-9600
India ¹	<200	200-2000	2000
USSR ¹	365	365-730	(uniform beds)
	275	275-550	(fairly consistent beds)
	200	200-365	(inconsistent beds)

¹ Reserves

Table 1: Coal resource/reserve classifications according to the maximum distance in metres between observations.

The following commonly accepted definitions of "measured", "indicated" and "inferred" are taken from McKelvey (1976, p.3).

"Measured - Resources are computed from dimensions revealed in outcrops, trenches, mine workings and drill holes. The points of observation and measurement are so closely spaced and the thickness and extent of coals so well defined that the tonnage is judged accurate within 20 percent of true tonnage.

Indicated - Resources are computed partly from specified measurements and partly from projection of visible data for a reasonable distance on the basis of geologic evidence.

Inferred - Quantitative estimates are based largely on broad knowledge of the geologic character of the bed or region and where few measurements of bed thickness are available."

The measured class is the only one for which the uncertainty is defined quantitatively. The meanings of inferred and indicated are ambiguous and hence subject to misinterpretation. The considerable range in distance cutoffs shown in Table 1 reflects varied definitions and experience in resource estimation. The ranges are often modified subjectively to reflect local geology of a coal bed. The result of using such classification schemes is an inconsistent partitioning of coal resources into classes which have little quantitative value in the decision-making process.

Estimation methods which provide quantitative

statements of geologic assurance avoid the problems inherent in the classification schemes and offer the advantages of consistency and reproducibility. Statistical estimation methods are not necessarily more objective because subjective input is required in the geological interpretation of data, the choice of a model and the choice of confidence level. Where data are insufficient to permit geological interpretation, an estimate cannot be prepared by any conventional method or statistical method based on sampling. At low information levels, only the methods of subjective probability provide quantitative statements of assurance.

Popoff (1966), in a review of conventional reserve estimation methods, suggested a two-fold purpose for these procedures: (1) valuation of the deposit and (2) illustration of the distribution of the variables. This division corresponds to global estimation and local estimation as used by Matheron (1971). Local estimates in the form of isopach, isoquality, structure contour and other isoline maps are used for the selection of areas of economic interest. Selection of coal which is to be strip mined is often first performed using a minimum bed thickness and a maximum overburden ratio or depth. As exploration progresses and information becomes available on the hydrogeology of the enclosing beds, quality characteristics of the coal and engineering properties of the enclosing materials, further

selection is made of economically interesting coal.

Although statistical methods can be and have been used for local estimation, the lack of coal quality data and engineering parameters precludes the illustration of and selection according to these variables in this study. Local estimation methods will be used to illustrate the distribution of variables and estimate subcrop boundaries but will not be used for selection. Local estimation methods will be discussed in the chapter on statistical methods.

Resource estimation as used in this study refers to the global estimation of the quantity of coal in-situ in a bed without selecting local areas of economic interest. Specifically, the resource estimation equation is:

$$\text{Volume} = \text{Area} * \text{Thickness}$$

1.2 Objectives

The objectives of this project were: 1) to identify causes of uncertainty in the estimation of area and average thickness of coal zones using exploration data for three coal zones in two areas of southern Saskatchewan. 2) to compare statistical models of the spatial variability of seam thickness and structural configuration with conceptual models of coal geology, applying the Theory of Regionalized Variables developed by Matheron (1963) and in particular to apply the techniques of structural analysis and kriging to

the comparison. 3) to investigate alternative methods of statistics and probability which can be employed in coal resource estimation, and 4) to apply some of the statistical methods to exploration data from southern Saskatchewan.

CHAPTER 2

2. Geology of Selected Coal Zones

The Ravenscrag Formation of Paleocene age covers about 10,000 square miles of southern Saskatchewan, and is coal-bearing throughout this area. Exploration data for three coal zones in two localities were selected; two in the Estevan coalfield (shown in Figure 2) and a third not located in the Estevan coalfield, chosen because of the closely-spaced, systematic drilling pattern. Due to the confidential nature of the data, the precise location of the third site cannot be given.

2.1 Previous Work

Early work on the geology of the coal-bearing strata of southern Saskatchewan was restricted to exposures in the Souris River valley between Estevan and Roche Perceé. Sir James Hector, travelling with the Palliser Expedition in 1857, measured a section in the Souris River valley and assigned a Tertiary age to the lignite coal measures. Underground mining of the lignite began in 1887 after geological investigations in the area by A.R.C. Selwyn in 1873 and G.M. Dawson in 1875. A comprehensive description of the exposures along the valley walls of the Souris River, Long Creek and Short Creek is found in Dowling (1904). MacLean (1918) added further descriptions of the coal seams

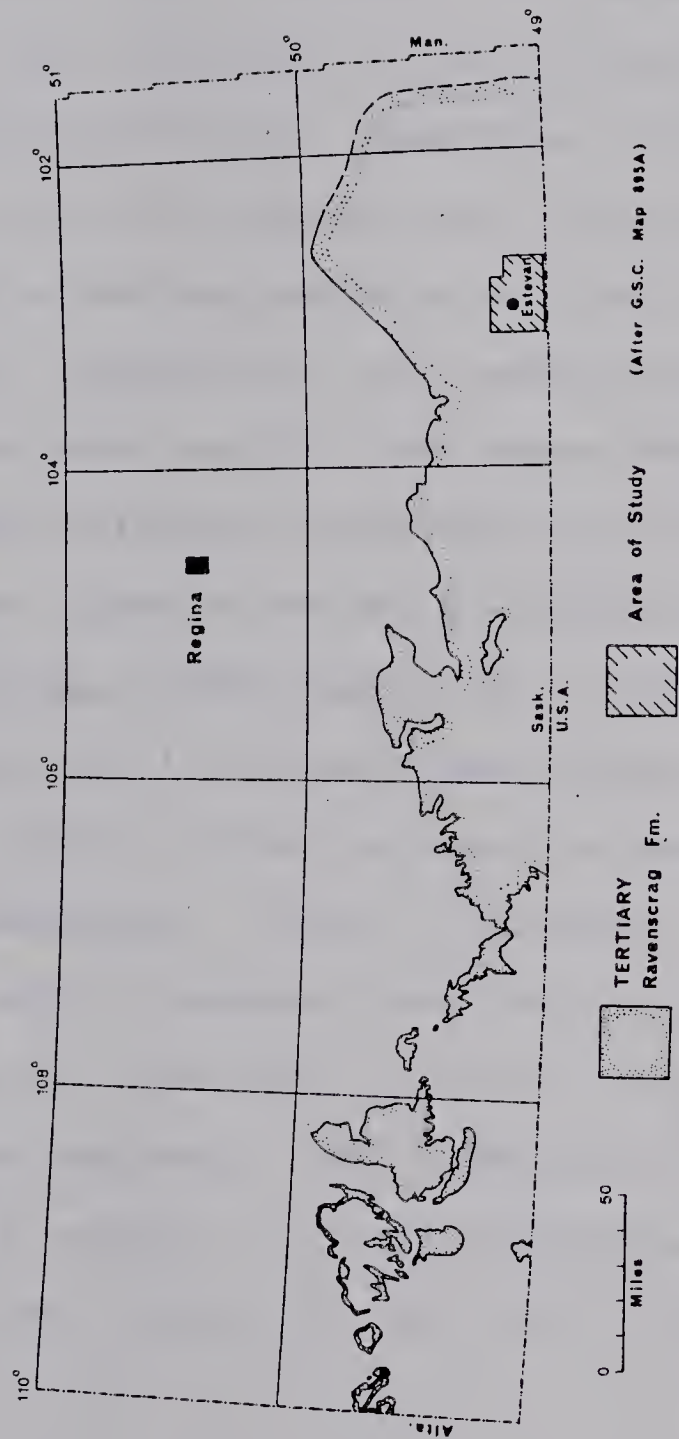


FIGURE 2. Location map, southeastern Saskatchewan.

in the Souris River coalfield.

Although the exploration for coal was most active in the Estevan area, the Tertiary stratigraphy of southern Saskatchewan was deciphered in the Cypress Hills area where Upper Cretaceous-Paleocene transition strata are well exposed. The term Ravenscrag was first applied to coal-bearing strata at Ravenscrag Butte by Davis (1918). Fraser *et al.* (1935) recognized two parts of the Ravenscrag of differing aspect and age. The term Upper Ravenscrag was used to describe the Paleocene coal-bearing part while Lower Ravenscrag was applied to the Cretaceous non-coal-bearing part. Fraser *et al.* (1935) mapped the distribution of the Ravenscrag Formation in southern Saskatchewan and correlated the isolated Souris River sections as part of their Upper Ravenscrag Formation. Their regional geology and stratigraphy until recently has been the only source of information on the formation. In 1935, Berry described the flora of the Whitemud and Ravenscrag Formations, and Furnival (1946) renamed the Lower Ravenscrag the Frenchman Formation on the basis of his work in the Cypress Hills area.

More recently, Holter (1972) made extensive use of coal exploration boreholes to correlate individual coal zones in the Estevan coalfield. The petrographic composition of some seams in that area was studied by Cameron and Birmingham (1971) and Broughton (1972). Whitaker (1967, 1974a, 1974b)

produced a series of maps and sections illustrating the general stratigraphy and structure of southern Saskatchewan for the purpose of groundwater exploration. This thesis is based on data collected and interpreted during the lignite evaluation program described by Whitaker (1972).

The first coal resource estimates in southern Saskatchewan were produced by Dowling (1913). Mackay (1947), using more realistic criteria, produced new estimates for the Royal Commission on Coal. Additional knowledge of the area and revised resource classification schemes reduced Mackay's estimates by one-half to those of Latour and Christmas (1970). Finally, on the basis of 700 boreholes drilled in 1972 and 1973, and 500 boreholes of comparable quality, Broughton et al. (1974) estimated the total quantity of measured and inferred coal resources of immediate economic interest to be 5.7×10^9 tons.

2.2 Regional Geology

The areas which form the basis for this study are located in the Interior Plains physiographic province and within the Western Canada sedimentary basin. They lie on the northern flank of the Williston Basin, an ellipsoidal structural depression centered in North Dakota. Christopher et al. (1973) summarized the the geological setting of the area. The Precambrian erosional surface dips southwestward at 12 to 20 feet per mile as an irregular monocline, except

in the southeast where dips to the south of up to 50 feet per mile are recorded. Local domal features originated with or were rejuvenated by Laramide movements (Kent and Simpson, 1973).

A basal clastic sequence records marine transgressions across the craton in Late Cambrian and Early Ordovician time. Subsequent to the development of the Williston Basin in Early Ordovician time, a thick carbonate-evaporite sequence was deposited (Webb, 1964). Although interrupted by an hiatus between the Silurian and Middle Devonian, sedimentation continued into the Mississippian, to be followed by a long period of uplift and erosion.

During the Jurassic, evaporites, carbonates, shales and sandstones were deposited in the area. Following uplift in the Cordillera in late Jurassic/early Cretaceous time, large volumes of clastics were deposited around the margins of the Cretaceous Boreal and Gulfian seas. Non-marine sandstones and marine shales intertongued as the seas transgressed, joined and finally receded to the south and east as further late Cretaceous and Tertiary uplift and vulcanism occurred to the west.

The early Paleocene Cannonball Sea (Lemke, 1960) represents the last marine incursion into the interior plains before the area was covered by an extensive alluvial plain represented by the Ravenscrag Formation. As a result

of the late Tertiary Laramide orogeny, southern Saskatchewan was uplifted and subjected to erosion. Thin stream-bed conglomerates represented by the Cypress Hills and Wood Mountain Formations accumulated with erosional unconformity on the Ravenscrag Formation (Taylor, 1964). Sands and gravels of the Empress Group (Whitaker and Christiansen, 1972) occur as valley fill deposits in pre-glacial and early glacial valleys on the bedrock surface. An extensive blanket of glacial drift, locally in excess of 900 feet thick, now covers much of the area.

2.3 Geology of the Ravenscrag Formation

Furnival (1946) and Fraser et al. (1935) provide the most recent published descriptions of the Ravenscrag in southern Saskatchewan.

The Ravenscrag Formation consists of grey and buff-weathering shales, fine sandstones, siltstones, and sandy shales and conformably overlies the late Upper Cretaceous Frenchman Formation (Furnival, 1946). Lignite seams are abundant and thin laminae of carbonized plant material occur. Fossil tap roots, lithified tree trunks and stumps in growth position have also been found in the formation. Bentonite beds form a minor component of the succession; the sandstones are fine to very fine grained and exhibit cross bedding and local channeling and filling.

Fossils collected from the Ravenscrag include fresh-water invertebrate, fish, turtle and crocodile remains. Berry (1935) concluded that the floral assemblages were representative of a humid, temperate climate, and Fraser et al. (1935) interpreted the depositional environment as an alluvial plain covered by forests, swamps and marshes. Azimuth measurements on cross-stratification (Carrigy, 1971) and heavy-mineral analyses (Rahmani and Lerbekmo, 1975) have suggested sediment transport from the northwest for the westernmost exposures of the Ravenscrag.

2.4 Coal Geology

Thick seams of lignite (greater than 3 feet) in the Ravenscrag are confined to four major basins (Broughton et al., 1974). Three to six seams occur near the surface in each of the basins and are separated by clastic intervals varying from 25 to 150 feet thick. All samples analysed by Tibbetts (1975) are lignite.

MacLean (1917, p. 38) characterized seams in the Souris River valley as:

"...not continuous through the area. In some places they split up, or pinch out completely, to start again at some distance from the last observed occurrence."

Dowling (1904, p. 9) correlated groups of seams he termed horizons which:

"...may contain several seams but in each, workable seams occur in places."

Throughout an area of coal deposition, individual coal seams may thicken, thin, split into thinner units separated by rock or disappear altogether. The term "zone" is used here to refer to any interval of strata which contains coal in one or more seams and which can be correlated over a wider area than any individual seam.

Petrographic studies have been restricted to the Estevan zone in the Estevan coalfield. Cameron and Birmingham (1971) recognized ten petrographic units varying from 3 to 12 inches in thickness in a column of lignite 98 inches in height. They concluded that the maceral composition favoured a dominantly forest-moor environment of deposition with indications of reed-moor and open-water environments. Broughton (1972) recognized seven environmental transitions in a 145 inch column of the Estevan zone. Six transitions occurred from the dominant forest-moor facies to the less frequent reed-moor and one occurred from the reed-moor to the open-water facies.

The general character of the Ravenscrag Formation is very similar to coal measures in the Sydney Coalfield described by Hacquebard and Donaldson (1964). Their conceptual model of a flood-plain depositional environment is an appropriate framework for interpreting coal exploration data for the study areas.

In Hacquebard and Donaldson's model, river channels

meandered across broad areas of low relief carrying sediment eroded from an uplifted area. Peat accumulated in large forested swamps and marshes which covered the flood-plain. Overbank fines and sand, deposited in crevasse splays as a result of floods interrupted peat accumulation. Occasionally channel migration or switching resulted in erosion of narrow channels in a peat deposit, and during pulses of orogenic uplift, floods of clastics buried and preserved the peat accumulations. As the sediment flow decreased, plants stabilized the channels and peat accumulation resumed.

2.5 Data Compilation

All exploration data used in this study are from boreholes. Lithologies penetrated were described by a geologist and most holes were logged at a scale of 1"=20' using single-point resistance, spontaneous potential, gamma ray, gamma-gamma density and caliper logs. Gamma ray and gamma-gamma density logs at an expanded scale of 1" to 2' were run over the major seam intervals.

A coal zone comprises depositional events which can be identified and correlated using subsurface techniques. Letters were assigned to the identifiable beds of clean coal in a zone in alphabetic order from the topmost bed down. For operational consistency, each bed of coal one foot thick or thicker was identified as a seam, with seams separated by barren strata at least two feet thick. Inorganic partings

less than two feet in thickness often occur in seams and the combination of coal beds in the seam was represented by the range of letters. The Estevan C-G seam would contain the coal beds C, D, E, F and G. Figure 3 illustrates this nomenclature as applied to a coal zone.

The thickness of a seam as recorded is the total interval from the top to the base of the seam. The net coal thickness, in contrast, is the seam thickness minus any non-combustible material which could occur in beds less than 2 feet thick. These terms are illustrated in Figure 4. Data on the location and identity of boreholes and the stratigraphy and coal seams penetrated were coded, keypunched and entered into a computer data file which formed the basis for this study.

Because of thickness and depth considerations, not all seams in a zone at a borehole might reasonably be mined. Therefore a method was devised to combine selected seams of a zone into a single unit termed a potential mining zone. Seams which were mathematically acceptable at each borehole according to the criteria described below were treated as a unit having a bottom depth equal to the base of the lowest coal seam chosen and a net coal thickness equal to the total of the net coal thicknesses of the accepted seams. Criteria used for selection of seams from each zone for inclusion in the potential mining zone in each borehole were:

1. Seams with five feet or more of net coal are

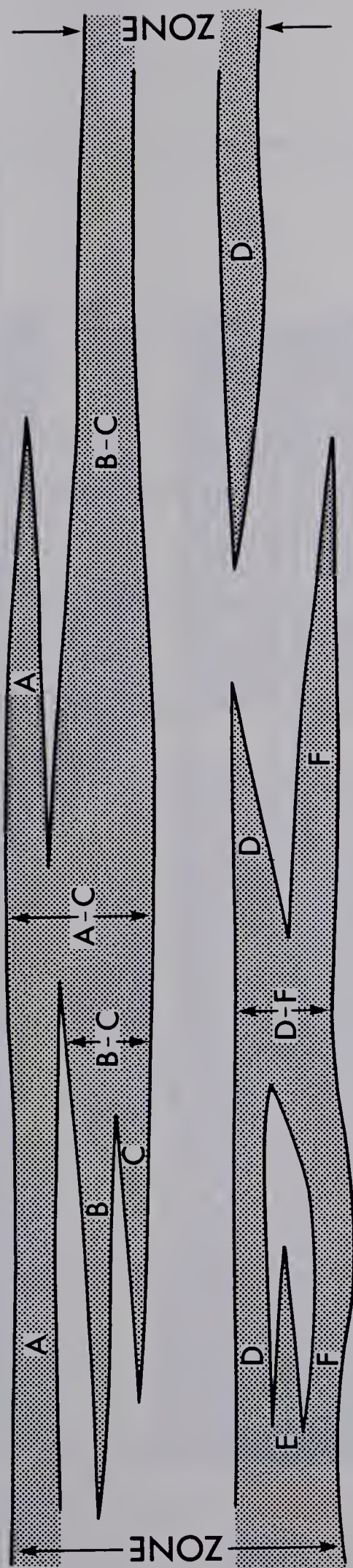


FIGURE 3. SEAM NOMENCLATURE APPLIED TO A HYPOTHETICAL COAL ZONE

SEAM NUMBER	ZONE NAME	NAME MODIFIER	LITHOLOGY	SECTION (in feet)	NET COAL (in feet)	SEAM THICKNESS (in feet)	ZONE THICKNESS (in feet)
1		A	Coal	2	2	2	
				8			
2	ESTEVAN	B C	Coal	5	5	12	28
		D	Shaly Coal	1			
		E	Coal	5	6		
				4			
3		G	Coal	2	2	2	
			TOTALS	28	15	16	28

Figure 4. Diagrammatic explanation of coal thickness terms.

always included.

2. Seams with less than five feet of net coal but with three feet or more are included if the incremental overburden ratio (overburden or rock material above the seam and below the next higher seam or surface divided by the coal thickness) is less than 15:1, or if underlain by a seam fitting criterion 1.

3. Seams with less than three feet of net coal and with two feet or more are included when underlain by a seam fitting either criteria 1 or 2.

OR

When overlain by an acceptable seam provided that the rock interval between the seams is less than twice the thickness of the lower seam.

The validity of the above criteria is dependent upon assumptions about the value and end use of the coal and the presently-practicable mining methods employed in southern Saskatchewan.

In some boreholes no seams in a zone were acceptable under the above selection criteria. Where evidence of erosion or non-deposition could be found in adjacent boreholes, the entire area in which the zone was too thin or missing was excluded from consideration in creating an

isopach map and in the subsequent resource quantity calculation. Where the lack of acceptable seams appeared to be restricted to a single borehole and did not extend to the surrounding area, a zero value for net coal in the potential mining zone was used for resource quantity estimation and for isopaching the net coal values.

Most coal zones are truncated by the bedrock erosional surface which developed after the Paleocene and prior to the onset of glaciation. To predict the location of the subcrop of the potential mining zone beneath glacial deposits, structure contour maps of the top of the zone and the bedrock surface were produced from borehole data by computer programs using various algorithms for estimating the value of a surface at the nodes of a regular grid. Although grid intersections form a regular geographic basis for surface comparisons, the choice of a grid spacing involved a trade-off between the desired level of detail in a contour map and the expense of creating very fine grids. A grid spacing of 500 metres was selected for the Estevan area whereas a 100 metre distance between nodes was used for the small-scale area. The grids were then contoured and algebraically compared using the SURFACE II graphics package.

Few exploration boreholes were drilled in stream valleys where recent erosion has removed the overlying till and exposed the bedrock surface and often the coal zones proper. Bedrock surface grids produced from borehole

information thus usually did not reflect such valleys. Selected contour lines from the published 1:50 000 scale topographic maps were digitized and a surface topography grid was produced. This surface topography grid was compared to the bedrock surface grid, and where a surface elevation value was lower than the corresponding estimated bedrock elevation, the surface elevation was substituted into the bedrock grid, adding the detailed information from the surface topography to the bedrock grid data. The location of the subcrop of the coal zone on the bedrock surface was then estimated by algebraically comparing the modified bedrock grid and the coal zone structure grid.

2.6 Estevan Area

The Estevan coalfield is located in southeastern Saskatchewan (Figure 2); the location and distribution of the 340 boreholes in the coalfield used in this study are shown in Figure 5.

The region is flat to gently rolling prairie dissected by the Souris River, Long Creek and Short Creek. The maximum relief from the bottom of the river valleys to the International Boundary in the southeast is about 200 feet (67 m) (Figure 6). Meneley et al. (1957) believe that the Souris River and Long Creek occupy meltwater channels which were marginal to the Weyburn glacial lobe at two different times.

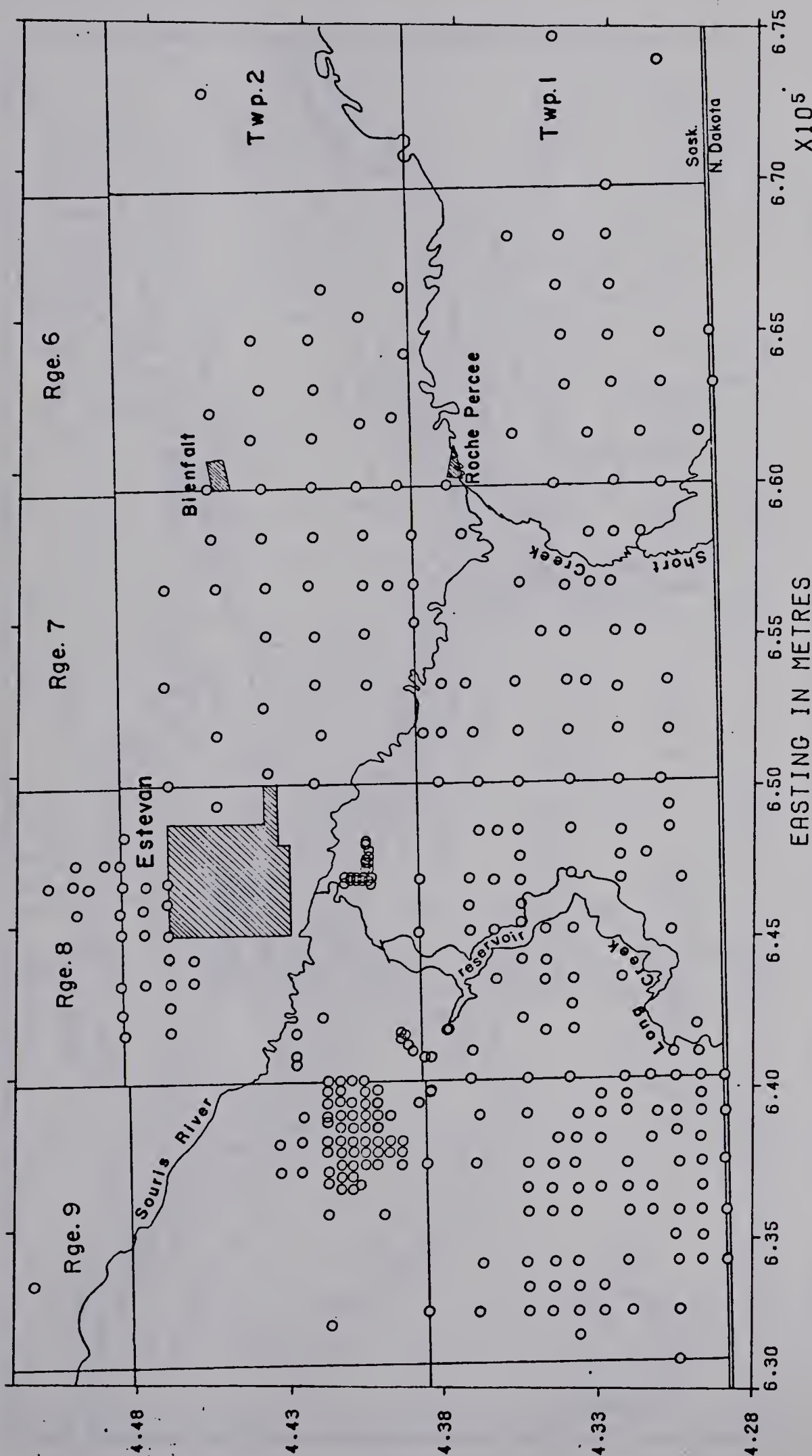


FIGURE 5. DISTRIBUTION OF BOREHOLES IN THE ESTEVAN COALFIELD.

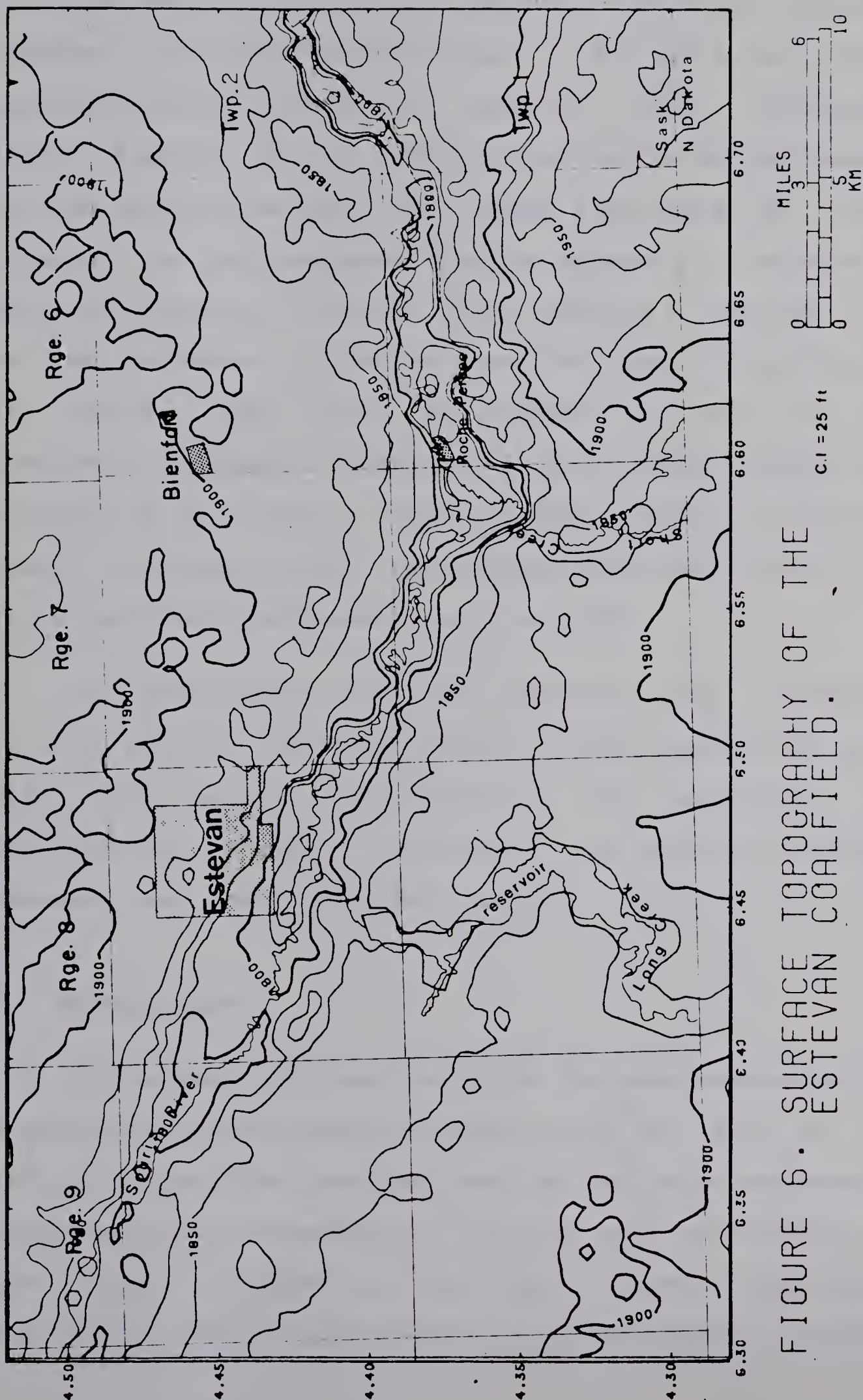


FIGURE 6. SURFACE TOPOGRAPHY OF THE ESTEVAN COALFIELD.

The Estevan coalfield underlies a plateau of bedrock bounded to the west, north and east by the valley cut by the northeast-flowing preglacial Missouri River (Whitaker, 1974a; Meneley et al., 1957). The elevation of the bedrock plateau varies from 1825 feet to 1950 feet above sea level (Figure 7). The northwest-trending channel of a preglacial river tributary to the major river isolates a bedrock high to the southwest of the main upland. Sands and gravels of the Empress Group cover the bottoms of most of the preglacial channels. Incision of the meltwater channel now occupied by the Souris River exposed bedrock (including coal) to a depth of 100 feet or more below the upland level in an east-west band about a mile in width.

At least five mineable coal zones have been identified in the Estevan coalfield (Holter, 1972). Because of their wide areal extent, contrasting seam character and availability of data, the Estevan zone and the underlying Boundary zone were chosen for study.

2.7 Estevan Zone

The Estevan zone was studied in the area bounded on the south by the International Boundary, on the east by the 670 000 metre UTM easting and to the north and west by estimated subcrop boundaries. The zone was intersected in 176 boreholes (shown in Figure 8); incomplete sections of the Estevan zone are preserved in some 15 boreholes located

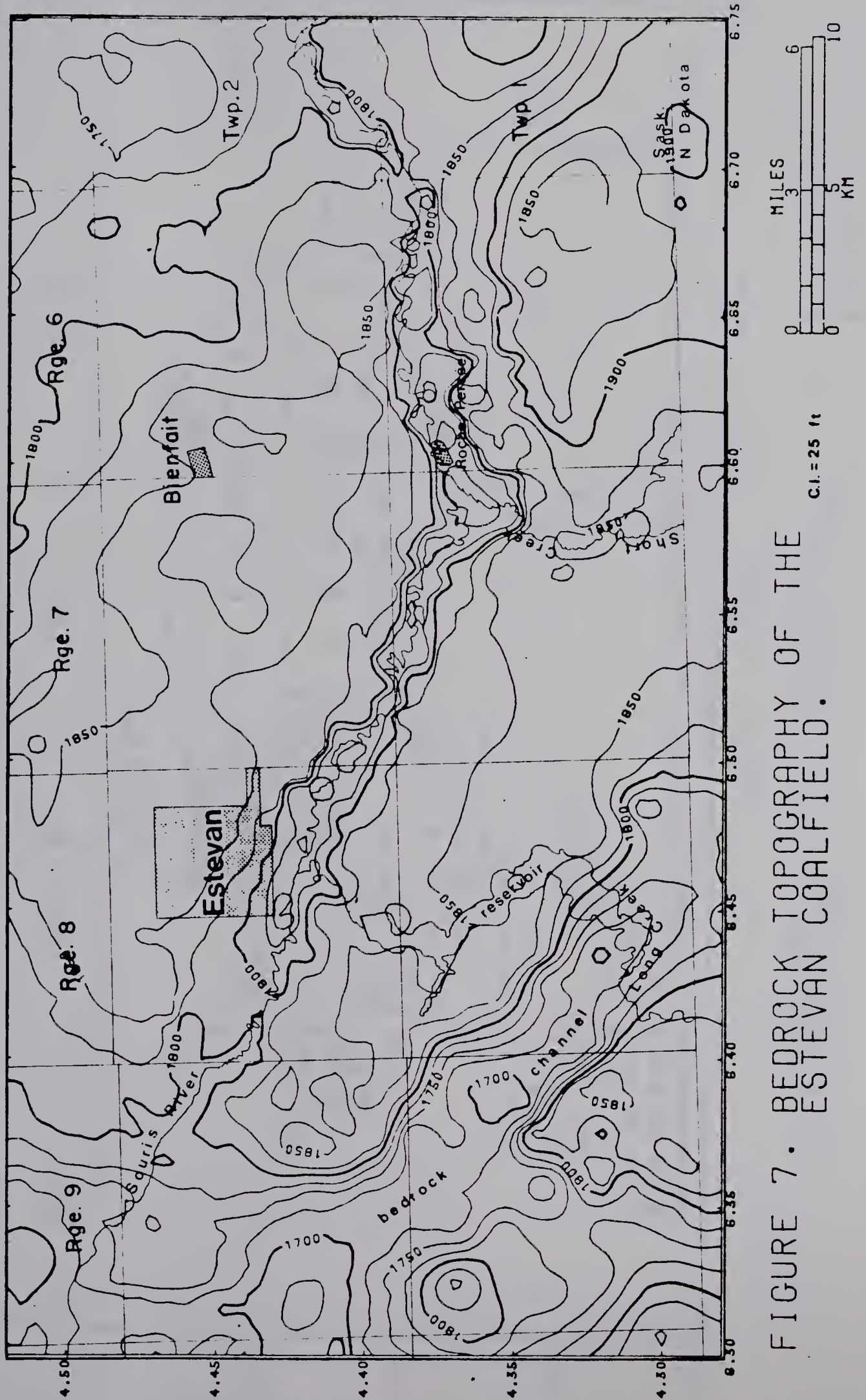


FIGURE 7. BEDROCK TOPOGRAPHY OF THE ESTEVAN COALFIELD.

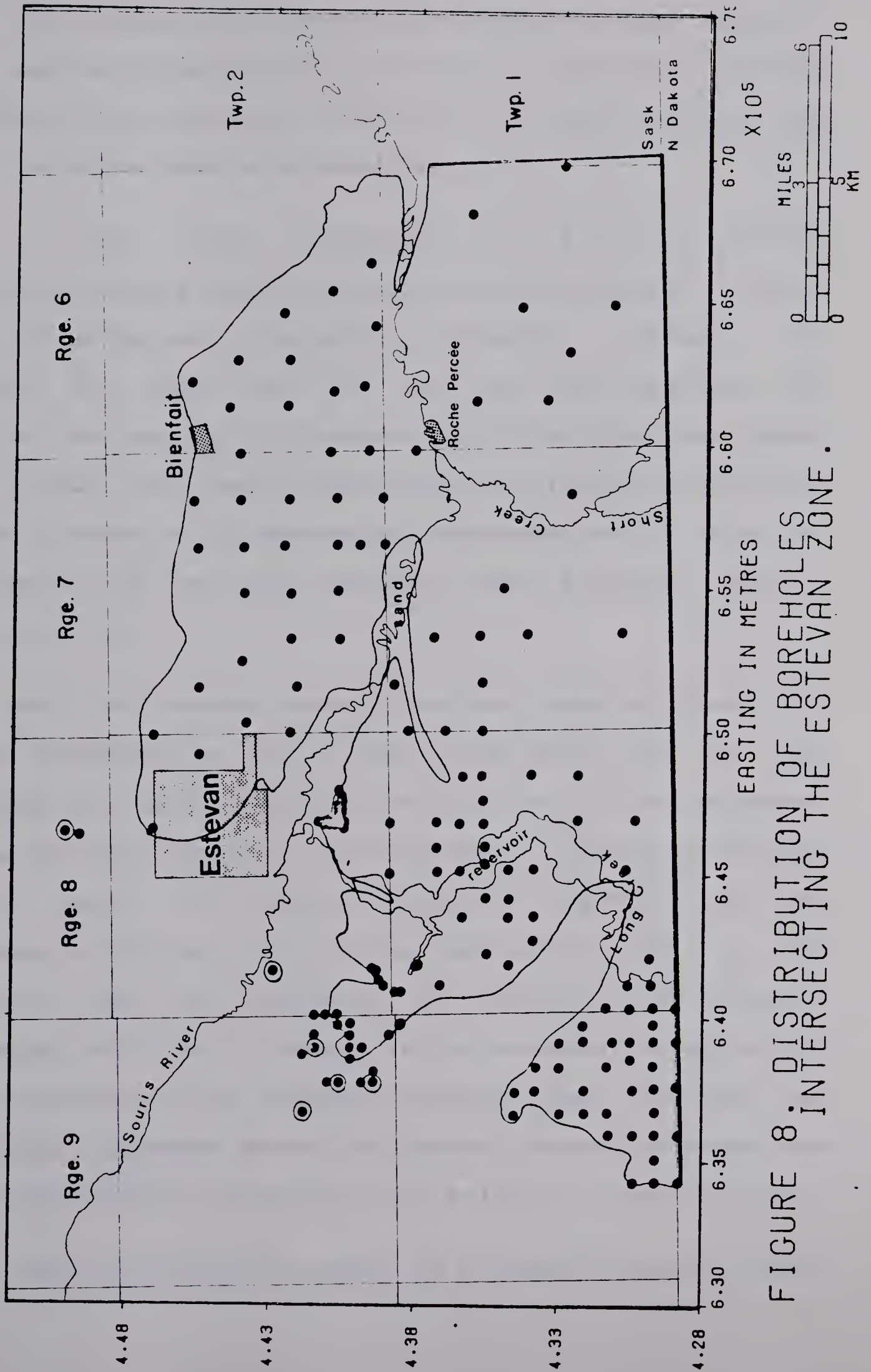


FIGURE 8: DISTRIBUTION OF BOREHOLES INTERSECTING THE ESTEVAN ZONE.

near or outside the subcrop edge where the upper seams in the zone have been removed by glacial or preglacial erosion. In these latter boreholes the top of the remaining zone was used for structural interpretation.

A sand body, interpreted as a stream channel contemporaneous with coal accumulation, was mapped for about 9 km along the north boundary of Township 1, Range 7 W2 (Figure 8). After most of the zone was deposited, the channel was apparently abandoned and filled with two upper coal beds. The area in which the coal filling was too thin to be mineable or is missing was considered as an area of non-deposition and was excluded from resource quantity calculations.

The zone surface generally strikes east-northeast and dips southeasterly at 20 feet per mile with the dip steepening to greater than 30 feet per mile to the southwest along the east flank of a south-plunging trough underlying Roche Perceé and Bienfait (Figure 9). The dip of the zone appears to flatten out to 12 feet per mile or less at the subcrop under and southwest of Estevan. A small south-plunging anticline is present in the southwest corner of the map southwest of the bedrock channel. The anticline may continue northeast across the bedrock channel although seam correlations are not sufficiently reliable to confirm this.

Local structure is present as northwest-trending swales

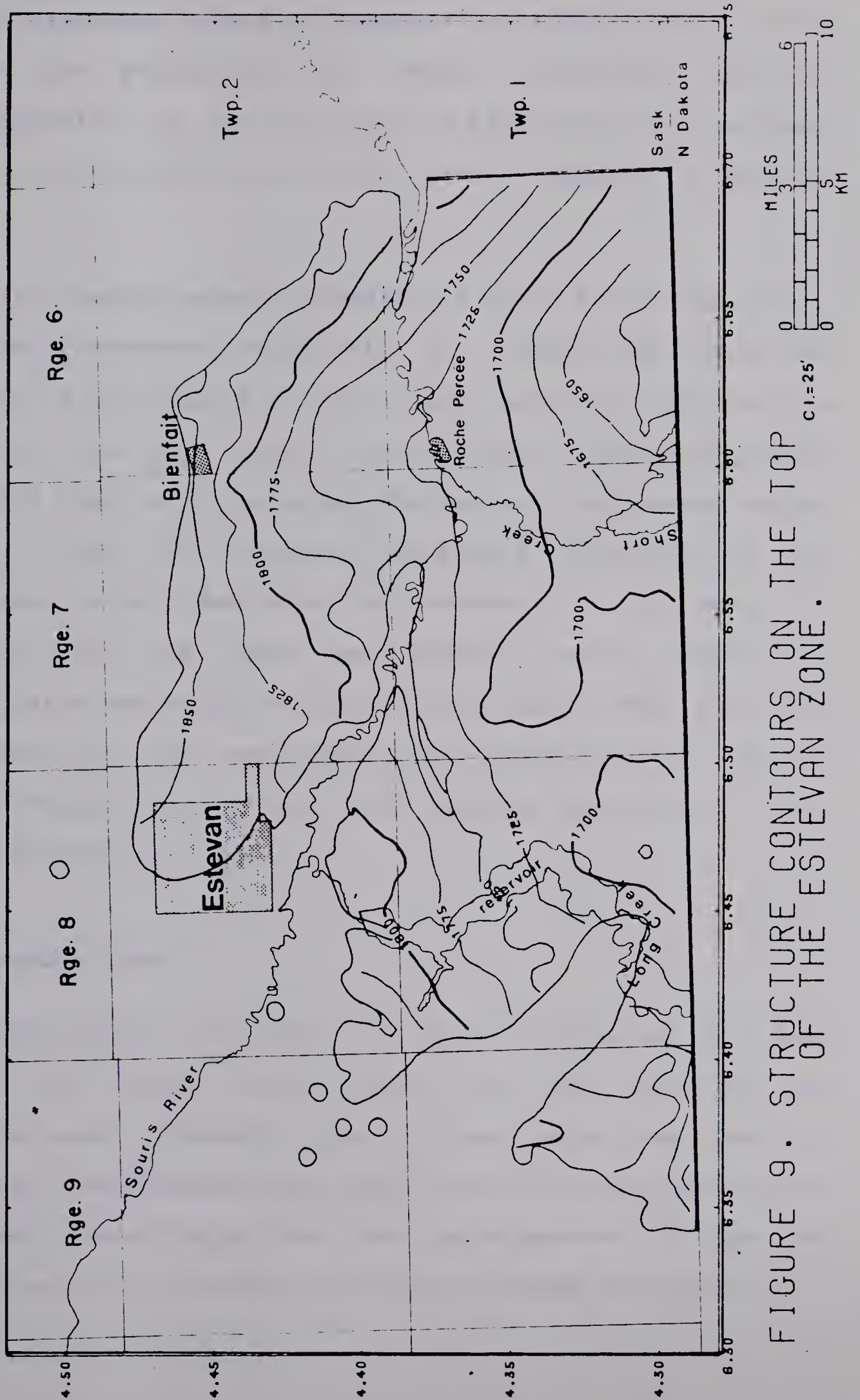


FIGURE 9. STRUCTURE CONTOURS ON THE TOP OF THE ESTEVAN ZONE.

of low amplitude having an apparent wavelength of one to two miles. The orientation of these structural features perpendicular to the direction of Pleistocene ice movement and near seam subcrop and valley walls suggests a glacial origin.

The Estevan zone is composed of up to 9 coal beds which can be correlated separately or combined in seams. An average of two seams is found in each borehole although as many as four may occur. The average thickness of the complete zone is 14 feet, and the net coal thickness varies from 2 feet (the minimum acceptable according to the criteria) to 18.4 feet with an average of 9.5 feet. An average of 1.4 seams per borehole were accepted in calculating the total net coal thicknesses. The net coal thickness in the zone tends to be greater in the west and north (Figure 10), but each area contains exceptions to this generalization.

2.8 Boundary Zone

The Boundary coal zone lies 20 to 86 (average 60) feet below the Estevan zone. Bounded on the south by the International Boundary, and to the north and west by subcrop, the Boundary zone was limited by sand deposition to the east. These limits and the distribution of the 160 boreholes which intersect the zone are shown on Figure 11.

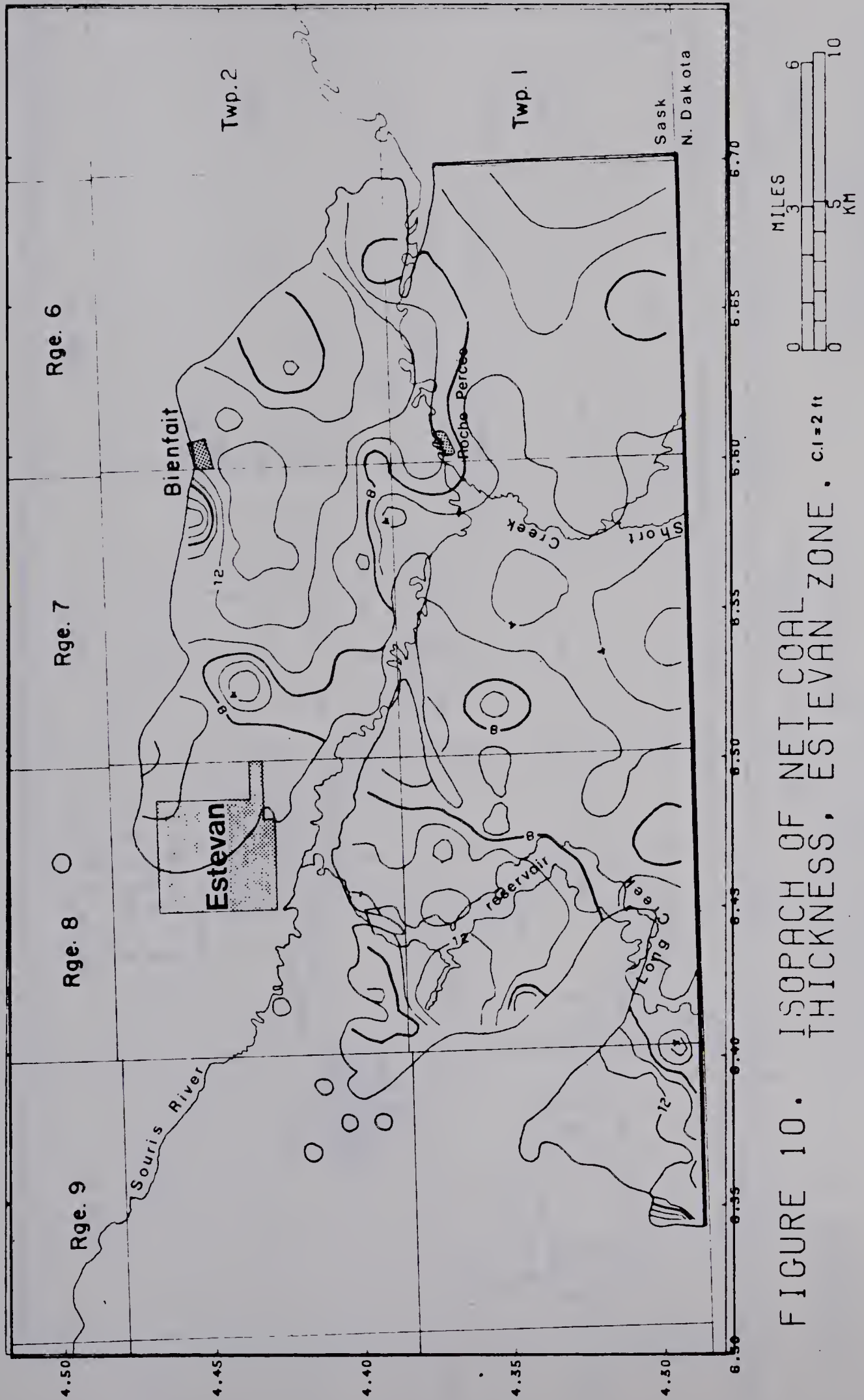


FIGURE 10. ISOPACH OF NET COAL THICKNESS, ESTEVAN ZONE. C.I.=2 ft

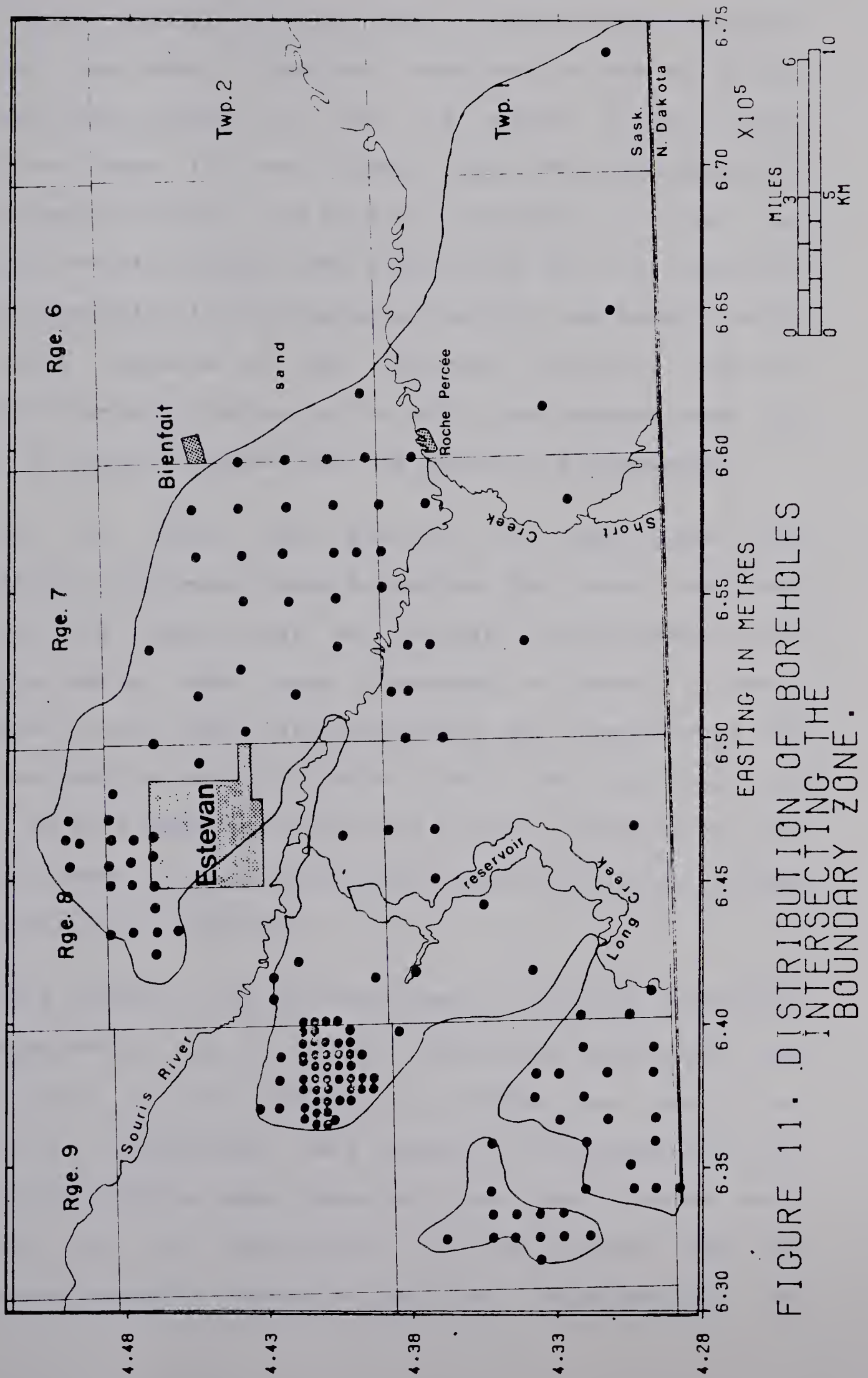


FIGURE 11. DISTRIBUTION OF BOREHOLES INTERSECTING THE BOUNDARY ZONE.

Due to the wide spacing of boreholes over the southeast part of the area, structure contours on the top of the Boundary zone (Figure 12) lack the detail of the local structure found in the Estevan zone. The zone generally strikes east-northeast and dips to the south at 25 feet per mile but the dip becomes more easterly on the west side of a slight depression located between Bienfait and Roche Perceé. The local features on the regional structure echo the northwest-trending swales on the overlying Estevan zone but appear to be more subdued and are smaller in dimension.

Up to twelve coal beds in the zone have been tentatively correlated among boreholes. The zone comprises one to five seams with an average of two seams in each borehole, and a total zone thickness of about 9 feet. Thickness of the potential mining zone was calculated in 151 holes and set to zero in 9 holes in which the seams were too thin. Up to 3 seams were selected in some boreholes but the average number of seams used in forming the potential mining zone was 1.2 per borehole.

Zero values of net coal thickness in several boreholes are apparently due to local thinning of seams below the cutoff value for the selection criteria and could not clearly be interpreted as a change in lithology as in the case of the Estevan zone. These zero net coal values were included in the construction of the isopach map and subsequent resource estimation. Net coal thickness in the

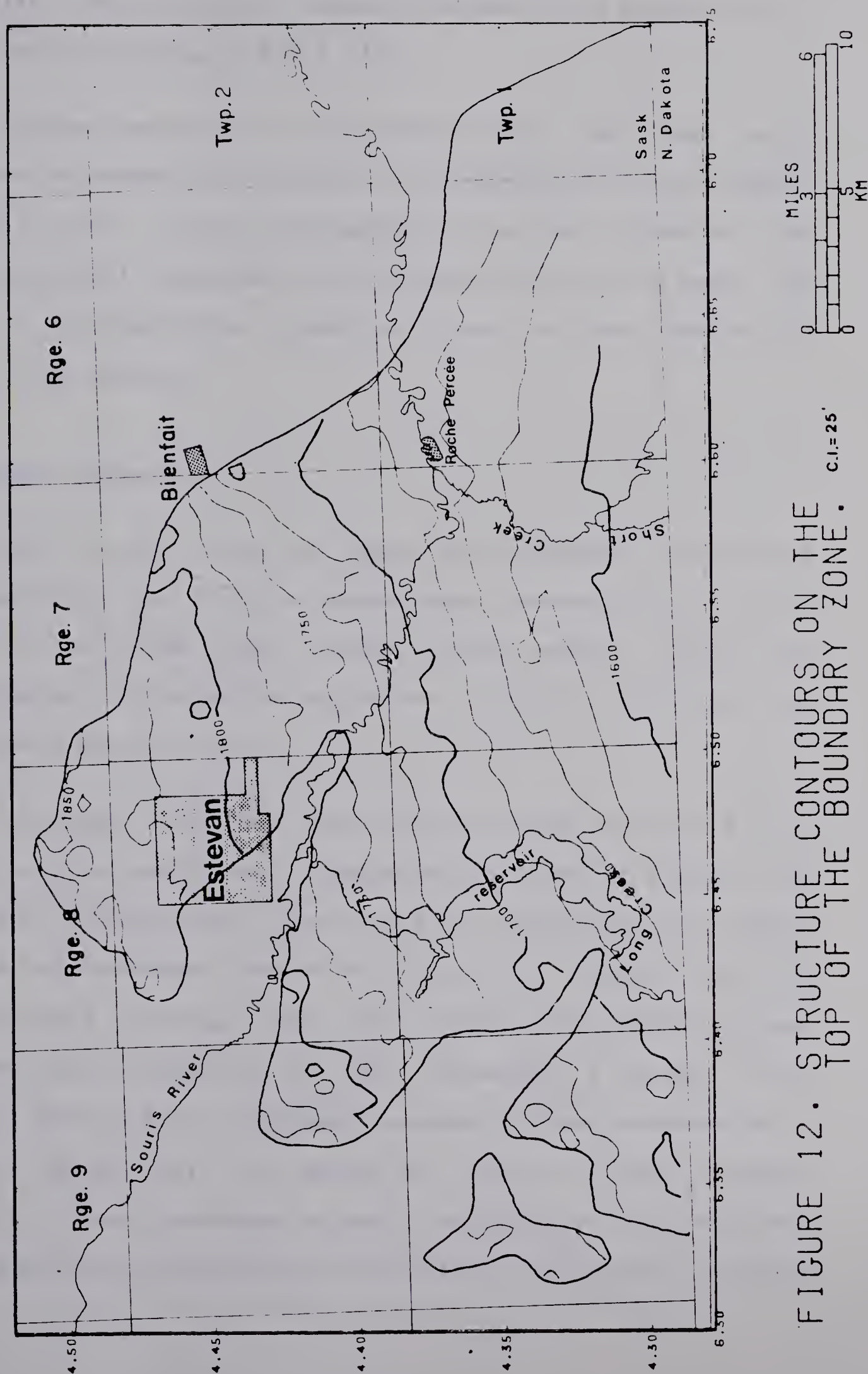


FIGURE 12. STRUCTURE CONTOURS ON THE TOP OF THE BOUNDARY ZONE. C.I.=25'

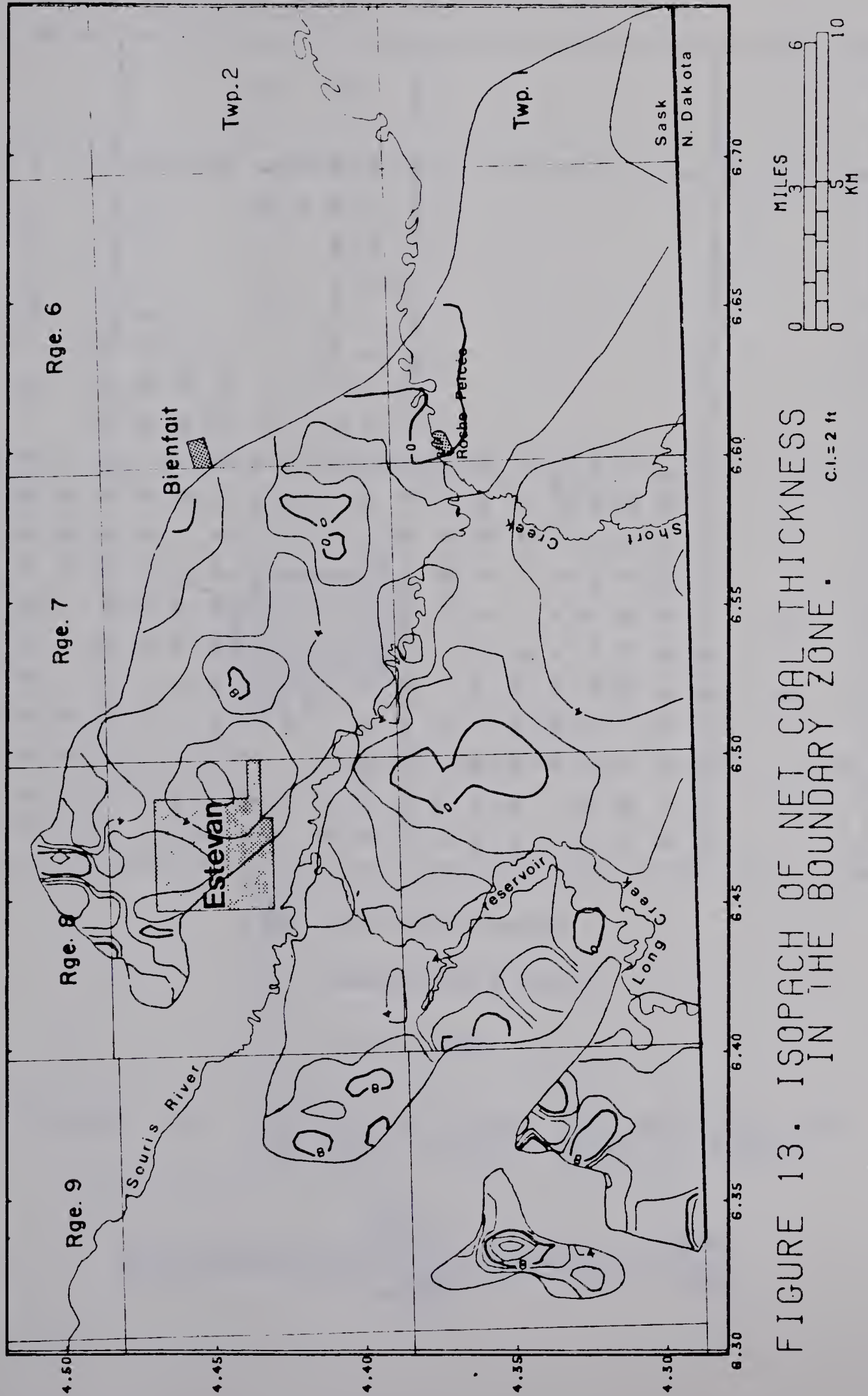
potential mining zone varies from zero to a maximum of 13 feet with an average of 5.3 feet.

Thicker sections of coal occur in the west and north but the thickness distribution as illustrated by the isopach of net coal (Figure 13) appears to be very irregular. The numerous small closures of the isopach lines is in part due to the interpolation algorithm used in the SURFACE II contouring package.

2.9 Small Scale Area

Data in the form of over 420 borehole logs were available for the study of small scale variability of a coal zone in an area about three miles square. Figure 14 illustrates the distribution of the control boreholes and surveyed section lines.

The area lies on the gently sloping south wall of a broad valley. The surface topography is shown in Figure 15. A misfit stream which flows along the thalweg of the valley across the northeast corner of the area is joined by two intermittent streams from the south. The bedrock surface (Figure 16) is composed of two elements, a broad, flat valley floor to the northeast bounded to the southwest by a steeper valley wall. The break in slope of the bedrock surface trends southeast across the centre of the area. The valley wall was dissected by two tributary streams draining



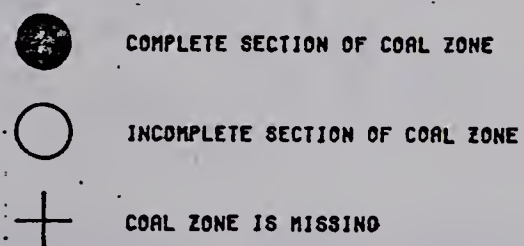
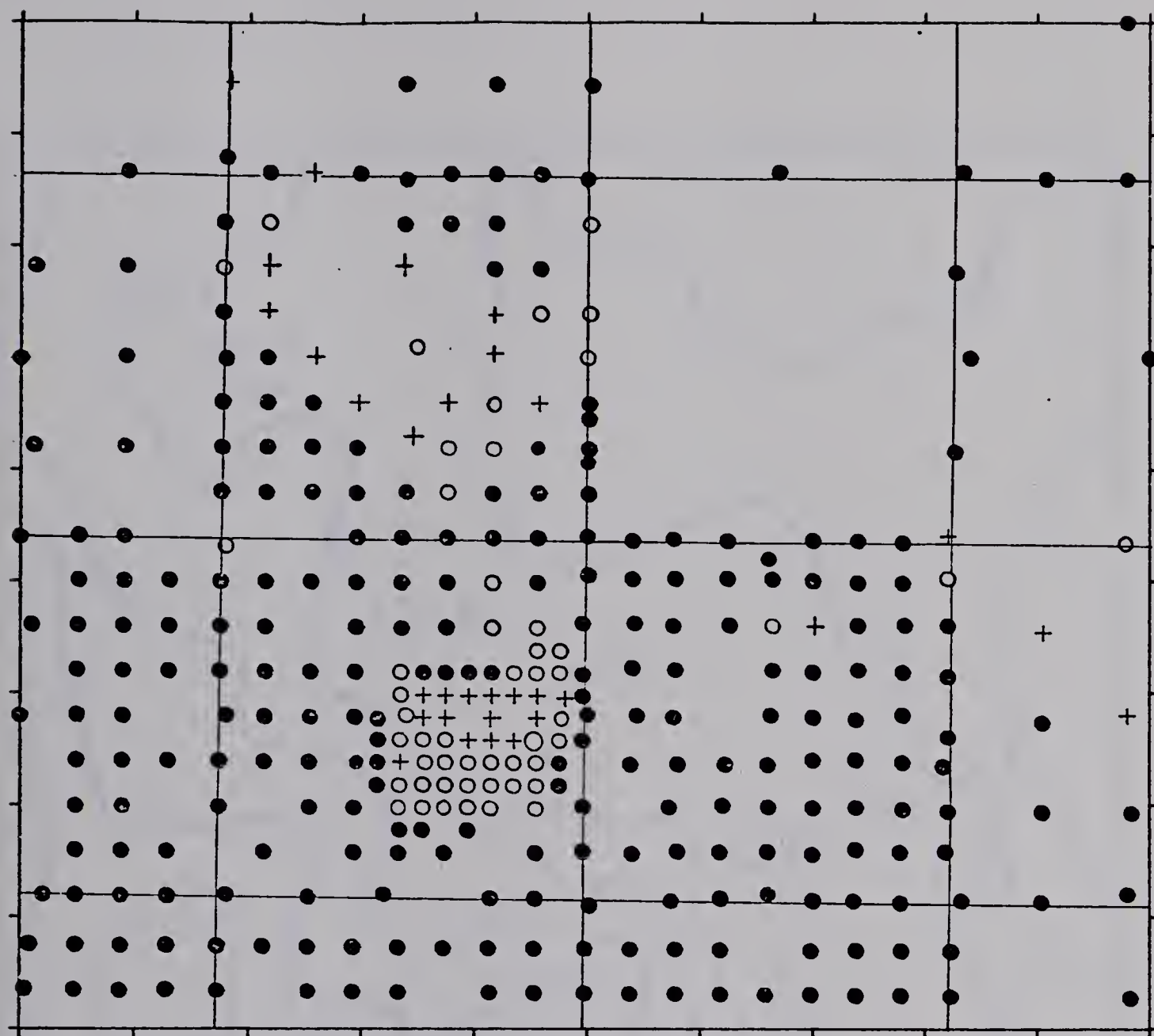


FIGURE 14. DISTRIBUTION OF BOREHOLES
IN THE SMALL SCALE AREA.

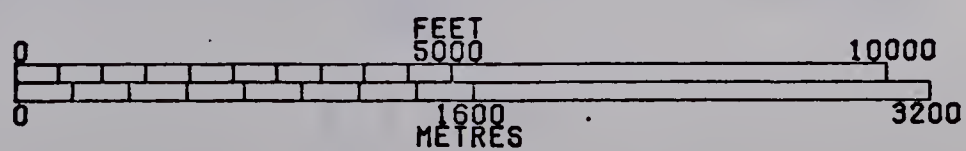
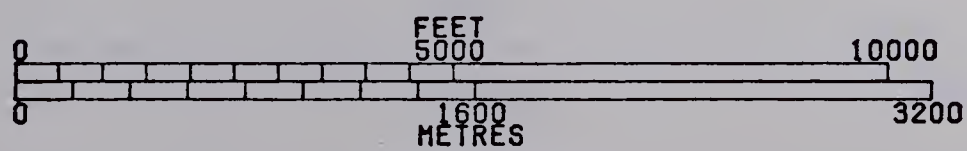




FIGURE 15. SURFACE TOPOGRAPHY OF THE
SMALL SCALE AREA.



C.I. = 20 feet

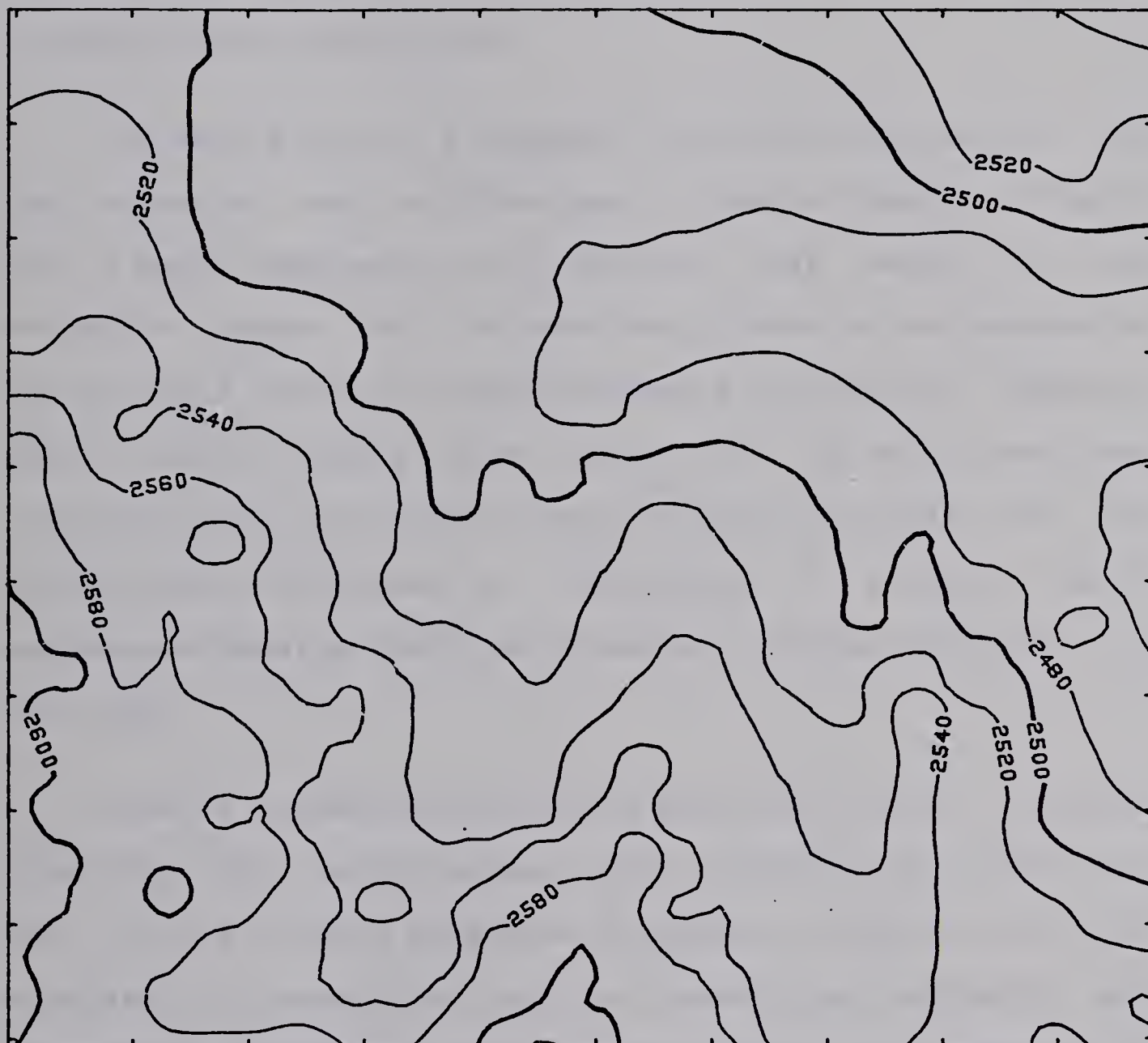
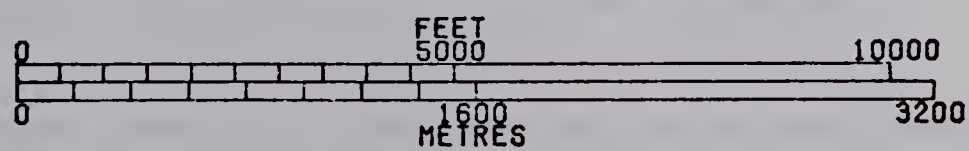


FIGURE 16. BEDROCK TOPOGRAPHY OF THE
SMALL SCALE AREA.



C.I. = 20 feet

the upland to the south. Glacial till and discontinuous sands and gravels of the Empress Group overlie the bedrock surface and range in thickness from 70 feet in the valley to 20 feet on the valley wall.

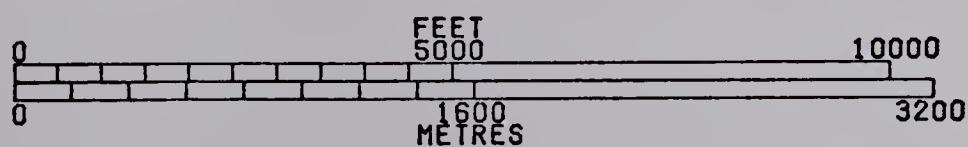
The coal zone has a regional dip of 30 feet per mile to the northeast but the structure is locally complex (Figure 17). A small depression 40 to 60 feet deep occurs in the southeast corner of the area and appears to be bounded to the west and north by a north-trending anticlinal flexure. Local normal faults with offsets of up to 20 feet were inferred along the trend of the structure but could not be traced over distances of one-eighth of a mile. A small northeast-plunging synclinal structure crosses the centre of the area.

Similar structures have been ascribed to salt collapse (DeMille, 1964; Christiansen, 1967). Solution and removal of salt in the Prairie Evaporite Formation of Devonian age has resulted in subsidence of the overlying sediments and structural adjustment along normal faults. Salt solution of the Prairie Evaporite was active during the Tertiary and may have controlled sediment dispersal and coal accumulation locally through subsidence of negative elements.

The coal zone is composed of up to six beds but the lower two are thin and erratic in distribution. A complete section of the zone consists of an upper seam separated by a



FIGURE 17. STRUCTURE CONTOURS ON THE
BASE OF THE COAL ZONE,
SMALL SCALE AREA.



C.I. = 20 feet

sand parting from a lower seam. The parting increases in thickness locally in the structural depression in the southeast, a fact which may indicate that the area was a positive element at the time of deposition, a remnant of salt which dissolved after the deposition of the Ravenscrag. The distribution of the zone in the boreholes is indicated in Figure 14.

Figure 18 is an interpretation of the areal distribution of the coal zone. A sand-filled channel which existed during coal deposition has been inferred from boreholes to occur in a narrow east-west band. The zone has been truncated by preglacial erosion at the foot of the valley wall except where it was preserved in the previously-mentioned synclinal flexure. Downcutting in tributary valleys removed the coal from two isolated areas.

Net coal thickness in the zone, excluding values affected by erosion and non-deposition (Figure 19), ranges from less than 8 feet in the southwest to more than 16 feet in the central area, with an average of about 12 feet. Local thickenings occur adjacent to the sand channel but values appear to be erratic over the remainder of the area.

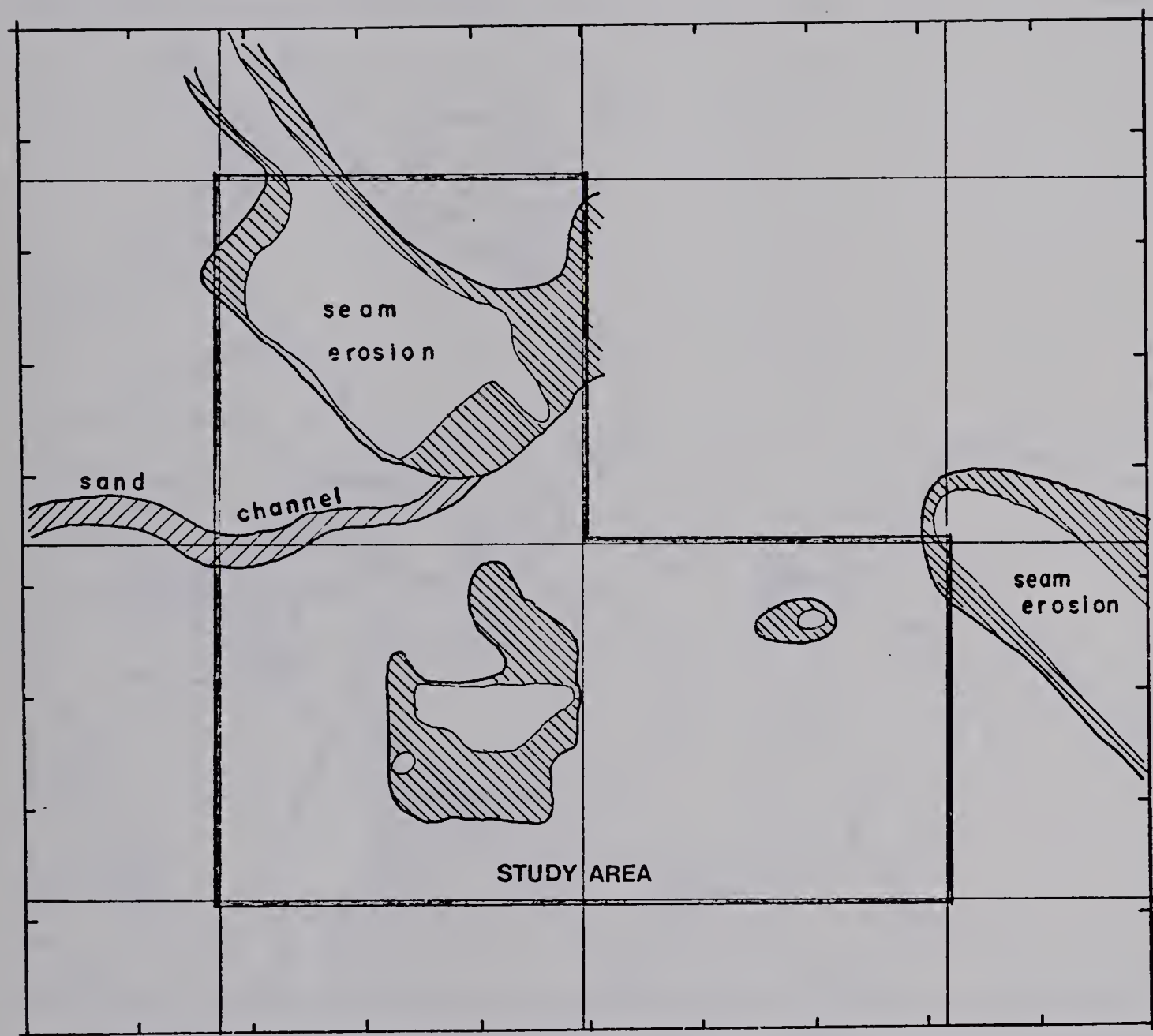
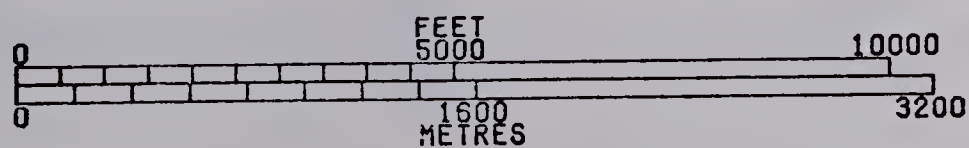


FIGURE 18. SAND CHANNEL AND EROSIONAL AREAS IN THE COAL ZONE, SMALL SCALE AREA.



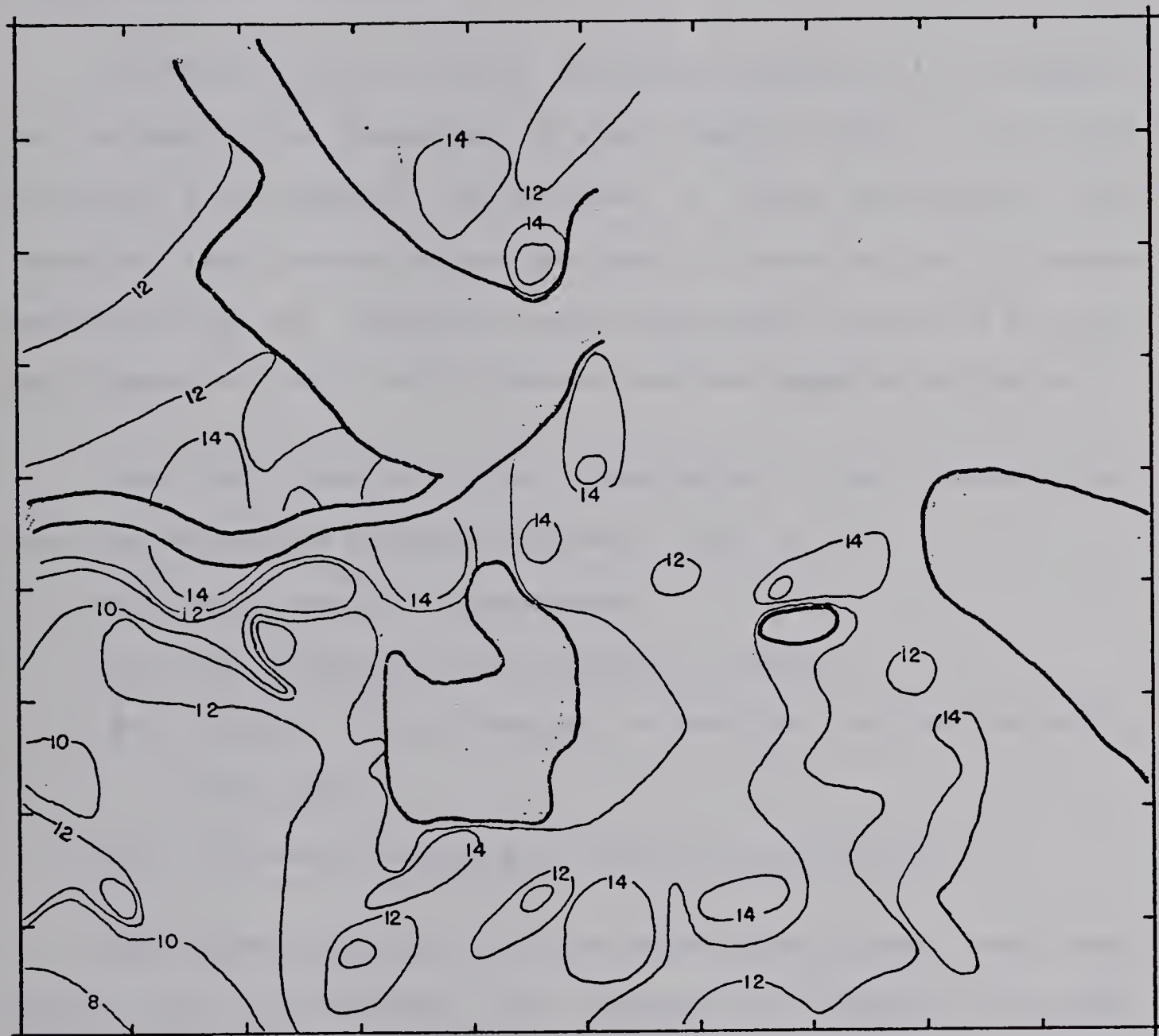
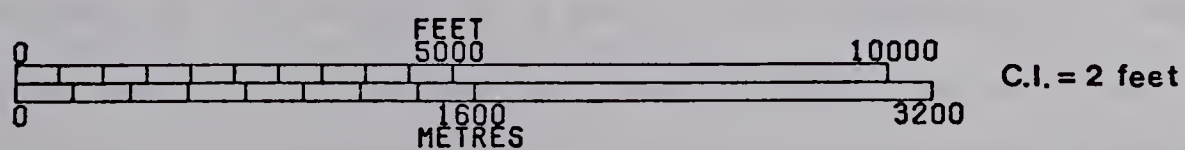


FIGURE 19. ISOPACH OF NET COAL THICKNESS OF THE COAL ZONE IN THE SMALL SCALE AREA.



CHAPTER 3

3. Statistical Methods

In 1965, Koch and Gomez employed statistical techniques to estimate the thickness of some lignite beds in Texas but they did not consider the problem of area estimation. As results, they presented the arithmetic mean of the thickness observations in boreholes and confidence intervals for the mean based on the t distribution and the sample variance.

For their results to be meaningful, four assumptions must be satisfied (Koch and Gomez, 1965, p 4):

- (1) each seam is homogeneous
- (2) the boreholes are drilled at random
- (3) results from different boreholes are statistically independent
- (4) the observations are normally distributed.

The third assumption is the most significant and most likely to be violated in reality. For example, consider measurements of the height of adult males passing a street corner. The height of the next man to pass the corner cannot be predicted by the value of a particular measurement taken previously, and is statistically independent. There is no a priori reason to suspect that the next individual will be tall or short but rather that the height of all adult males forms a frequency distribution characterized by certain

parameters such as a mean and variance. According to the third assumption seam thickness as observed in boreholes is similar in character to the above process. To continue the analogy, consider a field in which men have been assembled and are now standing shoulder to shoulder. An isoline map of the height of the men would appear chaotic. Giants, midgets and those of average height would be randomly arranged in the field.

This model does not fit previous observations of coal seam thicknesses or geological models of peat deposition. In outcrops along valleys and in mines, coal seam thicknesses are observed to vary relatively continuously. If considered as a mineable zone in which the contribution of several seams may be combined, the net coal thickness has a regional continuity with local thickenings and thinnings of coal. A simplistic analogy of a similar process is men passing by the street corner in groups of similar height: the relative position at which an individual arrives in the sequence of groups is significant for accurate prediction of the individual's height as location is significant for accurate prediction of coal seam thickness.

The processes of peat accumulation at any one point are controlled by many factors. A coal zone probably represents ten or more discrete configurations of peatland and alluvial channels and the coal thickness at any point represents the sum of these processes. As each of the major peat

depositional events occurred (and shifted) reasonably uniformly over an area, the sum of these processes has a relatively continuous spatial structure. Minor variations in bed thickness due to differential compaction, growth patterns of vegetation, erosional channelling and water table level are impossible to detect in boreholes spaced on an average of more than half a mile apart. Any model used to describe coal thickness variation must take into account not only the seeming random component but also a structured aspect.

From the above discussion it follows that not all the results from different boreholes are statistically independent. Observations taken close to one another are more likely to be similar than observations separated by a great distance. Statistical dependence might be expected between thickness measurements from closely spaced boreholes while observations widely spaced would be statistically independent. The dependence or correlation between samples of the same phenomenon at different locations is called spatial autocorrelation (Agterberg, 1974, p. 314).

The assumption that the boreholes are drilled at random (Assumption 2) implies for an autocorrelated variable such as seam thickness that the arithmetic mean of the observations is a biased estimator of the average thickness. Areas which are more heavily sampled than the average density contribute more weight to the mean than is

appropriate for an unbiased estimator.

To summarize, the assumptions made by Koch and Gomez (1965) are not intuitively appealing. The coal seam thickness is not randomly distributed spatially, and there are a priori reasons to expect patterns to occur. On the other hand, the coal thickness cannot be predicted exactly because variations occur at random locations due to small scale processes. Finally, an irregular sampling pattern results in a fragmented picture of the structured and random aspects of the phenomenon.

Equations will be introduced in the remainder of the chapter to describe the properties of some random processes and the estimation of their parameters. In these formulae, 'Z' will refer to a structural surface elevation, net coal thickness or any other continuously mappable variable which exhibits spatial correlation. The location of any point in the plane will be referenced as "x" and that of the i-th point location as "x(i)". The i-th measurement has a value "Z(i)". The location of the point or area which is to be estimated is "x(o)" and "Z(o)" is the value of the estimate.

3.1 Stationary Stochastic Processes

Mathematical models of processes which could be used to describe coal thickness variation over an area are stationary stochastic processes in the plane (Matern, 1960,

p. 11). A stochastic process is stationary if the expected mean value is a constant and the covariance function of two observations depends on the distance between the points and not their location.

This may be described by the following equations. Let $Z(x)$ be a random variable at the location x in the plane. Then the mean function of Z is

$$m(x) = E[Z(x)] = \text{constant} \quad (3.1)$$

and the covariance function is defined as

$$C(x,y) = E[Z(x)Z(y)] - m(x)m(y) \quad (3.2)$$

where E is used to denote 'expectation'. The symbols x and y represent point locations.

The autocorrelation function of the process is

$$r(x,y) = C(x,y) \cdot [C(x,x)C(y,y)]^{-1/2}$$

which can be rewritten as

$$r(x,y) = \frac{C(x,y)}{\sigma} \quad (3.3)$$

where σ^2 is the population variance.

Since the covariance function depends only on the distance h between x and y , (3.3) can be rewritten as

$$r(h) = \frac{C(h)}{C(0)} = \frac{C(h)}{\sigma^2} \quad \text{where } h = x-y$$

$C(0)$ is the covariance of an observation to itself and it is theoretically the population standard deviation, σ .

This model is in wide use in time series analysis for measurements taken at regular time intervals. The distance

between measurements is called the lag. The behaviour of the autocorrelation function with distance can be studied using a correlogram. An experimental autocorrelation coefficient $r(k)$ is calculated for all pairs of measurements k lags apart and plotted on the ordinate with the lag as the abscissa. In general, the coefficients decrease from 1 to 0 and even attain negative values as lag increases. Examples of correlograms of geologic variables may be found in Agterberg (1970; 1974, Chapter 10) and Krige et al. (1969).

Permissible models of autocorrelation functions in two dimensions have been discussed by Matern (1960), Krige et al. (1969) and Agterberg (1970). Agterberg concluded that the form

$$r(h) = C \exp(-ah) \quad (3.4)$$

could be fitted to experimental correlograms as a model of the autocorrelation function. If the coefficient C is less than one, the phenomenon is discontinuous near the origin. The coefficient a is a constant which scales the decrease in correlation to the distance h .

Matern (1960) reviewed previous work on spatial variation and studied the efficiency of unrestricted random sampling, stratified random sampling, Latin square designs and systematic sampling of stationary and isotropic processes with a decreasing correlation function. He applied his results to optimum sampling of forest tracts.

Agterberg and Chung (1973) computed a two-dimensional anisotropic autocorrelation function for the sulfur content in the Harbour seam, Sydney coalfield. They used the experimental autocorrelation coefficients to predict the sulfur content using the best linear unbiased estimator (BLUE). The BLUE of a statistical parameter is a linear combination of all the known values, $Z(i)$; it is unbiased; it has the minimum variance of all possible linear, unbiased estimators.

In the case of a stationary random function, the BLUE of an unknown point $Z(o)$ may be characterized by

$$Z(o) = \sum a(i)Z(i) \quad i = 1, N \quad (3.5)$$

where $\sum a(j)C(ij) - \mu = C(oi)$

$$\sum a(i) = 1 \quad (3.6)$$

the $a(i)$ are the weights of the $Z(i)$ used to form the weighted average $Z(o)$. $C(ij)$ is the covariance between sample i and sample j . $C(oi)$ is the covariance between the point to be predicted and sample i . The Lagrangian multiplier, μ is used to obtain a minimum. The second condition, that the sum of the weights is unity, assures unbiasedness.

If the mean of a variable is non-stationary or only weakly stationary, the correlogram has several operational drawbacks as a measure of spatial variation. The variance of a non-stationary process increases with the size of the field sampled and if the variance is not finite, the

covariance and the autocorrelation function are undefined.

3.2 Intrinsic Random Functions

A weaker hypothesis to replace the assumption of stationarity is the intrinsic hypothesis (Matheron, 1971, p. 53). He defines an intrinsic random function as having increments which are wide sense stationary. That is,

$$E[Z(x+h)-Z(x)] = m(h) \quad (3.7)$$

and

$$E[(Z(x+h)-Z(x))^2] = 2\gamma(h) \quad (3.8)$$

where E denotes the expectation. The function $\gamma(h)$ on the right hand side of 3.8 is called the semivariogram or more commonly the variogram. The expression $m(h)$ is the expected difference between observations a distance h apart and is called the drift.

This formulation appears to be more convenient in that it can accomodate a linear trend in $Z(x)$ and $\gamma(h)$ is defined even if no a priori variance exists for the variable. If the variogram remains bounded with distance (finite variance) the relationship

$$\gamma(h) = C(0) - C(h) \quad (3.9)$$

exists between the variogram and covariance. The phenomenon is wide-sense stationary if the drift is constant and the variance is finite. The variogram (serial variation function of Jowett (1955)) is a basic tool in Matheron's Theory of Regionalized Variables. It is used to characterize the

spatial variation of regionalized variables which he defines as very irregular functions of location composed of a random aspect and a structured aspect. Continuous phenomena measured in one or more spatial dimensions are regionalized variables.

Using the relationship between the variogram and covariance (3.9), the BLUE of a stationary random function (3.6) may be rewritten as

$$Z(o) = \sum a(i)Z(i) \quad (3.10)$$

$$\sum a(j)\gamma(ij) + \mu = \gamma(oi) \quad i=1, N \quad (3.11)$$

$$\sum a(i) = 1$$

where $\gamma(ij)$ is the value of the variogram between the pair of samples i and j and $\gamma(oi)$ is similarly the value of the variogram for the point to be estimated o and the sample point i . This method was termed kriging by Matheron in honour of D.G. Krige who used a similar form of regression of the actual grade of ore blocks on the grade predicted from samples. Although Matheron's theory is very rich in applications, the following discussion will be confined to two topics: structural analysis and kriging.

3.3 Structural Analysis

The structural properties of a variable may be studied using experimental variograms. The theoretical variogram (3.8) can never be obtained but the variogram of samples taken over a finite area may be computed using the formula

$$\gamma(h) = 1/2N [Z(x(i)) - Z(x(i+h))]^2 \quad (3.12)$$

N is the number of pairs of samples separated by the vector h with a direction θ where

$$\tan \theta = y/x \quad (3.13)$$

and

$$h^2 = x^2 + y^2 \quad (3.14)$$

If sample points are regularly distributed along a line of length L then the experimental variogram can be estimated for h up to $L/2$ but is most reliable near the origin. When sample points are irregularly spaced in the plane, pairs of points are classed into distance intervals, $h \pm dh$. The class width, $2dh$ is selected so that most classes have 30 pairs of observations or more to ensure a stable variogram estimate. For each distance class, the drift

$$m(h) = 1/N \sum [Z(x(i)) - Z(x(i)+h)], \quad (3.15)$$

the variogram, and the average distance between pairs are calculated. If the variogram is estimated without regard for the direction of the vector h , it is called the average or isotropic variogram.

Anisotropy in the spatial structure of a variable can be detected if variograms are computed in several directions. Since sample points are rarely available on lines in the direction of interest, a pair is included if the vector is within an angular tolerance of the desired direction. An angular tolerance of $\pm 30^\circ$ is acceptable since only general trends are of interest in the structural

analysis. Figure 20 illustrates how pairs of points are included in experimental variograms.

The purpose of structural analysis is to fit a geologically reasonable model of the variogram function to the observed experimental variograms(s). The model fitted is used for the purpose of estimation and although many functions might fit the experimental points, Matheron (1971) suggests a restricted range derived from theoretical processes. Two classes of models are used in practice: variograms which are bounded and variograms which continue to increase with distance (Figure 21).

Bounded variograms rise to a sill and remain constant with increasing distance. They are characteristic of phenomena which have a finite variance (the sill), are wide-sense stationary and obey the relation (3.9). The distance at which the model rises to the sill is the range or zone of influence of the process. Points separated by a distance greater than the range are statistically independent. If the range measured in one direction differs markedly from that observed in another direction, anisotropy in the variable is indicated.

One of the most common bounded models is the spherical scheme defined as:

$$\gamma(h) = C \left[\frac{3}{2} \frac{h}{a} - \frac{1}{2} \frac{h^3}{a^3} \right] \quad h < a \quad (3.16)$$

$$\gamma(h) = C \quad h > a$$

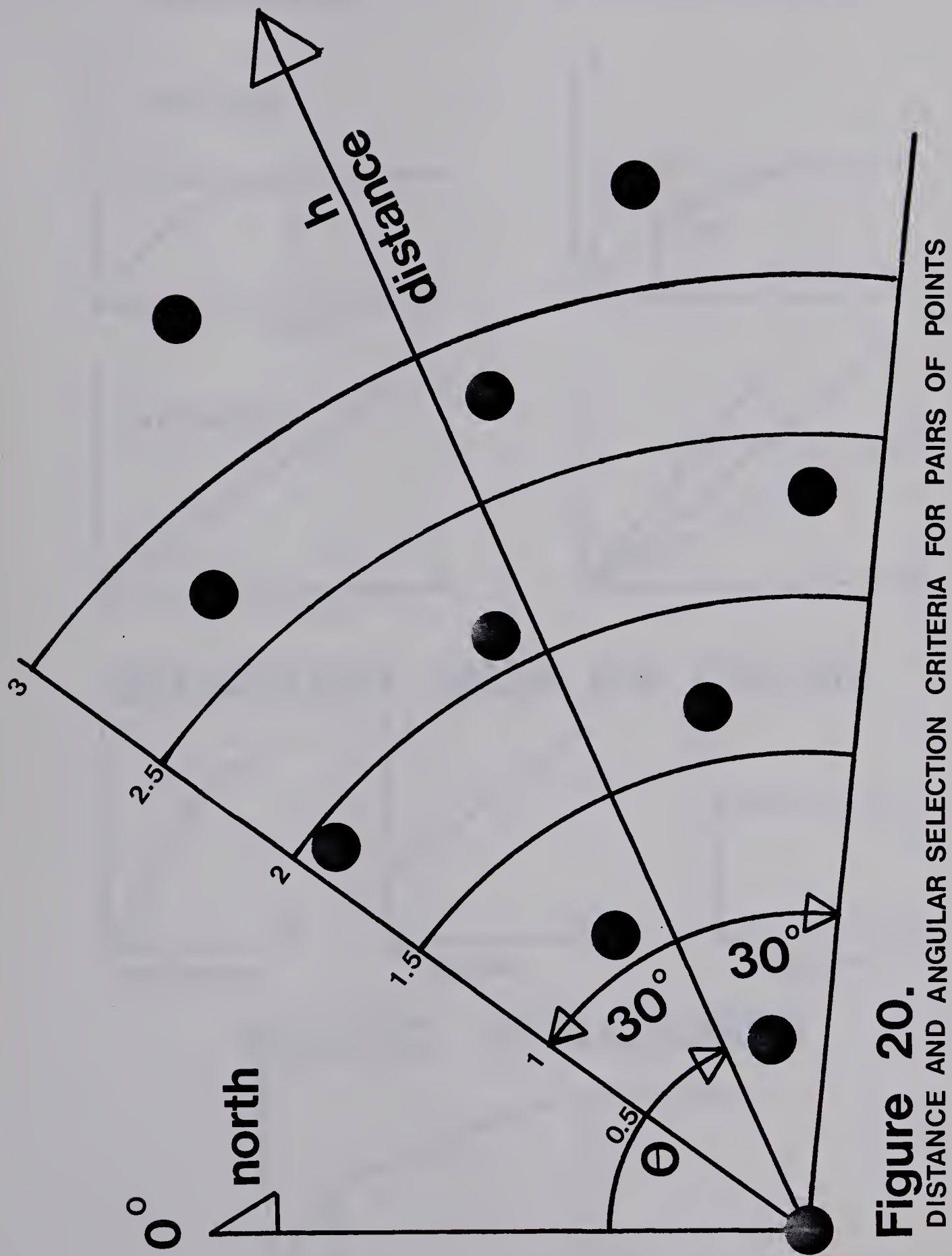
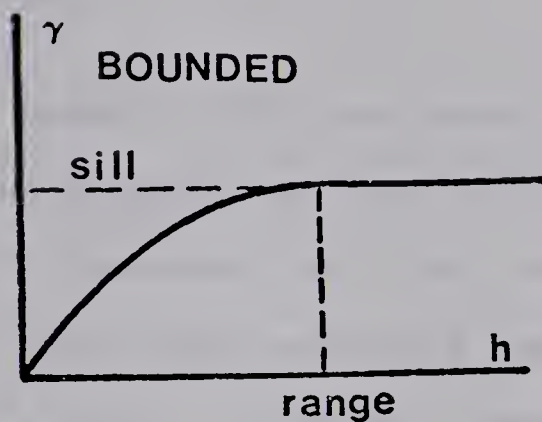
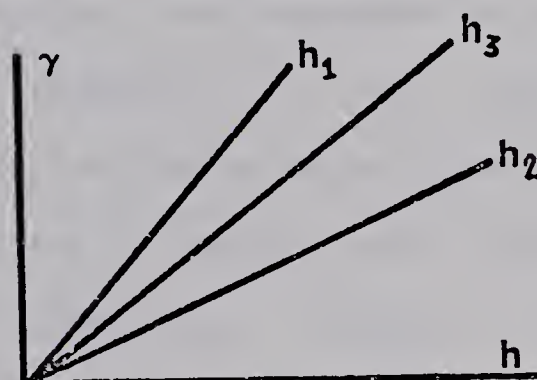
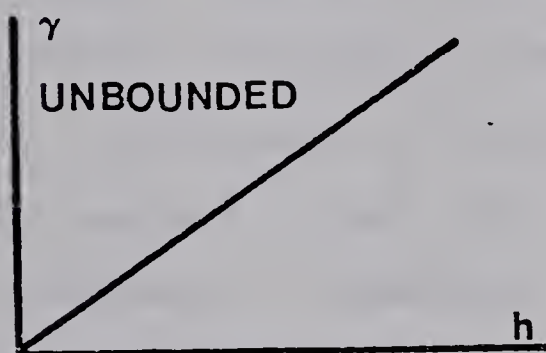
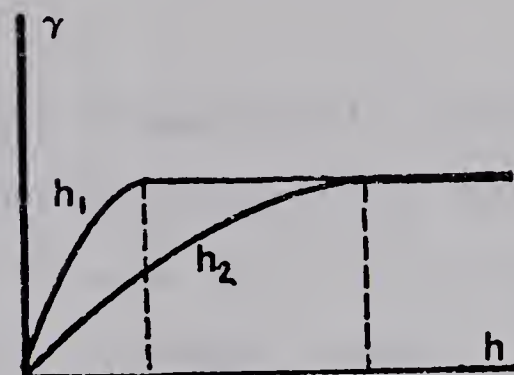


Figure 20.
DISTANCE AND ANGULAR SELECTION CRITERIA FOR PAIRS OF POINTS

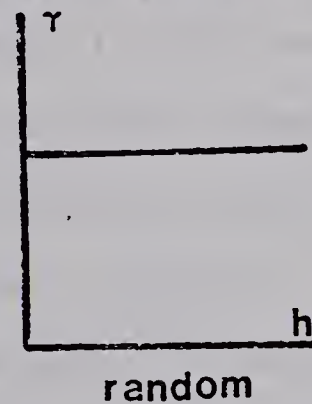
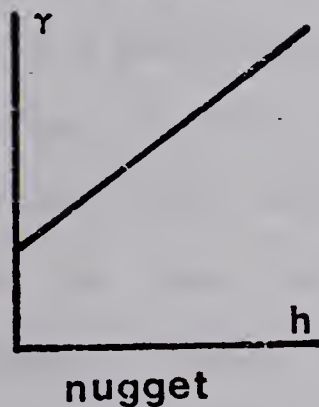
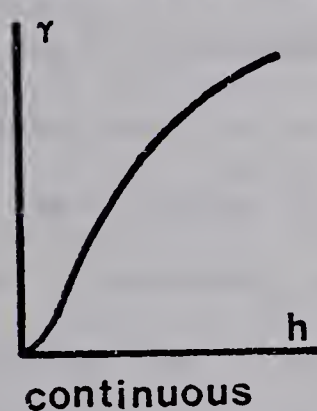
MODELS



ANISOTROPY



BEHAVIOUR NEAR the ORIGIN



NESTED STRUCTURES

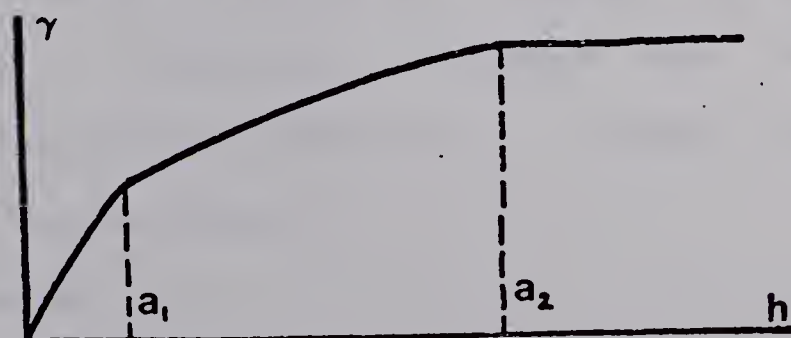


Figure 21. Characteristics of Variograms

where a is the range of the variogram and C is the variance or sill.

Serra (1968) has shown that such transitional processes can be observed at the scale of microns, centimetres, metres and kilometres in the grade of iron in the Lorraine Iron Formation. The nature of processes with ranges shorter than the closest sampling interval cannot be measured on an experimental variogram but can be inferred in the model fitted to the data. An experimental variogram which clearly shows a break in slope may be modelled as two or more nested or intermeshed structures of different ranges and intensities (Figure 21).

Variograms which are not bounded characterize non-stationary phenomena with a non-constant drift (3.15) and a variance that is a function of the size of the area sampled. Such variograms are often linear and may indicate anisotropy by a different slope in each direction. Because the variogram is not bounded, there is no range or zone of influence of sample points. Transition phenomena with ranges shorter than the sampling interval appear in experimental variograms as a non-zero intercept even though such processes are spatially continuous. A linear variogram is modelled using the equation

$$\gamma(h) = bh \quad (3.17)$$

where b is the slope and h is the distance.

The behaviour of the variogram near the origin is at the same time important and difficult to determine. The interpretation has a critical effect on the weighting given to samples in linear prediction and on the value of the estimation variance. The detailed information required is available only where continuous exposures of the geological phenomena are available. The dense drilling required to collect such information for buried coal deposits is often not justified. Modelling the nature of the variogram between the origin and the first few experimental points is necessarily an art of some skill and subjectivity.

Figure 21 indicates the shape of four types of variograms near the origin. The continuous type is representative of bed thickness and surface elevations measured without error. Errors in measurement or slight discontinuities in the phenomena introduce what is referred to as a nugget effect. The random type of variogram corresponds to the spatial structure of the height of adult males randomly arranged in a field or the thickness of a coal seam under the assumptions made by Koch and Gomez (1965) and discussed earlier.

The nugget effect is so called because of the effect that very concentrated nuggets, small relative to the volume of a sample, have on the experimental variogram of gold values. Analogous problems occur in coal quality observations which are dependent upon the physical volume of

the sample. Sabourin (1975) has noted a nugget effect in the sulfur content of coal zones in Cape Breton.

Since borehole observations are point observations of continuous surfaces, the experimental variograms were interpreted in this study as continuous near the origin with the possibility of a nugget effect from errors in observation. If a nugget effect is present, the models previously described (3.16 and 3.17) become

$$\gamma(h) = C_0 + C_1 \left[\frac{3}{2} \frac{h}{a} - \frac{1}{2} \frac{h^3}{a^3} \right] \quad h < a \quad (3.18)$$

$$\gamma(h) = C_0 + C_1 \quad h > a$$

and

$$\gamma(h) = C_0 + bh \quad (3.19)$$

where C_0 is the value of the nugget effect and $C_0 + C_1$ is the variance for the spherical model (3.18).

The purpose of structural analysis in this application is to identify variogram models which can be used for solving estimation problems. Although structural analysis is a powerful tool for data analysis, caution must be exercised in the geological interpretation of experimental variograms. Dutta and Rao (1977) discussed the problems encountered in the structural analysis of mixed populations. David (1974, pp. 68-142) provides an excellent discussion of practical techniques of variography as well as the inherent pitfalls. Some points on the experimental variogram may be ignored, and it can be used for estimation, if the model fitted is

consistent with most of the data.

3.4 Kriging

Once a model of the variogram function has been chosen by structural analysis, the model can be used to calculate the estimation variance for various estimators. The estimation variance is the variance of the distribution of possible errors made in estimating a true unknown value Z by a sample value or a combination of sample values, Z^* . Hopefully, an estimator will be unbiased such that

$$E[Z - Z^*] = 0$$

and the estimation variance

$$E[(Z - Z^*)^2]$$

will be a minimum.

The estimation variance of extending the value of a point sample to a line and to regular geometrical shapes has been charted for standard variogram models (Matheron, 1971, pp. 87-95). FORTRAN subroutines used to evaluate these auxiliary functions for the spherical scheme (equation 3.16) have been published by Clark (1976). Some commonly used estimators are:

- (1) the value of a central sample extended to the enclosing rectangle.
- (2) the mean of the corner samples extended to the rectangle.
- (3) the arithmetic mean of samples taken on a rectangular

grid.

- (4) the arithmetic mean of samples collected by random stratified sampling with rectangular strata.

The estimation variances of more complex geometrical relationships between the samples and the area estimated can be calculated as combinations of the elementary shapes. Kriging has the property of being the estimator which has the minimum estimation variance of all the possible linear combinations of sample points and is therefore preferable to most of the other estimators available.

Local estimation is the prediction of the unknown value of Z at a point $x(o)$ or the average value Z over a regular polygon which is small in comparison to the area sampled. The kriging system in this case is:

$$Z(o) = \sum a(i)Z(i)$$

$$\sum a(j)\gamma(ij) + \mu = \gamma(oi) \quad i=1, N$$

$$\sum a(i) = 1$$

The quantity $\gamma(ij)$ is the value of the variogram between sample points i and j and is easily evaluated from the variogram model. The $a(i)$ are the weights and μ is the Lagrangian multiplier. When $x(o)$ is a point, $\gamma(oi)$ is the value of the variogram between the sample point $x(i)$ and the point to be predicted $x(o)$. When $x(o)$ is a regular polygon, $\gamma(oi)$ becomes $\bar{\gamma}(oi)$, the mean value of the variogram between points in the polygon and the sample point $x(i)$. $\bar{\gamma}(oi)$ can be evaluated using the auxiliary functions discussed

earlier.

The system of equations is composed of a matrix of sample to sample variogram values

$$S = \begin{bmatrix} \gamma_{11} & \gamma_{12} & \gamma_{13} & \dots & \gamma_{1n} & 1 \\ \gamma_{21} & \gamma_{22} & \gamma_{23} & \dots & \gamma_{2n} & 1 \\ . & . & . & . & . & . \\ \gamma_{n1} & \gamma_{n2} & \gamma_{n3} & \dots & \gamma_{nn} & 1 \\ 1 & 1 & 1 & & 1 & 0 \end{bmatrix}$$

a vector of sample to unknown variogram values

$$U = \begin{bmatrix} \gamma_{01} \\ \gamma_{02} \\ . \\ . \\ . \\ \gamma_{0n} \\ 1 \end{bmatrix}$$

and the vector of weights which are the unknowns

$$A = \begin{bmatrix} a_1 \\ a_2 \\ . \\ . \\ . \\ a_n \end{bmatrix}$$

The system is written as

$$SA = U$$

and solved for A by rewriting as

$$A = S^{-1}U$$

where S^{-1} is the inverse of the matrix S. The vector A is then used to weight the samples vector Z to form an estimate of $Z(o)$. The estimation variance by kriging is

$$\sigma^2 = \sum a(i) \gamma(o_i) - \bar{\gamma}(o) - \mu$$

where $\bar{\gamma}(o)$ is the mean variogram value of all points in the

polygon to be estimated to all other points in the polygon.

If $x(o)$ is a point,

$$\bar{\gamma}(o)=0$$

otherwise

$$\bar{\gamma}(o)=\iint \gamma(x-y)dx dy \quad x,y \in X(o)$$

Auxiliary functions can be used to evaluate $\bar{\gamma}(o)$ for regular shapes.

Global estimation is the prediction of the average value Z of a variable over the areal extent of that variable. The kriging system of equations is identical to that in the local estimation problem. The values of $\bar{\gamma}$ are estimated by the sum

$$\bar{\gamma}(oi)=1/l \sum \gamma(x(i)-x(j))$$

where $x(j)$ is a point on a square grid located at random over the area and l is the number of grid points within the polygon $x(o)$. Since the boundaries of most areas are irregular, the grid spacing must be such that there are greater than 200 grid intersections in an area for a stable estimate of $\bar{\gamma}(oi)$. $\bar{\gamma}(o)$ is estimated by a similar discrete summation method.

3.5 Non-Stationary Phenomena

In contrast to a wide-sense stationary process which has a constant mean function and the weakly stationary process which has a constant mean for a local area, the mean function of some variables clearly depends upon the

location. Structural surfaces of inclined and disturbed strata are examples of variables where

$$m(x) = E[f(x)] \quad \text{is not constant.}$$

Agterberg (1970), Parsley (1971) and Matheron (1971) have suggested models of such non-stationary phenomena.

Agterberg (1970) proposed that each observation of a geologic attribute in space is the sum of three components:

$$\text{DATA} = \text{TREND} + \text{SIGNAL} + \text{NOISE}$$

Variation called "signal" at a large scale might become "trend" at a small scale and similarly "noise" might become "signal" as more detailed sampling became available. The "trend" component is the large scale "regional" variations which may be represented by the fitting of deterministic polynomials to the data. The signal, according to Agterberg (1970, p. 120) is "...weakly stationary... [and] ...characterized by its autocorrelation function". Noise is the purely random and uncorrelated component caused by rapid variation over short distances and measurement errors. His approach to modelling spatial variation, as evidenced by the terminology, is adapted from time-series analysis. The use of deterministic polynomials to represent the trend is the familiar trend surface analysis (Whitten, 1975). The statistical model for the signal is a weakly stationary random function of distance.

Parsley (1971) described the components of variation in mapped geologic data in the following manner:

$$\text{TOTAL} = \text{REGIONAL} + \text{LOCAL} + \text{RESIDUAL}$$

To separate the three components, he employed a low order trend surface to estimate the regional component and then fitted successively higher order polynomials to deviations from the regional trend until serial-correlation coefficients computed for residuals indicated that the residuals were not autocorrelated. The use of a high-order trend surface to model the local variation contrasts with Agterberg's choice of a stochastic or random function.

Matheron's geostatistical model of non-stationary processes has been described by Delfiner (1976, p. 51) as

$$\text{DATA} = \text{DRIFT} + \text{RESIDUAL}$$

The drift is his term for the mean function and the fluctuation or residual is the random component. The drift is similar to the trend component of Agterberg's model and is represented by local deterministic polynomials. The residual is assumed to be a random function with a spatial structure which can be modelled by a variogram function.

In practice, the variogram can be a biased estimator of the covariance function of the residual component because the drift $m(x)$ is not known but must be estimated (Delfiner, 1976). If the drift is evident as in the homoclinical dip of a bed, the experimental variogram of the residuals along the strike is probably a good estimator. If trends are present but are not constant across the area studied, a more comprehensive method for identifying spatial structure is

based on the theory of intrinsic random functions of order k (IRF- k) and their generalized covariances (Matheron, 1973).

Delfiner (1976) provides an introduction to linear prediction using IRF- k theory. An intrinsic random function of order k is a random function whose k th order increments are weakly stationary. The spatial structure of the k th order increments are estimated as isotropic generalized covariances appropriate for the order k . Once an order k and the coefficients of the generalized covariance have been chosen, a modified form of kriging called universal kriging is used for local estimation. Universality conditions are equations of polynomials up to order k representing the drift effect which are added to the basic kriging system. The coefficients of the polynomial terms and the estimation variance can be computed as part of the solution.

Structural analysis of non-stationary phenomena using the variogram tends to be a biased estimator except in rare situations. An automated procedure has been designed for selecting the order k and the parameters of the generalized covariance. The method consists of estimating each sample point by all other sample points assuming orders 0, 1 or 2 and comparing the mean squared error of each order. The order with the lowest mean squared error is the best predictor. Once the order k is selected, the generalized covariance model which most closely approximates the observed estimation variance is chosen. The resulting

estimator is empirically the best estimator for the observations.

If samples are taken from heterogeneous surfaces composed of rough and smooth areas, the resulting estimated generalized covariance is suitable for neither area and may be biased if one of the areas is more heavily sampled. Furthermore, the model selected is only one of many models which fit the data. Another model may be more appealing when other information and conceptual geological models are taken into account.

3.7 Areal Methods

The preceding sections have been concerned with methods of estimating the value of a continuous variable at a location or the average of a continuous variable over an area. This section examines methods of estimating the area underlain by coal.

One method is to estimate the areal proportion of coal underlying the map area by

$$p = n/N$$

where n is the number of boreholes intersecting coal and N is the total number of boreholes. If p is distributed as the binomial distribution, confidence intervals for the estimate can be made. This model is based on the naive assumption that observations are statistically independent - ie. that

an observation located a short distance (say 5 feet) away from a previous observation of coal has the probability p of being coal. Switzer (1976) suggested that the estimator could be improved by systematic sampling on a square grid and that the estimation variance could be calculated from a form of autocorrelation function adapted from Matern (1960). His method requires a systematic sample pattern which is rarely available in practice.

Matheron (1971) has proposed another estimator of area based on systematic sampling. A square cell is centred around each sample point and the area estimate is

$$S = Na$$

where N is the number of cells in which the borehole intersected coal and a is the area of a cell. Since the location of the boundary is not known, the estimator has a relative variance dependent on the length of the boundary relative to the area. This is approximated for the isotropic case by the number of boundary segments between cells containing coal and cells without coal. For the method to be useful, the boundary of the area must be outlined by sampling and the sample spacing must be reasonable for the expected variability of the phenomenon. The formula for estimating the relative variance of the area estimator is

$$\frac{\sigma^2}{S^2} = \frac{1}{N^2} \left[\frac{1}{6} N_2 + 0.061 \frac{(N_1)^2}{N_2} \right] \quad N_1 > N_2 \quad (3.20)$$

This method is once again dependent upon the availability of systematic sampling.

Neither of these methods use the available structural data. In the present study, much of the area underlain by coal is bounded at subcrop so that the prediction of location of the subcrop is a form of area estimation. Grid manipulation methods permit surface comparison to facilitate prediction of the subcrop line. The subcrop line is the zero contour on an isopach of the depth of a seam below the bedrock surface. The isopach can be represented as the difference

Bedrock - Seam

for each grid node. The variance of the possible error made in estimating a surface at a grid node can be produced by universal kriging. The variance of the sum of two independent random variables is the sum of the individual variances

$$\sigma^2 (B+S) = \sigma^2(B) + \sigma^2(S)$$

Since the bedrock surface and the seam structure were formed by different processes and are estimated from different control points using different models they are considered here as independent. Confidence intervals about the isopach value at each grid intersection can be determined if the error of estimation is assumed to be normally distributed with a zero mean and a variance equal to the estimation variance. The location of the subcrop line for each confidence level can be displayed on a contour map. The area can then be planimetered or integrated digitally and a distribution of probability versus area can be computed.

Such a distribution would not be regular in shape since the area estimates may skew quite strongly.

The method of area estimation using subcrop lines is only a partial solution to the total problem since in some cases the areal extent of coal is bounded by a lithologic change to clastic facies. All three coal zones described previously have lithologic boundaries interpreted where they grade into sand bodies or other lithologies. The interpretation of the nature and extent of such boundaries is a subjective judgement made by a geologist based on often limited borehole data. Statistical inference about the location of such boundaries based on objective probability is impossible. The objective probability of an event may only be determined either theoretically from the physical characteristics of a mathematically-defined process or empirically as the result of a large number of trials.

Subjective probability offers a solution to statistical inference when the objective probability approach cannot be used. Subjective probability is the degree of belief or personal opinion of the likelihood that an event will occur. Expert geological opinion can be used to define a cumulative probability distribution of the form $P(X > x)$ for many types of parameters. For the areal extent of a coal seam, there are only three parameters of the distribution which can be reasonably defined: the maximum, the minimum and the mode or most likely value. The triangular distribution (Newendorp,

1975, p. 273) can be used to create a continuous cumulative probability distribution based on these three parameters.

CHAPTER 4

4. Applications to Irregular Sampling Patterns: Estevan Area

The location of coal exploration boreholes commonly does not form a systematic pattern, a fact which precludes the use of statistical techniques based on a regular geometrical configuration of samples. Non-systematic sampling of spatially correlated variables gives rise to the problem of weighting observations to form an unbiased estimate. Kriging and subjective probability appear to offer solutions to the problem of providing quantitative uncertainty limits to coal quantity estimates from irregularly distributed borehole data.

4.1 Location of Coal Subcrop

In section 3.6, a method was proposed which would predict the location of coal subcrop lines and allow confidence limits to be placed on the estimated locations. A procedure for implementing the method is as follows:

- (1) Perform a structural analysis of the borehole data for the bedrock and coal zone elevations. Select models of the experimental variograms and the order k if a drift is indicated.
- (2) Estimate the elevations of the bedrock and the coal zone using kriging at the nodes of a regular grid. Save the estimation variance for each estimate on separate grids.

- (3) Modify the bedrock grid to reflect stream erosion in recent valleys. This is performed with a surface topography grid based on contours digitized from maps.
- (4) Subtract the coal zone surface grid from the modified bedrock grid to form a grid of isopach values. Where grid values are negative, the coal zone is predicted to lie at elevations above the inferred bedrock surface and is assumed to have been removed by erosion. The zero contour interpolated from the isopach grid values on a contour plot is interpreted as the best estimate of the subcrop of the top of the zone.
- (5) Combine the estimation variance for the bedrock surface with the estimation variance for the coal zone surface at each grid node to form an estimation variance for the isopach grid value. The distribution of possible error made in estimating the isopach should be symmetrical about a zero mean value (because the kriging estimator is unbiased) with a variance equal to the estimation variance (because the errors of estimation for the bedrock and the coal zone are assumed to be independent). Although there have been few studies of actual error distributions using kriging, David (1974, p. 17) suggests that the normal distribution is a safe if not conservative assumption.
- (6) Subtract (or add) one or more standard deviations of the estimation error at each grid node to form grids of isopach values, each grid with a constant cumulative

probability that the real isopach thickness at a particular node is greater than the calculated isopach value. The cumulative probability that the true unknown value (X) is greater than or equal to a value (x) is derived from a cumulative normal distribution with a mean equal to the estimated isopach and a variance equal to the estimation variance and is written

$$P(X \geq x)$$

For a distribution with a mean m and a variance s^2 , some values of P are:

$$P(X \geq m-2s) = 0.977$$

$$P(X \geq m-s) = 0.841$$

$$P(X \geq m) = 0.500$$

$$P(X \geq m+s) = 0.159$$

Four grids of isopach values are created according to the above equations and are contoured.

The probability that the real unknown area of coal (X) is greater than the area enclosed by the zero contour line (x) is the same as the probability that the real isopach thickness at a grid location is greater than the estimated grid value.

- (7) Create a cumulative probability distribution for the area enclosed by the subcrop lines. Using four grids with probability values $P(X > x) = .98, .84, .50$ and $.16$, the areas corresponding to the subcrop lines can be plotted against probability to form a distribution.

Structural analysis of the surfaces was based on experimental variograms produced by a program VARIOGRAM and an automated variogram-fitting routine in KRIGPACC, a proprietary software system of Aquitaine Company of Canada Ltd. Five experimental variograms were calculated for each variable: an isotropic variogram and four directional variograms made at 45^0 intervals. The analysis performed by KRIGPACC reports the residual sum of squares for kriging using universality conditions of order 0, 1 and 2. This can be useful to select an order of polynomial if a drift is indicated. For each order, several sets of coefficients for the generalized covariance are suggested, each accompanied by a selection criterion.

Several points must be made about the choice of an order k of drift and a model of the variogram of residuals. First, the order k which minimizes the residual sum of squares is not always the wisest choice. The minimum number of data points required to estimate a point using kriging with a quadratic drift is 12 while only 6 are needed if a linear drift is assumed (Delfiner, 1975, p. 65). If there is only a marginal difference in the residual sum of squares criteria between the first and second order increments, then selecting the linear drift would permit extrapolation beyond the limits of data control.

If a drift is indicated in the analysis and selected, then the sample weights (and hence the estimate) do not

depend only on the form of the variogram but are determined primarily by the universality conditions and hence the geometry of the data points and the point to be estimated. The choice of a model for the variogram of residuals is not critical to making estimates since

"...the fundamental indeterminability will only affect the variances of our optimal estimators and not the estimators themselves" (Matheron, 1971, p. 189).

Care was taken to model the residual variogram as realistically as possible since the variance of the estimator was to be used in constructing confidence limits.

Experimental variograms for the elevation of the bedrock surface are displayed in Figure 22. The average variogram indicates a transition type phenomenon rising from the origin to a peak of approximately 2400 ft² at about 6 km and dropping down to 1600 ft² at about 8 km. The cause of the "bump" in the average variogram is more easily seen in the directional variograms. The variogram oriented at 45° (and those at 0° and 90° to a lesser extent) shows the effect of a systematic drift between 2 km and 8 km. The drift is caused by the pairing of points in the bedrock valley southwest of Estevan with points on the general level of the bedrock plateau. The variogram calculated at 135° parallel to the preglacial valley shows no drift effects and has been taken as the variogram of the residuals. The residual sum of squares calculated by KRIGPACC (Table 2) suggests that a linear drift minimizes the estimation

Table 2

Residual sum of squares (ft²) at data points estimated by
kriging

Order of IRF-k	Bedrock	-----Surface-----	
		Estevan	Boundary
0	5648	1912	2433
1	4930	1944	762
2	10750	1814	522

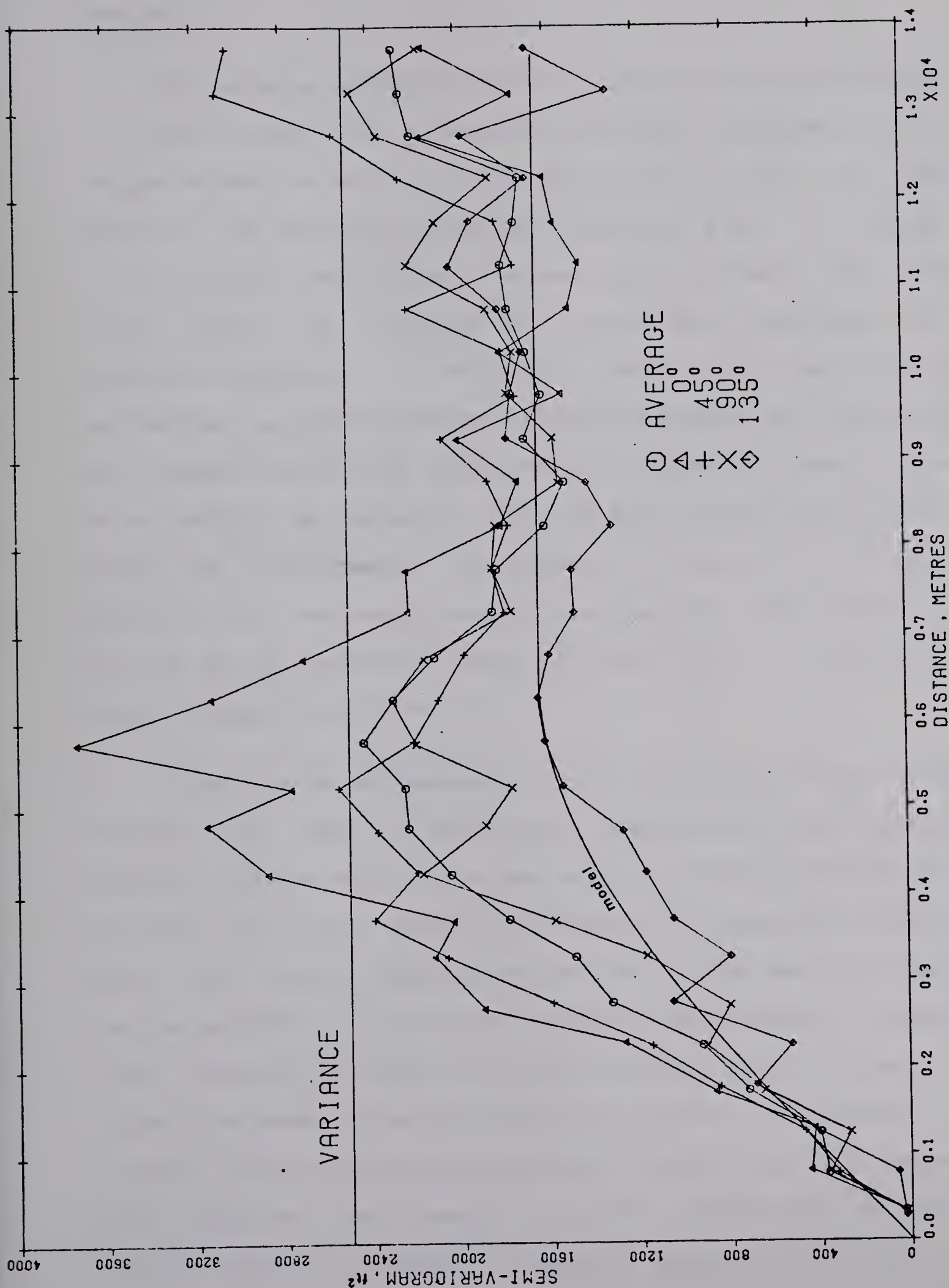
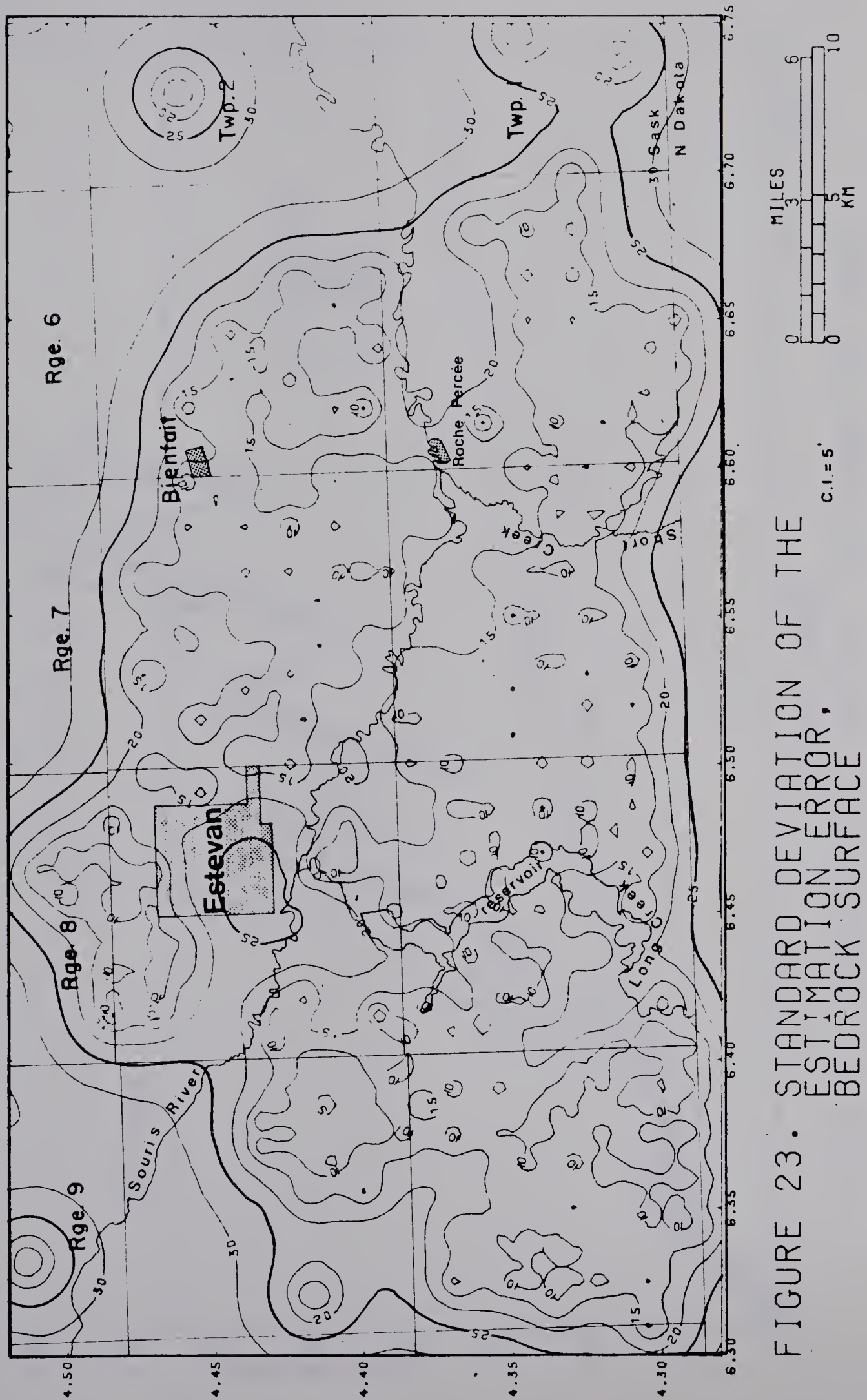


FIGURE 22. BEDROCK SURFACE, VARIOGRAMS AND MODEL.

variance.

The kriging parameters for the bedrock surface include: a linear drift and a spherical residual variogram with no nugget effect, a sill of 1650 ft² and a range of 6500 metres. The variogram model is plotted on Figure 22. Figure 7 is a contour map of the bedrock grid estimated by the above model and modified for the surface topography. The standard deviation of estimation error for the bedrock elevations has been contoured and is displayed in Figure 23. The standard deviation ranges from a theoretical zero at the data points to greater than 30 feet outside the drilled area. The distribution of values is controlled by the geometry of the sample points and the data void located in the valley of the Souris River is marked by a "ridge" of high standard deviation.

Experimental variograms for the top of the Estevan zone (Figure 24) show a transition phenomenon with no nugget effect, a short range structure with a sill of about 400 ft² at 800 metres and a marked anisotropy for distances greater than 2500 metres. The directional variogram computed along the approximate strike of the surface (65°) appears rounded with distance whereas variograms in other directions show a linear increase and drift components beyond a distance of 2.5 km. The residual sum of squares (Table 2) for the sample data indicate that there is little difference between orders. Because a systematic trend is evident in the dip of



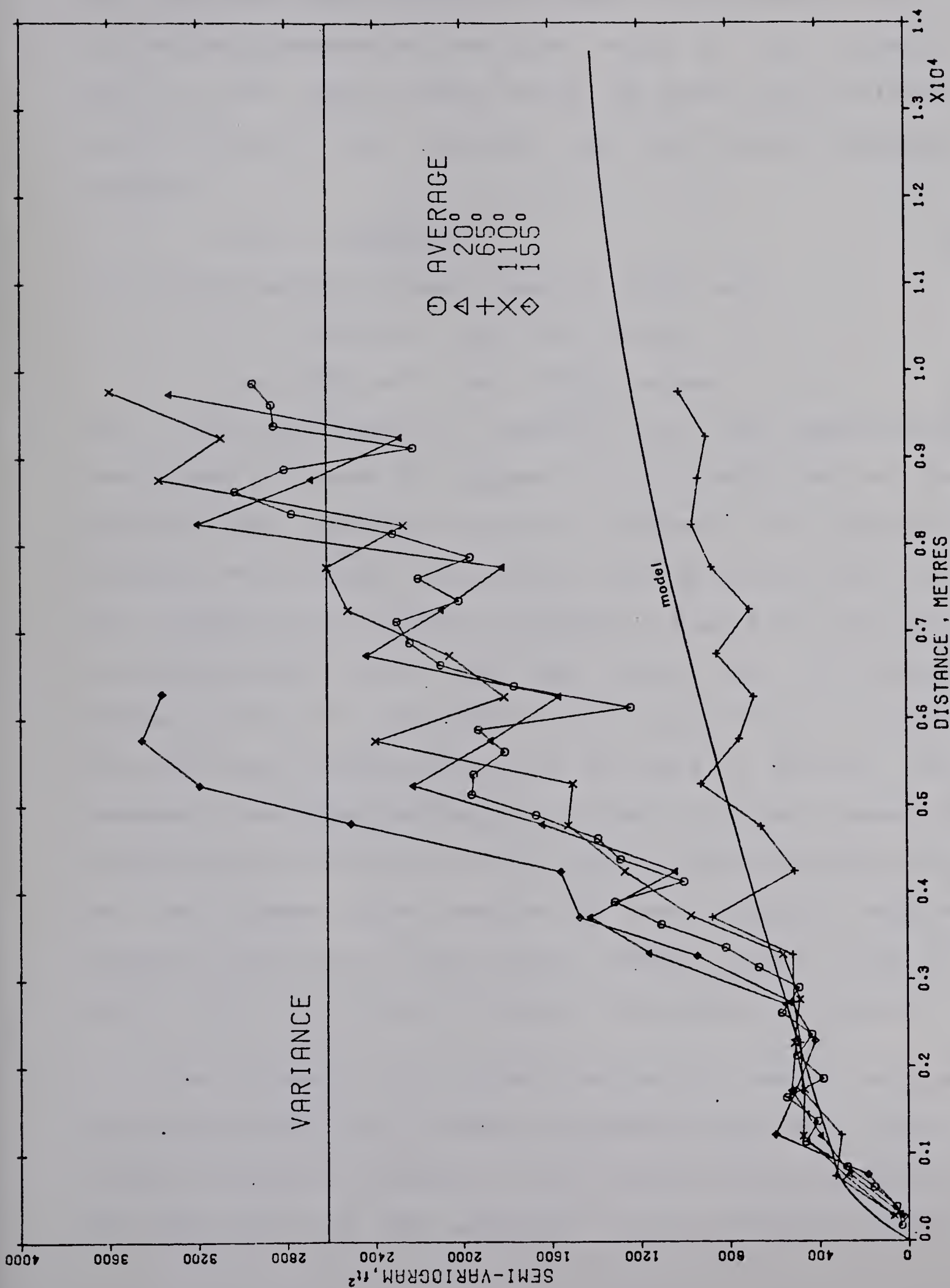


FIGURE 24. ESTEVAN ZONE SURFACE, VARIOGRAMS AND MODEL.

the bed and insufficient data points are available within a 2.5 km neighbourhood of many grid nodes in the southeast part of the map, a linear drift was chosen. The variogram model fitted to the residuals has two nested spherical models:

$$\gamma(h) = \gamma_1(h) + \gamma_2(h)$$

and the parameters of each (equation 3.18) are

$$C_1 = 225 \text{ ft}^2 \quad a_1 = 750 \text{ metres}$$

$$C_2 = 1200 \text{ ft}^2 \quad a_2 = 15000 \text{ metres}$$

The resulting model is plotted with the experimental variograms in Figure 24. Figure 9 is the contour map of the Estevan zone structure grid as estimated by universal kriging. The standard deviation of the estimation error for the Estevan zone structure is shown in Figure 25. The areas of poor control within the coal field have a standard deviation of 20 to 25 feet. In the area drilled at centres one mile apart north of the river and east of Estevan, the standard deviation varies from 15 feet to 20 feet except at locations very close to the data points. The standard error of the Estevan zone surface in the triangular nose of bedrock south-west of the bedrock channel varies from 10 feet to 20 feet, an area drilled at one-half mile centres.

The isopach of the interval between the bedrock surface and the Estevan zone is shown in Figure 26. The zero contour line is the best estimate of the location of the subcrop of the coal zone, and the gradient of the isopach surface

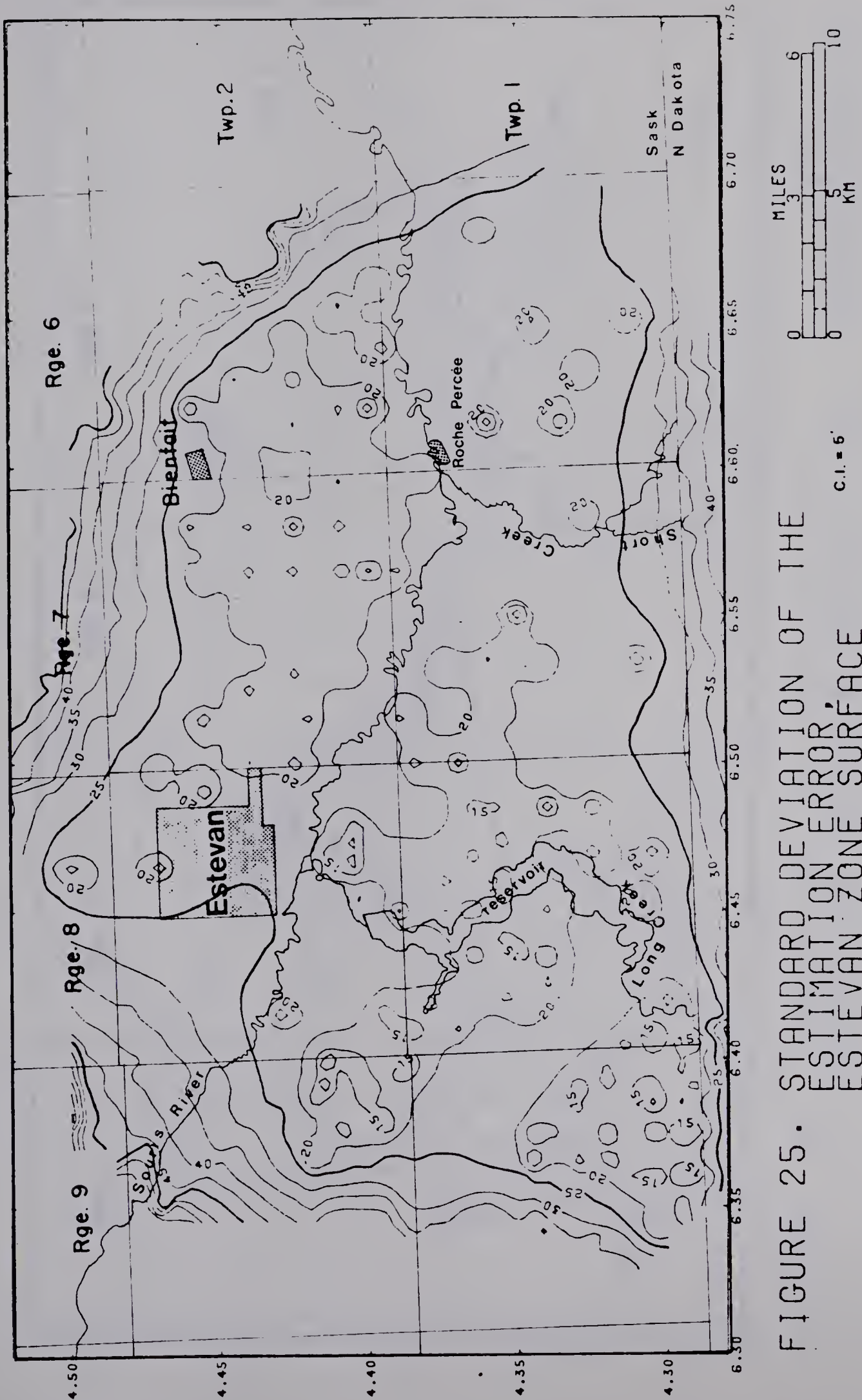


FIGURE 25. STANDARD DEVIATION OF THE ESTIMATION ERROR, ESTEVAN ZONE SURFACE

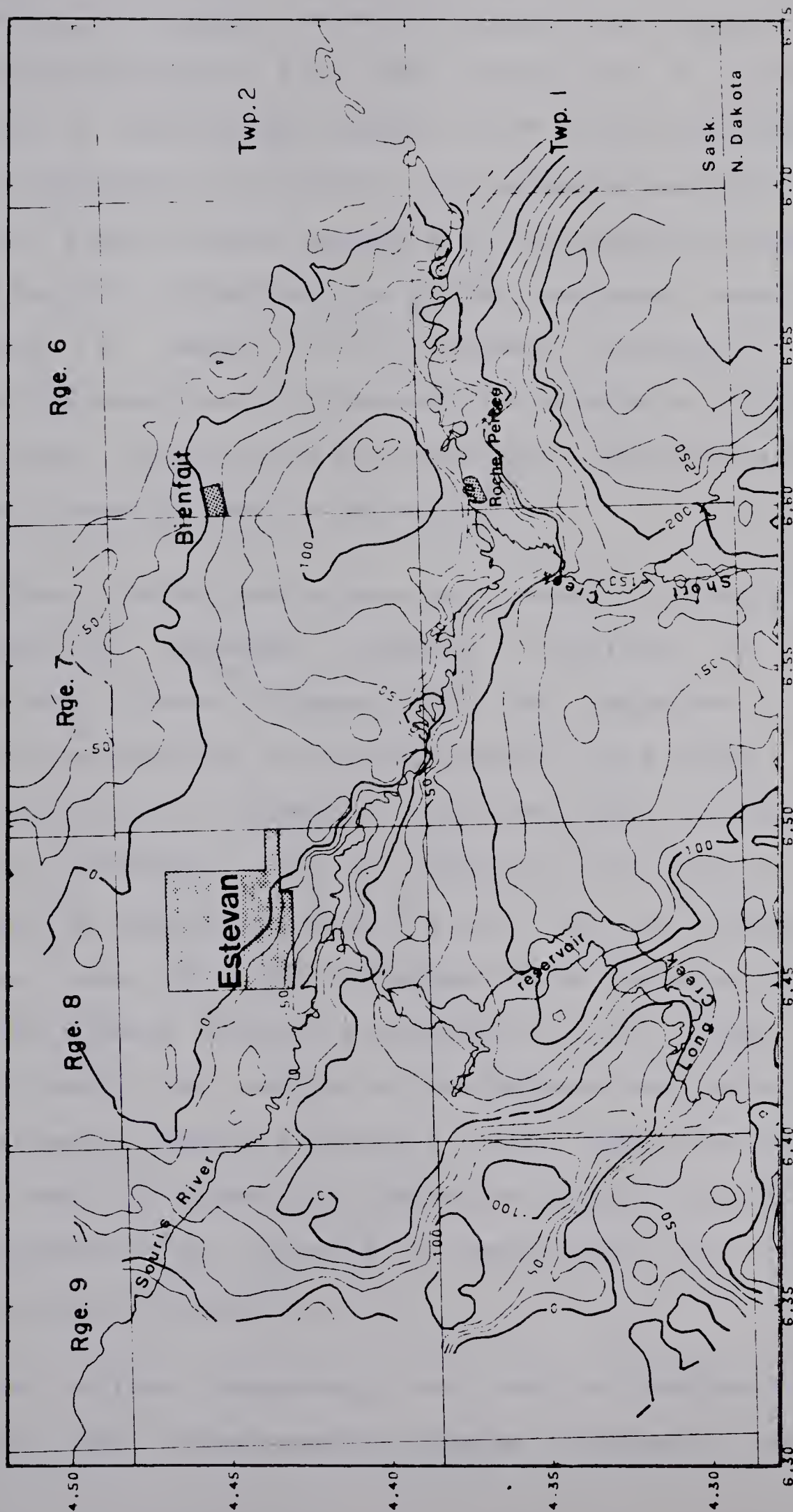


FIGURE 26. ISOPACH OF THE INTERVAL BETWEEN THE BEDROCK SURFACE AND THE ESTEVAN ZONE SURFACE. C.I. = 25'



indicates the angle at which the zone is truncated at the bedrock unconformity. This angle varies from 3° along the margins of the bedrock channel to 1° at the erosional edge to the northeast. In contrast, the estimated surface of the Estevan zone is almost parallel to the bedrock unconformity under the city of Estevan and in the southeast quarter of Township 2, Range 9. The standard deviation of the estimation error for the isopach is displayed in Figure 27. The values range from zero to 30 feet with the most common values between 20 feet to 25 feet.

These standard deviations were used to create lines representing estimated subcrop locations at various probability levels (Figure 28). The estimates diverge markedly in the area to the northwest but are closely spaced and sub-parallel elsewhere. Within the "best" subcrop line to the northwest, over 50 boreholes drilled at close spacings in Township 2, Ranges 8 and 9 did not intersect the Estevan zone. Detailed investigation of the area indicated that the bedrock surface is horizontal with a relief of 10 to 15 feet. The surface of the Estevan zone which can be reconstructed suffers a reversal of dip from the regional trend and is apparently almost horizontal. The structural interpretation is hampered by uncertainty in the data arising from two sources.

In shallow boreholes, the section studied may not include any recognizable marker horizons and the

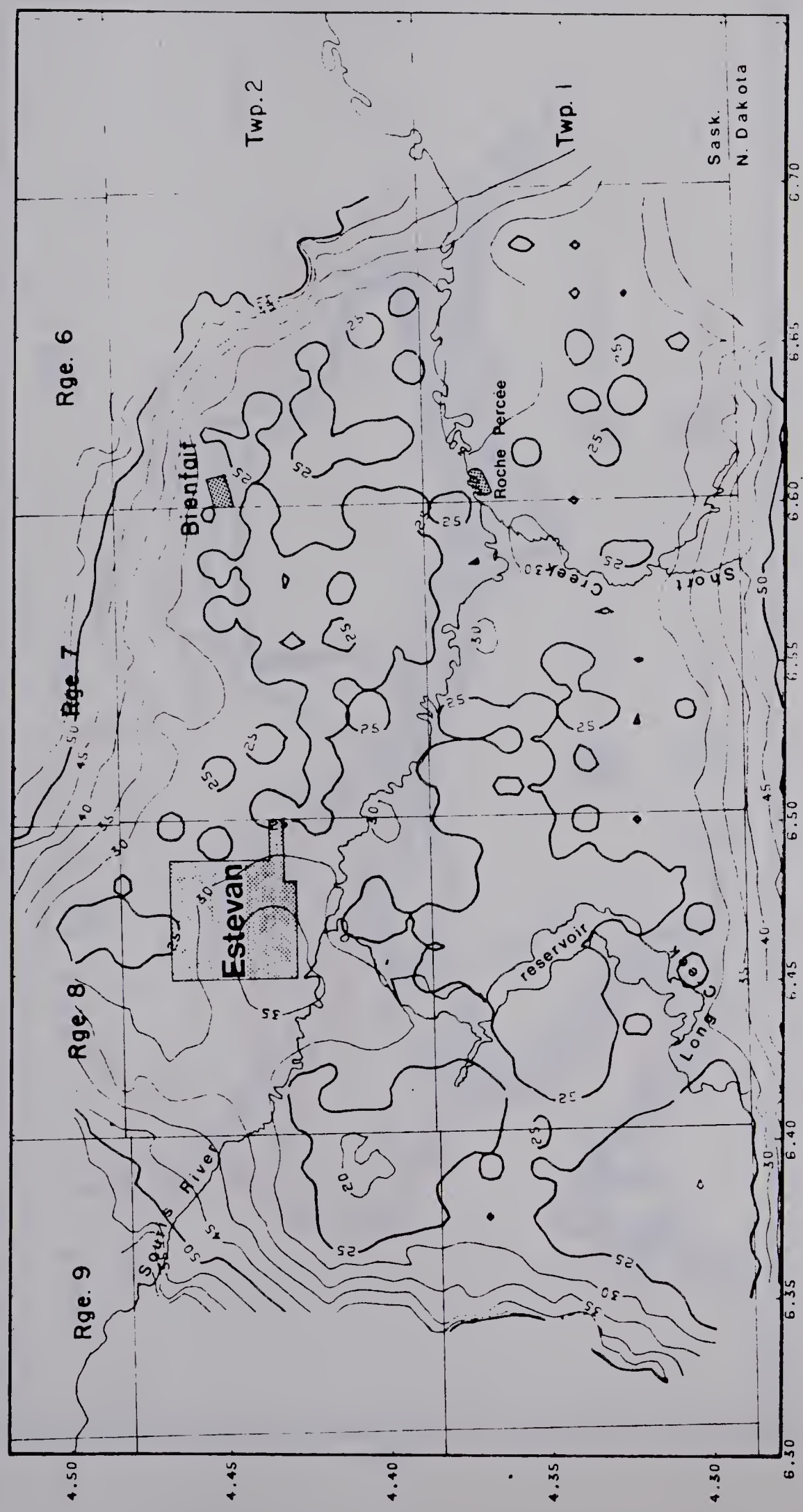


FIGURE 27. STANDARD DEVIATION OF THE ESTIMATION ERROR. ISOPACH BETWEEN THE BEDROCK AND ESTEVAN ZONE SURFACES. CI = 5'

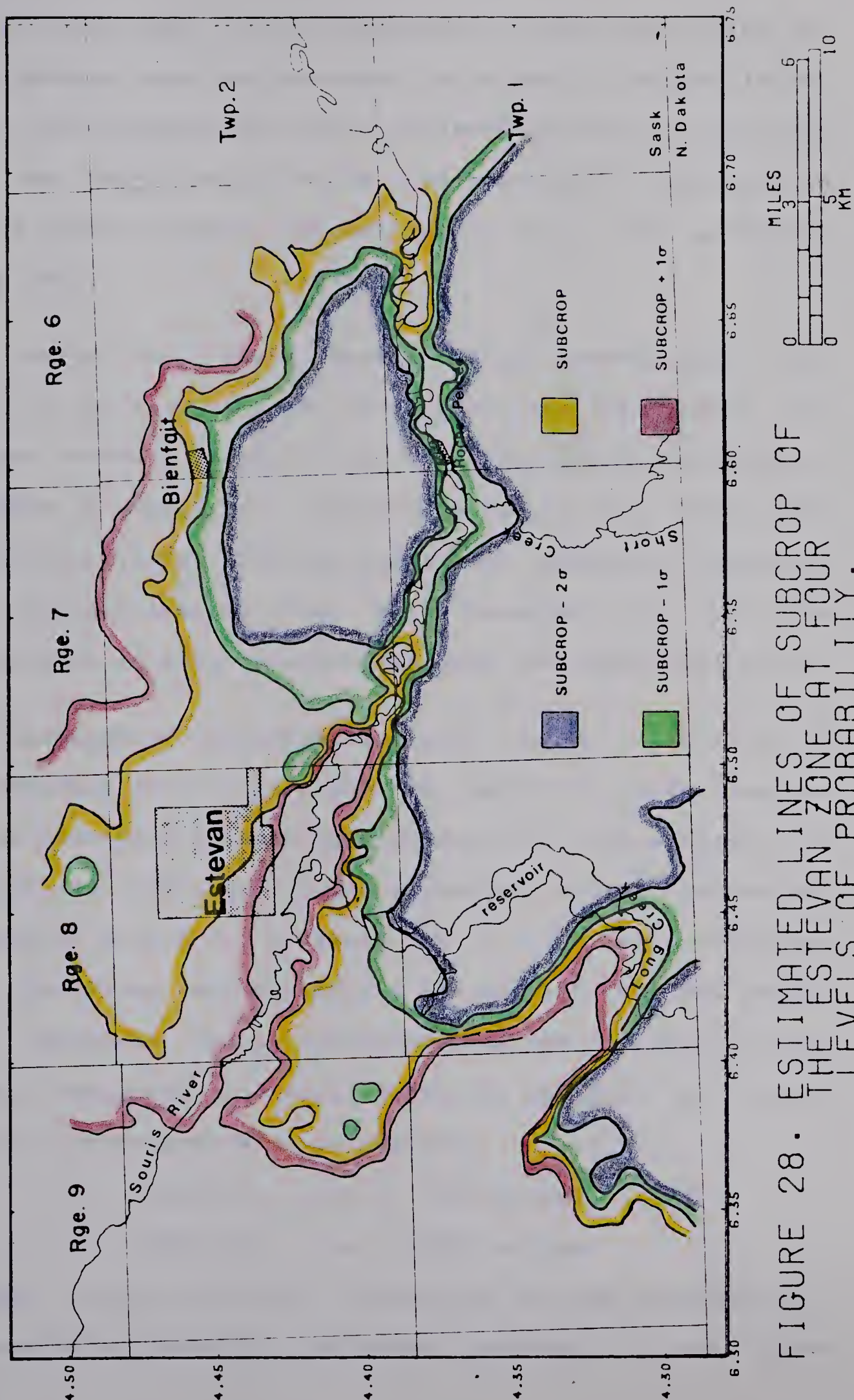


FIGURE 28. ESTIMATED LINES OF SUBCROP OF THE ESTEVAN ZONE AT FOUR LEVELS OF PROBABILITY.

correlations made are very subjective. Additional noise may be introduced into the data when the elevation mapped is not a true stratigraphic top but a synthetic horizon calculated from the elevation of the base of the lowest seam accepted and the gross thickness of coal accepted in the potential mining zone.

Clearly the "best" subcrop line overestimated the extent of the Estevan zone, the cause of this being the apparent reversal of dip in the southeast corner of Township 2, Range 9 which was carried over to the data void underlying Estevan. The mean minus one standard deviation line underestimates the area underlain by coal but approximates it much more closely than the "best" estimate.

Experimental variograms computed for the elevation of the Boundary zone (Figure 29) are similar to those computed for the overlying Estevan zone (Figure 24). The presence of a drift is indicated by the divergence of the directional variograms beyond a distance of 3 km. The variogram calculated along the approximate strike (65°) has the lowest drift component and is interpreted as the variogram of the residual component. The model fitted is composed of nested spherical structures with parameters:

$$C_1 = 300 \text{ ft}^2 \quad a_1 = 500 \text{ metres}$$

$$C_2 = 1200 \text{ ft}^2 \quad a_2 = 15000 \text{ metres}$$

Although a drift of order 2 minimized the sum of squares of the residuals (Table 2), the result produced by the first

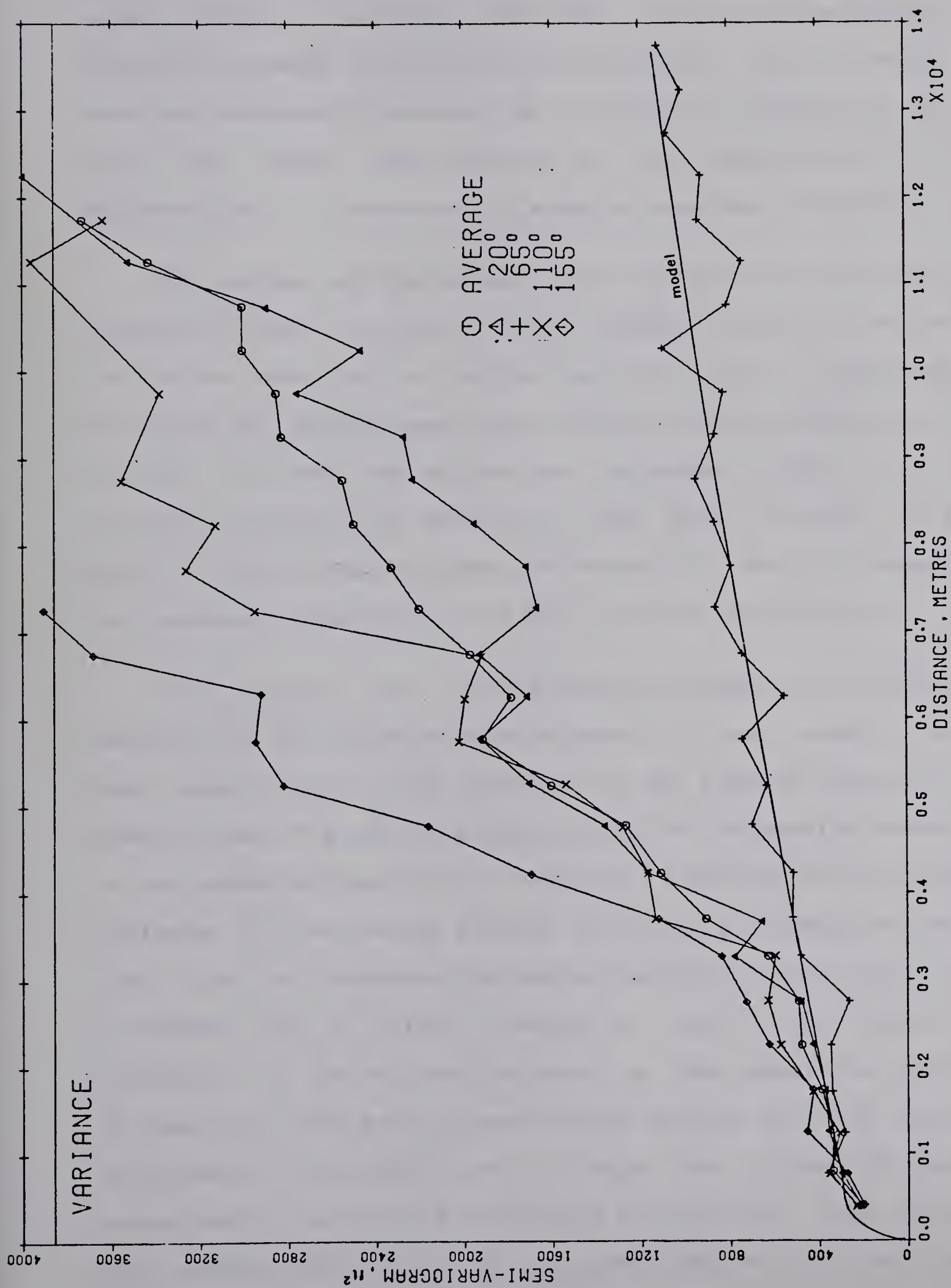
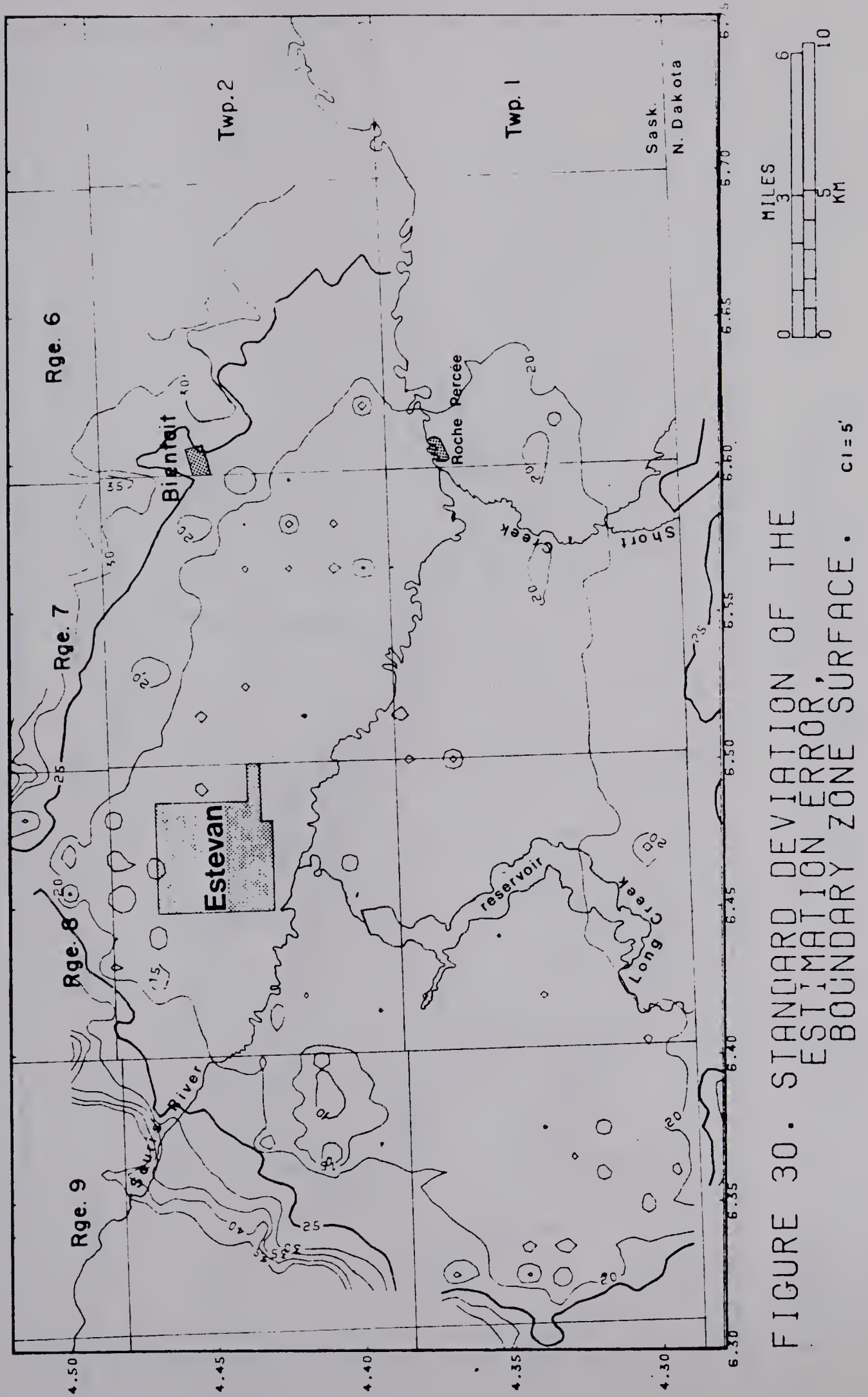


FIGURE 29. BOUNDARY ZONE SURFACE, VARIOGRAMS AND MODEL.

order drift is similar. The first order drift was chosen primarily because it permitted extrapolation over a wider area but secondarily because the structural analysis for the zone may have been biased by the concentration of observations in a structurally complex area near subcrop.

The surface of the Boundary zone estimated by universal kriging is shown in Figure 12. The standard deviation of the estimation error for the surface is contoured and displayed in Figure 30. The average value of the standard deviation is between 15 feet and 20 feet and decreases to zero at data points. The cluster of drilling at 400 metre spacing (1/4 mile) in the southeast corner of Township 2, Range 9 reduces the standard deviation in the area to less than 15 feet.

The isopach grid of the interval between the bedrock surface and the Boundary zone (Figure 31) was created by grid manipulation. The gradient on the isopach surface is greater than 1^0 near the predicted subcrop boundaries except to the north-northwest under the city of Estevan and to the southwest of the bedrock channel in Township 1, Range 9. The zone does not approach the bedrock surface to the east but is bounded by a lateral change to sand. The standard deviation of the estimation error for the isopach is shown in Figure 32. The grid values average between 20 to 25 feet of standard deviation and a large area of over 30 feet occurs under the city of Estevan in a data void. This grid was manipulated with the isopach grid (Figure 31) resulting



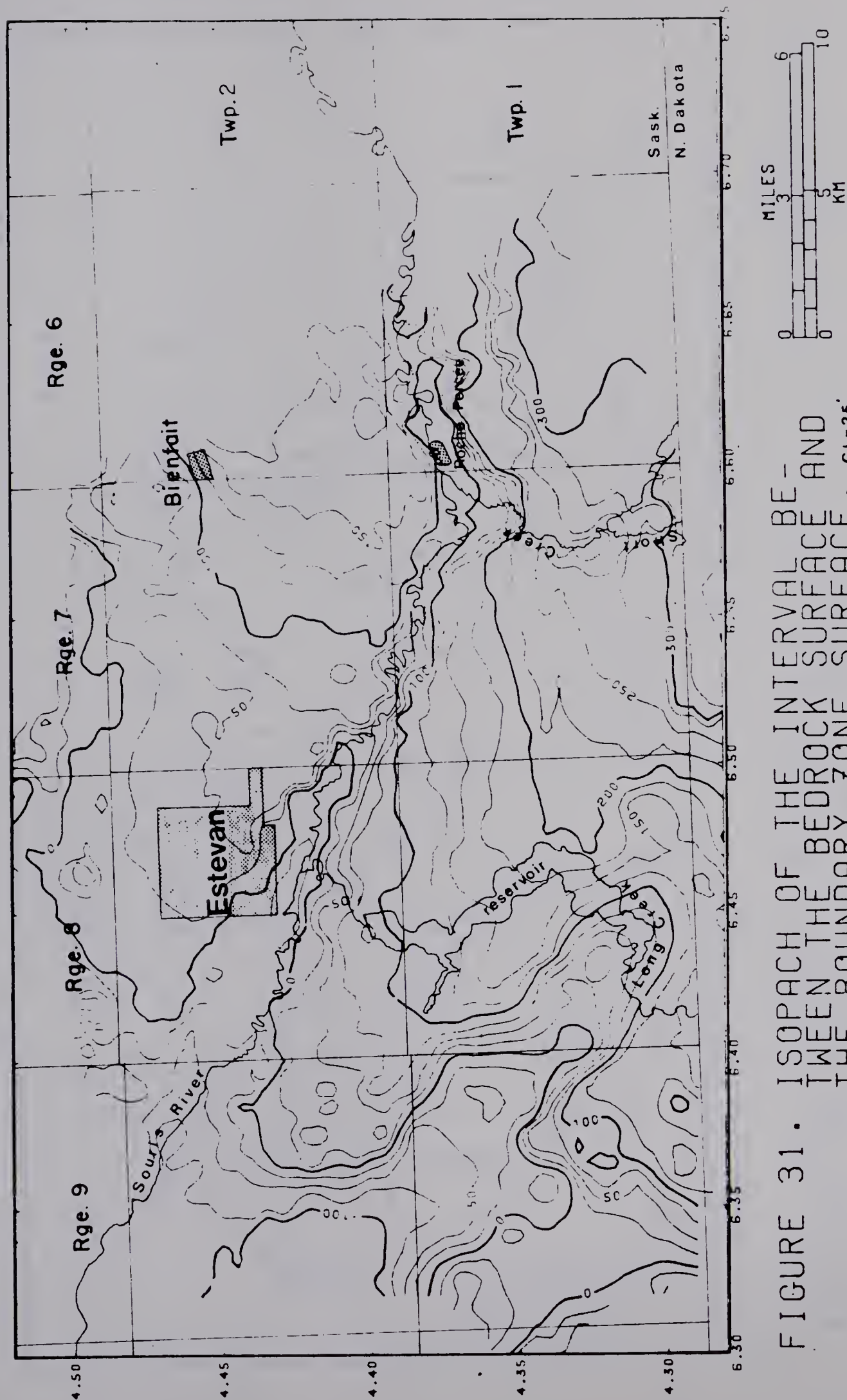
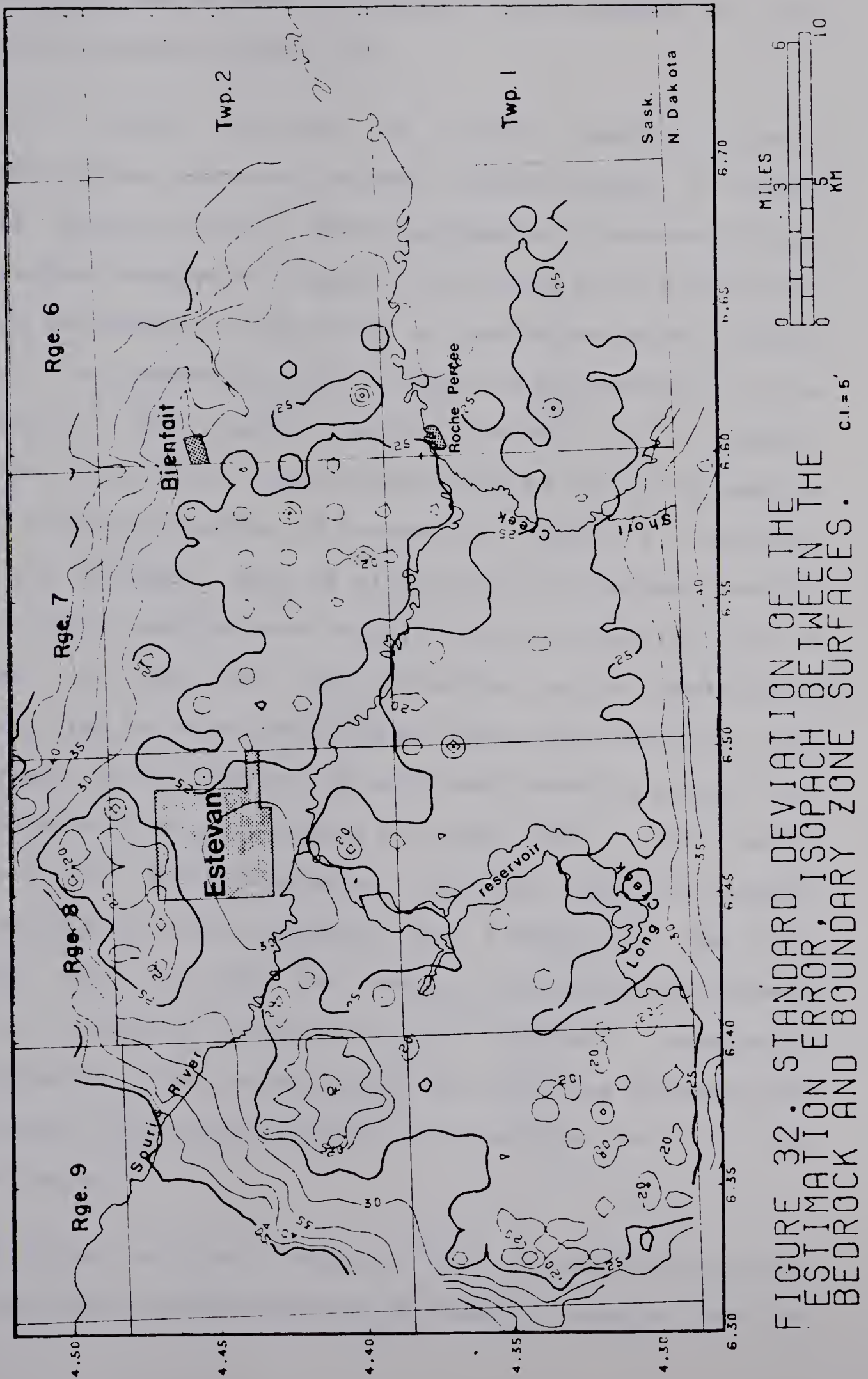


FIGURE 31. ISOPACH OF THE INTERVAL BETWEEN THE BEDROCK SURFACE AND THE BOUNDARY ZONE SURFACE. $CI=25'$



in the predicted location of Boundary zone subcrop at four probability levels (Figure 33).

The "best" estimate of subcrop location closely approximates the observed borehole results except southwest of the bedrock channel. Here, geological interpretation of the bedrock topography suggests that pre-glacial erosion has removed the Boundary zone along a north-northeast-trending valley. The Boundary zone intersected in boreholes to the northwest of this valley exists probably as a remnant isolated by erosion. Detailed drilling at 400 metre spacing in the southeast quarter of Township 2, Range 9 indicates that the Boundary zone is structurally disturbed near the subcrop edge, varying more than 30 feet in elevation over a distance of less than one kilometer. If the zone is not faulted, dips of up to 150 feet per mile are indicated over a distance of 400 metres and northwest-trending swales with an amplitude of 25 feet spaced at about 500 to 800 metre intervals may be interpreted. Although there is evidence that the Tertiary coal measures are faulted in the area (Holter, 1972, p. 176), the problem of correlation between shallow boreholes precluded a faulted structural interpretation. The presence of the overlying Estevan zone in boreholes corresponds roughly to structural lows in the Boundary zone.

Detailed drilling indicates that the structure of the coal zone near the subcrop edge is locally complex due to

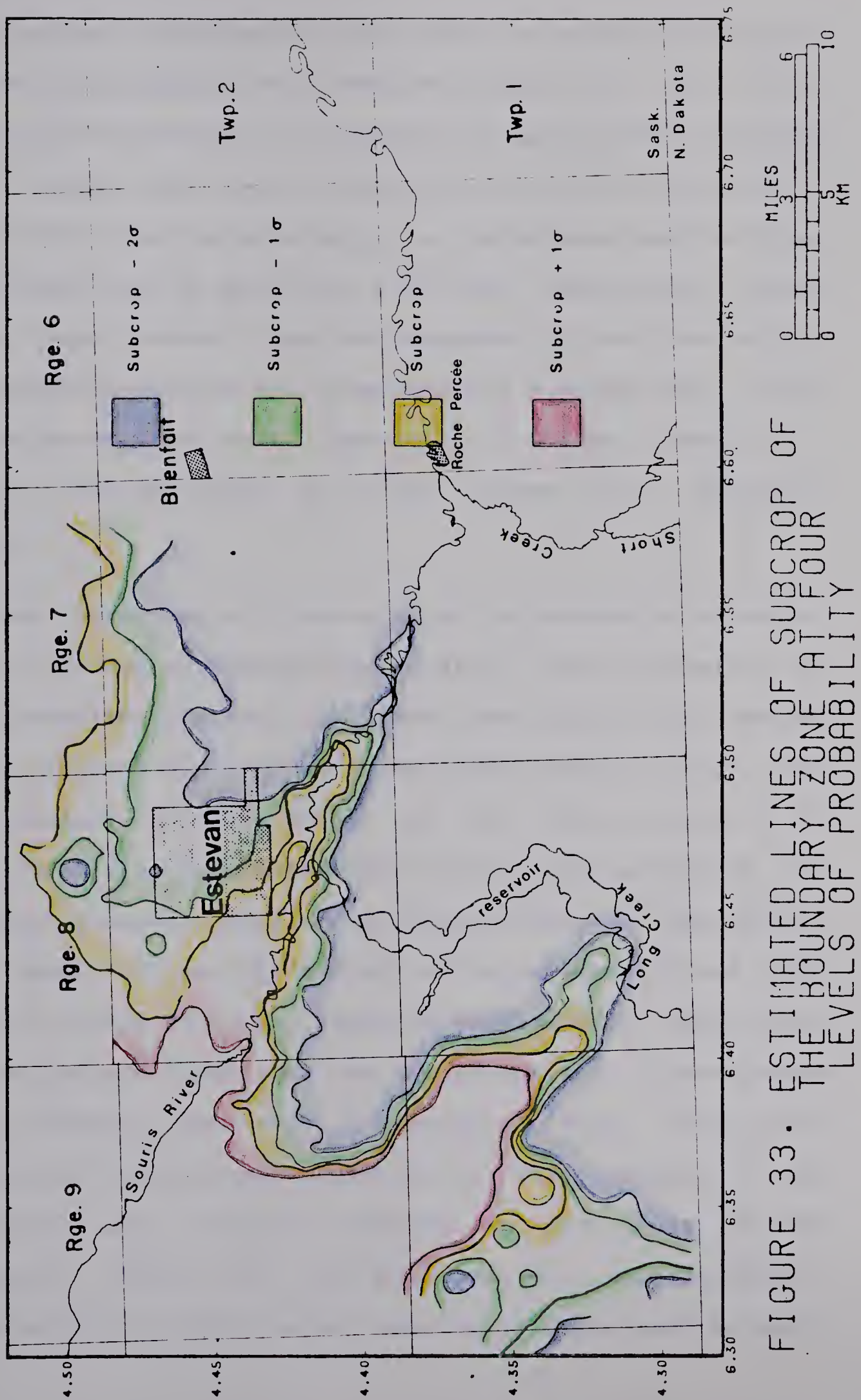


FIGURE 33. ESTIMATED LINES OF SUBCROP OF THE BOUNDARY ZONE AT FOUR LEVELS OF PROBABILITY

glaciotectonic deformation and cannot be sampled adequately at a drill spacing of more than 400 metres nor can it be adequately represented by estimates at grid nodes spaced 500 metres apart. The local structural information required to predict the location of subcrop in the Estevan coalfield can be obtained only by detailed drilling. Observation points spaced more widely than the dimension of local structures will sample more than one structure and a false trend would be inferred the data. Inadequate sampling results in regional extrapolation of false trends into unsampled regions.

The uncertainty of correlation compounded by a complex local structure extrapolated into data voids accounts for the overestimation of the area underlain by the Estevan zone. A similar although much more minor problem occurs for the Boundary zone southwest of the bedrock channel. The local structure is reflected in the variogram models of the residual component for the coal zone surfaces which have a short range (500 and 750 metres) and a relatively high sill (225 ft² to 300 ft²). The grids of the standard deviation of the estimation error show the rapid increase in uncertainty with distance away from a borehole. This uncertainty flattens out beyond about 1000 metres. The coarseness of the estimation grid (500 m) relative to the range of the variogram (500 m to 700 m) results in inadequate representation of the narrow area surrounding each borehole

in which the geology is known with great confidence. Because of the crude grid approximation, boreholes which do intersect the zone lie outside the margins of the higher confidence cumulative probability zones (.84 and .981) in Figures 28 and 33. A finer grid at least one half the range of the local structure (range of the variogram model) is required for adequate representation of the estimation variance. The cost of estimating a large number of grid nodes may be, as in this case, prohibitive.

An alternative approach to the problem of subcrop estimation is conditional simulation (Chiles, 1976, pp. 70-71). A conditional simulation is a simulation of a regionalized variable with the following characteristics:

- it has the same covariance as the phenomenon
- it passes through the data points.

There is an infinite number of such simulations with the same covariance which pass through the data values. If the simulations were averaged, the average value at any point would be the value estimated by kriging while the variance would be the estimation variance. Conditional simulations may be more useful than kriging estimates since the simulation values show the true variability of variable values whereas the kriging estimates are smoothed. The conditional simulations may be considered as possible models of the true (unknown) surface and the one which seems to fit the other information (such as boreholes which did not

intersect a zone) can be selected. If the cost of creating conditional simulations at appropriate scale is not too great, the method could be a viable alternative to the kriging technique.

4.2 Subjective Probability of the Area Underlain by Coal

Most damaging of all criticisms of area estimation by subcrop lines is that lithologic boundaries may account for much of the perimeter of an area. These boundaries are either depositional or erosional in nature. The depositional extent of coal is controlled by the paleoenvironment; a complex combination of factors including climate, topography, hydrology and time. Reconstruction of the lateral facies relationship of a peat-forming environment is difficult from the limited exposures available. McCammon (1975) demonstrated that even the use of sophisticated sampling rules devised with prior knowledge of the facies distribution cannot provide significant improvements over a systematic sample pattern in reconstruction of the lateral facies relationships in the Mississippi delta. A sinuous erosional channel is an example of a facies which is difficult to trace in subsurface.

Because the prediction of lithologic boundaries requires a great deal of interpretation, it is not amenable to a statistical approach based on objective probability. The use of subjective probability and cumulative probability

distributions of variables in resource potential evaluation has been described in EMR (1977) and Newendorp (1975). The variable under study here is the area underlain by coal. Three parameters of its cumulative probability distribution were estimated: the minimum probable area underlain by coal ($P[X > x] = 1$), the maximum probable area ($P[X > x] = 0$) and the most likely area ($P[X = x]$ is maximum). These values were estimated by outlines of the maximum, minimum and most likely extent of the coal zones under the most optimistic, pessimistic and reasonable interpretations of all the available data. These estimates are shown for the Estevan and Boundary zones in Figure 34 and Figure 35 and the values are tabulated in Table 3. These values were interpolated to form a continuous cumulative probability distribution (Figure 36) using the triangular distribution.

Table 3

Area estimates of the coal zones, Estevan coalfield

Cumulative probability	Area, square miles	
	Estevan	Boundary
1.0	132.3	147.8
---	171.8	202.3
0.0	192.3	227.1

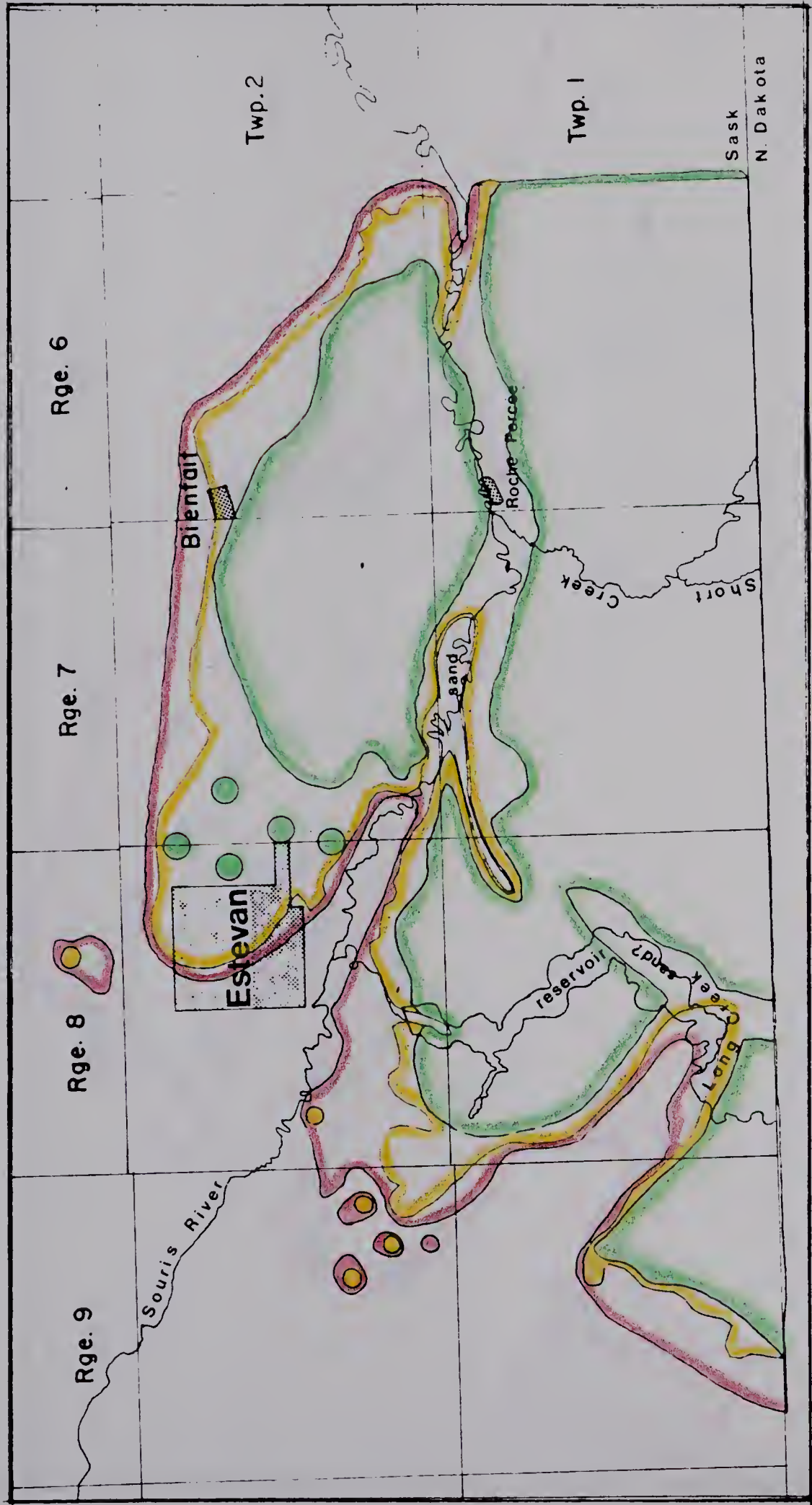


FIGURE 34. MAXIMUM, MINIMUM AND MODAL EXTENT ESTIMATES OF THE AREAL EXTENT OF THE ESTEVAN ZONE.

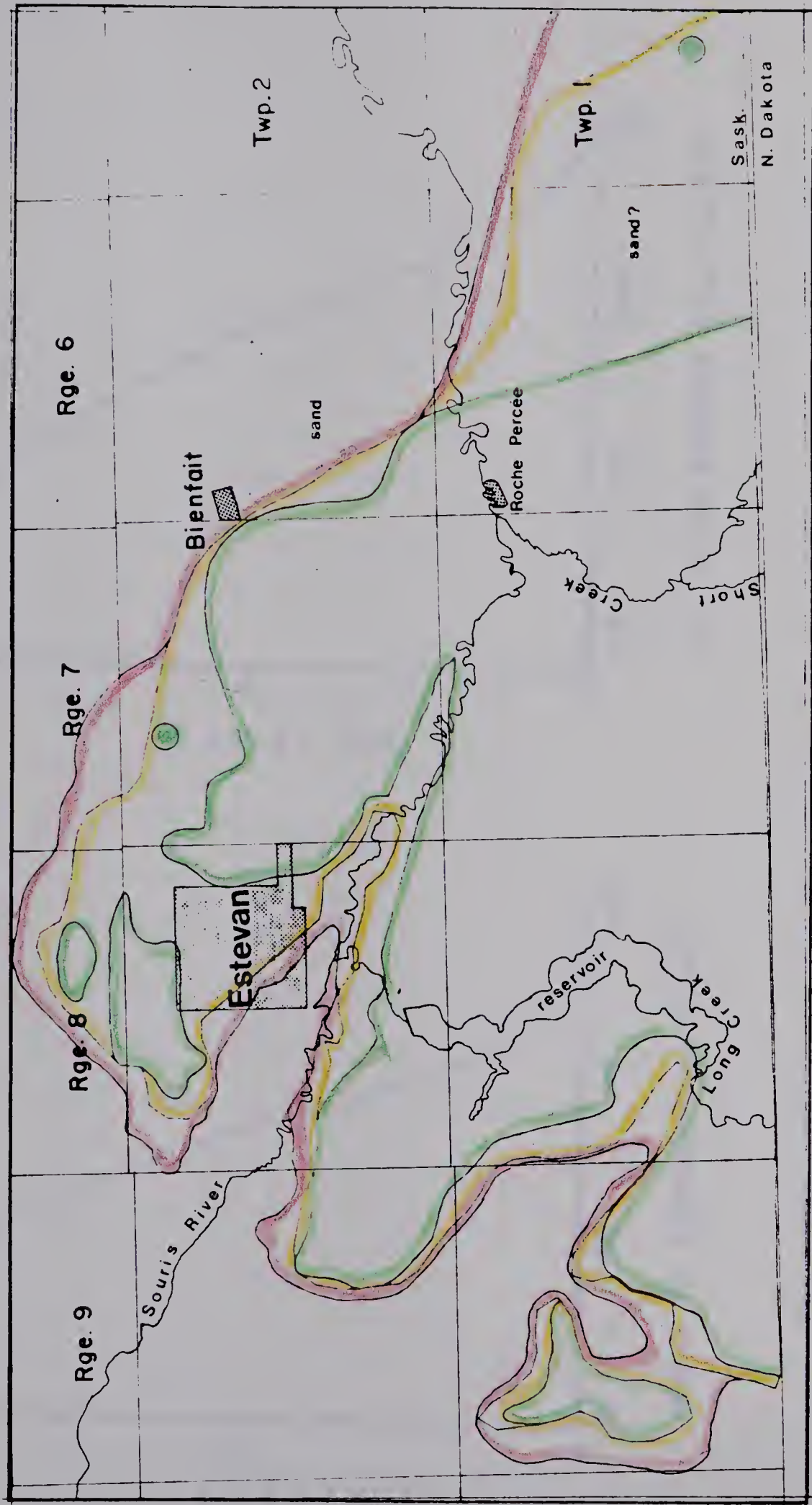


FIGURE 35. MAXIMUM, MINIMUM AND MODAL EXTENT ESTIMATES OF THE AREAL EXTENT OF THE BOUNDARY ZONE.

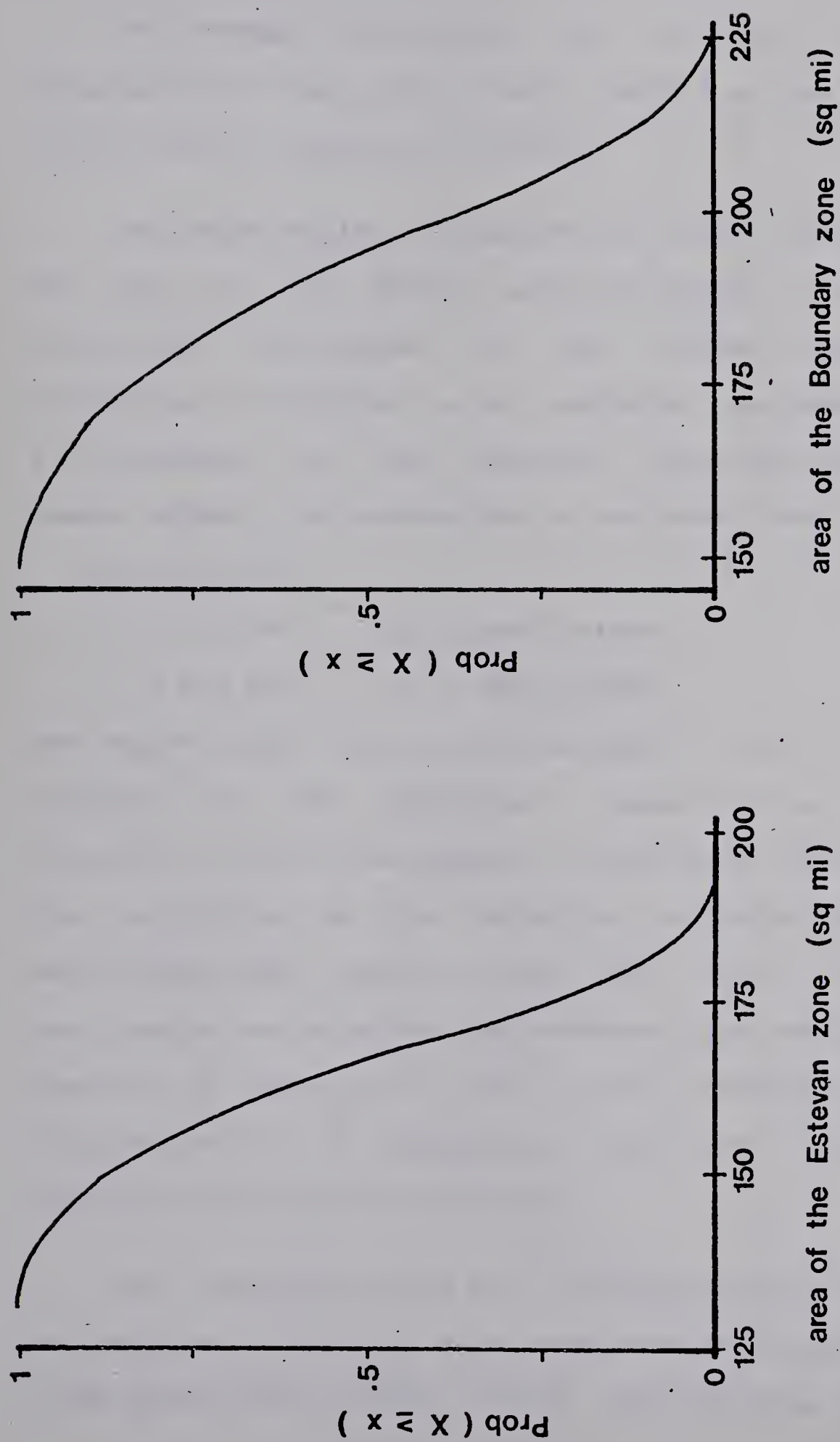


Figure 36 – cumulative probability distributions, areal extent of the coal zones

4.3 Average Thickness of Net Coal in a Zone

The average thickness of net coal was estimated by kriging within the best estimate (modal) of the areal extent of the zones (Figures 34 and 35).

The experimental variograms and sample variance for the net coal in the Estevan zone are shown in Figure 37. The directional variograms do not differ markedly and directional anisotropy is not indicated. The model fitted is a combination of two isotropic spherical schemes with a nugget effect. The parameters of the model are:

$$C_0 = 1.0 \text{ ft}^2$$

$$C_1 = 4.0 \text{ ft}^2 \quad a_1 = 1000 \text{ metres}$$

$$C_2 = 5.5 \text{ ft}^2 \quad a_2 = 4000 \text{ metres}$$

The nugget effect is used to represent a very short range component of the uncertainty caused by the inclusion or rejection of thin overlying or underlying seams into the zone according to the selection criteria. The variogram model rises quite rapidly within the first kilometre and then levels out at about 4 kilometres. The average variogram remains at this sill until drift effects cause a rise slightly beyond 9 kilometres. The drift effect is not important and was not modelled.

The variance of the area and the average covariance of the samples to the area were estimated as discrete sums over a 500 metre grid of 1789 points representing an area of

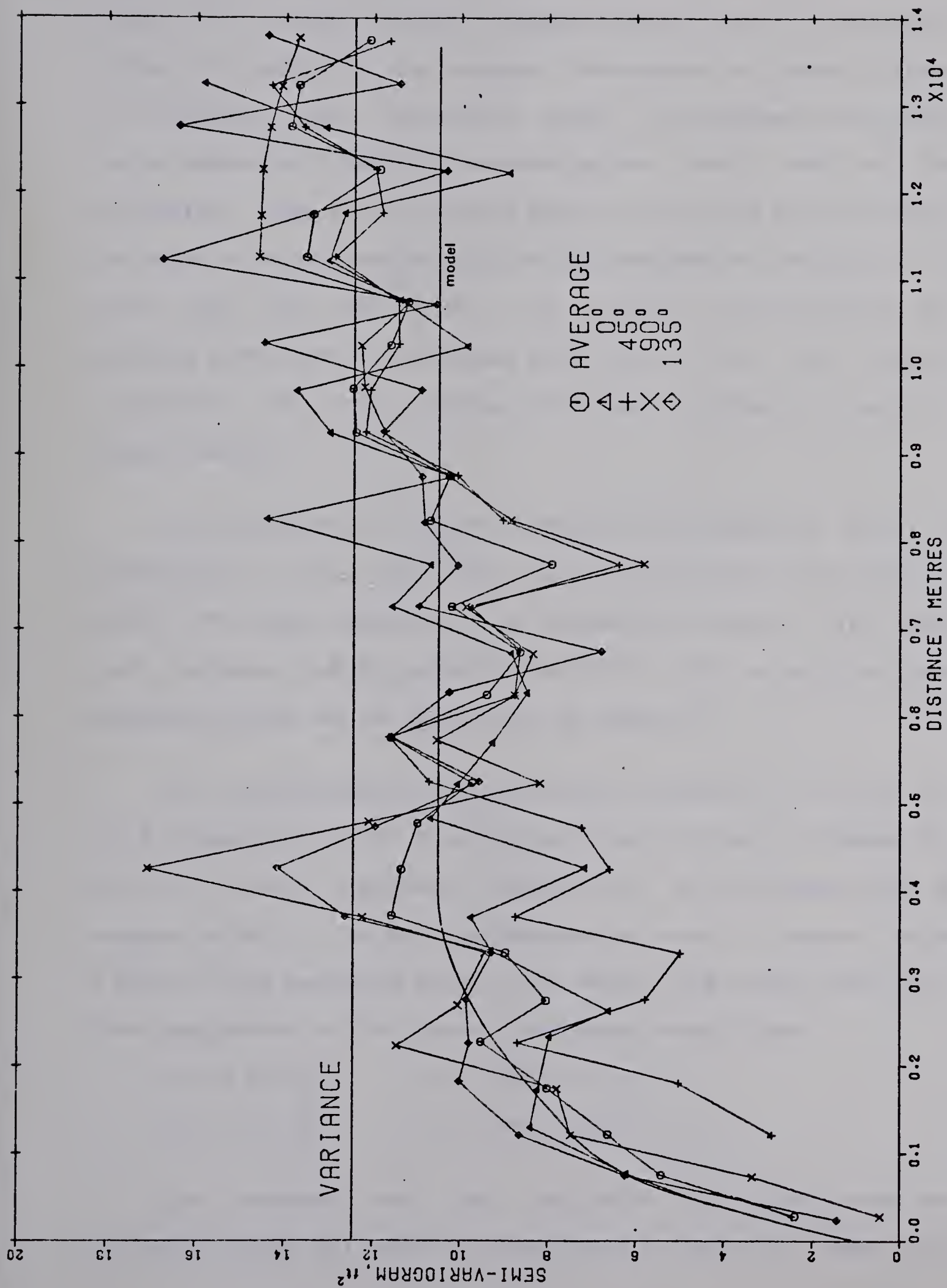


FIGURE 37. ESTEVAN NET COAL THICKNESS, VARIOGRAMS AND MODEL.

about 170 square miles. Sample values from 160 boreholes formed the basis of the average thickness estimate. Since the Estevan zone variogram model is composed of a short range component (1000 m) accounting for about 40% of the variation, the choice of 500 metres as a grid size resulted in about a 5% overestimation of the estimation variance. As grid size was decreased, the weights calculated by the kriging system did not change markedly nor did the average thickness but the variance of the area decreased towards a stable value.

The average net coal thickness of the Estevan zone is estimated to be 8.9 feet and the estimation variance is 0.085 ft^2 . This compares to an unweighted mean of 9.5 feet and variance of the mean of 0.077 ft^2 . The unweighted mean appears biased on the high side by about 7.

The experimental variograms and variance for the net coal thickness of the Boundary zone is plotted in Figure 38. The net coal thickness appears to be isotropic with no nugget effect. A transition phenomenon with a short range (1000 m) was modelled within the major long range structure. The parameters of the nested spherical models are.

$$\begin{array}{ll} C_1 = 1.0 \text{ ft}^2 & a_1 = 1000 \text{ metres} \\ C_2 = 4.5 \text{ ft}^2 & a_2 = 6000 \text{ metres} \end{array}$$

The average net coal thickness over the area was estimated from 161 sample values over an area of about 205

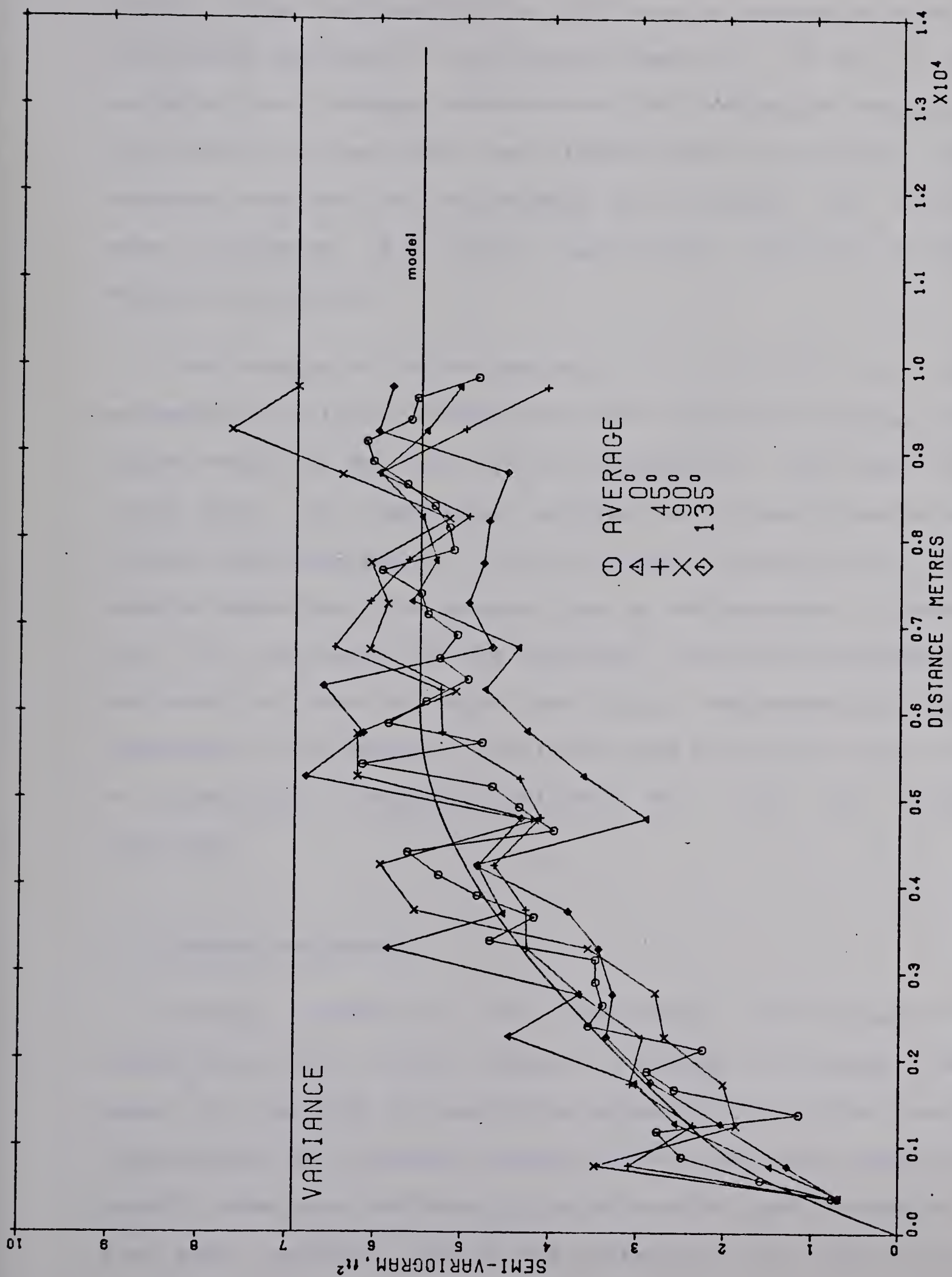


FIGURE 38. BOUNDARY NET COAL THICKNESS, VARIOGRAMS AND MODEL.

square miles represented by 2115 points located on a 500 metre grid. Because of the discrete summation of the area variance and average covariances, the estimation variance may be 3% to 4% too high. The relative error is less for the Boundary zone than for the Estevan zone because the short range structure is a less significant component of the Boundary zone model.

The average thickness estimate is 3.8 feet and the estimation variance is 0.057 ft^2 . The unweighted average of sample values is 5.3 feet and the variance of the mean is 0.043 ft^2 . The unweighted average is biased towards a greater thickness because of the disproportionate number of samples taken near the subcrop line to the northwest (Figure 11). In the case of the Boundary zone, the unweighted estimate is over a third too high, demonstrating the importance that spatial correlation has in the selection of an appropriate unbiased estimator for the net coal thickness.

4.4 Tonnage Estimates

Having estimated and represented the component variables of the volume equation (average thickness and area) in the form of cumulative probability distributions, the addition of a tonnage factor based upon specific gravity permitted the calculation of in-situ coal tonnages. The mean specific gravity was estimated to be 1.24 with a

minimum of 1.19 and a maximum of 1.29 (J. Irvine, personal communication). These values were taken as ± 2 limits of a normal distribution. The cumulative normal distribution was used for both the tonnage factor and the average thickness.

The evaluation of the resource equation was carried out by a simulation technique described by Roy (1975). In this process component variable distributions are sampled independently and the sample values are multiplied to form one estimate of the resource tonnage. The simulated sampling process was repeated 5000 times and the results were accumulated as a coal tonnage cumulative probability distribution. The simulation technique is particularly useful if the distributions of the variables in the resource potential equation are irregular or highly skewed and cannot be represented by analytical expressions. The area underlain by coal is an example of an asymmetric distribution.

The tonnage distributions created by the simulation runs for the Estevan and Boundary zones are displayed graphically in Figure 39. The parameters of the tonnage distributions and those of the component variables are tabulated in Table 4. The resource quantity estimated for the Estevan zone is twice that of the Boundary zone. The coefficient of variation and maximum/mean ratio of tonnages suggest that the Estevan zone is estimated with narrower relative confidence limits than the Boundary zone.

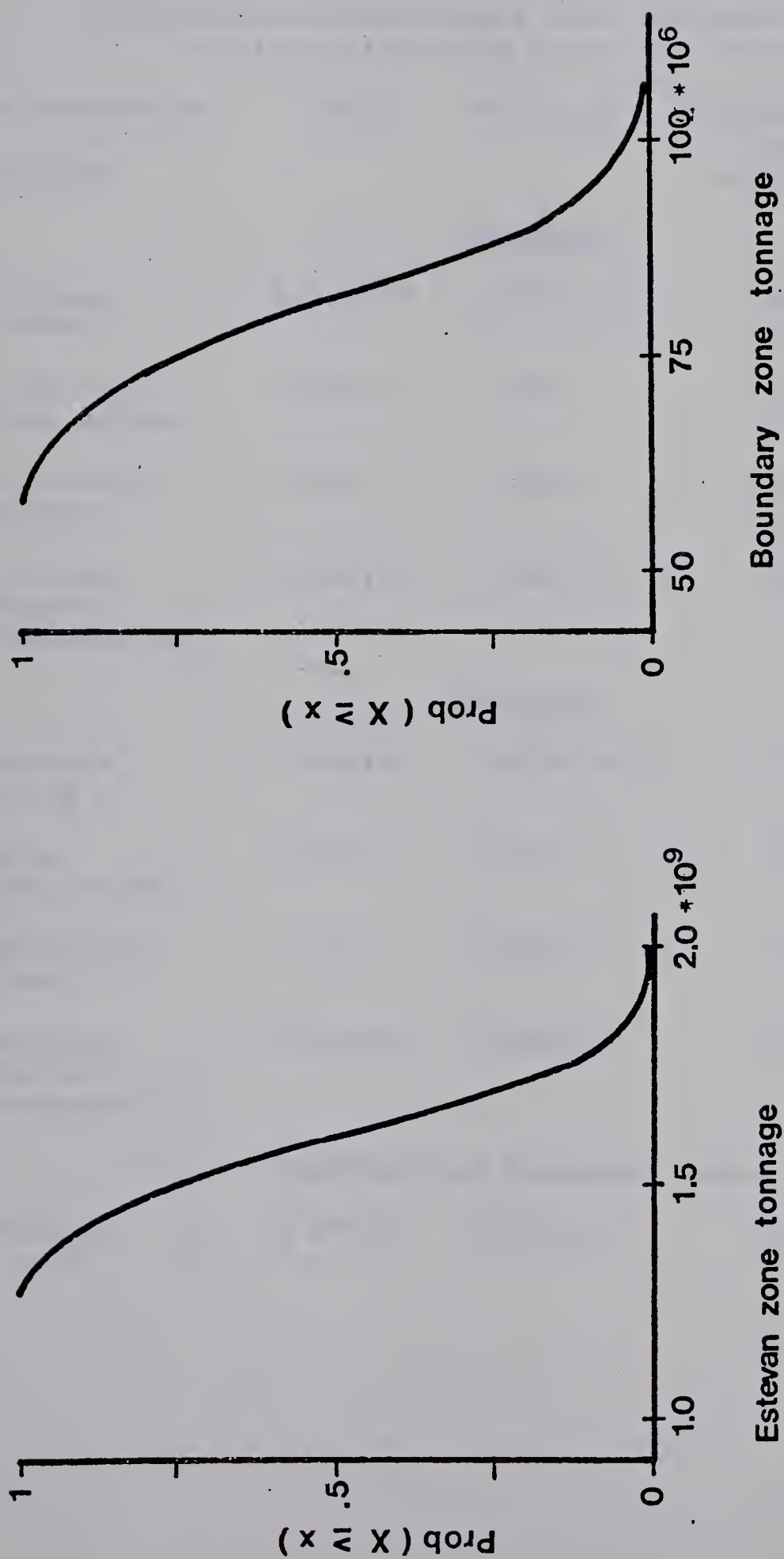


Figure 39 – cumulative probability distribution, short tons of coal resources

Table 4Parameters of estimated coal resource quantity
distributions and component variables

Distribution (Units)	Mean	Variance	Coefficient of variation	<u>maximum</u> mean
<u>Estevan</u>				
tonnage (tons)	1.59×10^9	$.200 \times 10^{17}$	8.9	1.3
area (sq. miles)	165.5	175.7	8.0	1.2
thickness (feet)	8.92	.0854	3.3	1.08
tonnage factor (tons/mi ² ft)	1.08×10^6	$.473 \times 10^6$	2.0	1.04
<u>Boundary</u>				
tonnage (tons)	796×10^6	$.812 \times 10^{16}$	11.3	1.4
area (sq. miles)	192.4	309.7	9.1	1.2
thickness (feet)	3.83	.05735	6.25	1.14
tonnage factor (tons/mi ² ft)	1.08×10^6	$.473 \times 10^6$	2.0	1.04
<u>Estevan and Boundary total</u>				
tonnage (tons)	2.40×10^9	$.278 \times 10^{17}$	6.9	1.3

If the confidence limits of the tonnage distribution are taken to be .977 then the range of values considered is the mean ± 2 standard deviations. This corresponds to the mean $\pm 18\%$ for the Estevan zone and the mean $\pm 23\%$ for the Boundary zone. The Estevan resource quantity estimate would fall in the measured resource category of McKelvey (1976) while the Boundary resource quantity estimate falls just outside the $\pm 20\%$ cut-off.

The percentage contribution of the component variables to the variance of the tonnage distributions is given in Table 5. In both zones the uncertainty in the areal extent of the zone accounts for over half the total uncertainty. The contribution of the average thickness variable ranks second and is more significant for the Boundary zone. The coefficient of variation for thickness in the Boundary zone (Table 4) is almost twice that in the Estevan zone. The coefficient of variation for the area of the Boundary zone is only slightly greater than that of the Estevan zone. In neither case does the variance of the tonnage factor contribute more than 6%.

The thickness of the Estevan zone is apparently well estimated from the fairly regular sample distribution (Figure 5). The area estimate suffers from the long subcrop perimeter which are structurally complex and inadequately sampled and from the presence of an erosional channel, the location and extent of which is difficult to define (Figure

Table 5

Components of the variance, tonnage distributions

Component	-----Zone-----	
	Estevan	Boundary
area	81.1	65.8
thickness	13.8	31.0
tonnage factor	5.1	3.2
tonnage	<u>100.0</u> percent	<u>100.0</u> percent

34). The thickness of the Boundary zone is less well defined because of the non-systematic location of samples (Figure 11) and because the eastern boundary of the areal extent is subject to several interpretations which vary widely (Figure 35). In both cases, any significant reduction in the uncertainty is dependent upon more detailed drilling to define the boundaries of the coal zone. Additional boreholes in data voids would improve the precision of the thickness estimate, particularly for the Boundary zone in which more than 80% of the variability occurs within a range of one to six kilometres of a point. The location of one additional borehole which would maximize the reduction in the estimation variance of the average thickness could be determined using methods described in Delfiner and Delhomme (1975).

CHAPTER 5

5. Applications to Systematic Sampling Patterns:

Small Scale Area

Three sections in the small scale area (Figure 18) were drilled over a period of three years at grid spacings of 800, 400 and 200 metres with some infill drilling in the fourth year at 100 metre spacing to define an erosional area (Figure 14). The proportion of boreholes which intersect coal is an unbiased estimator of the proportion of the area underlain by coal and the arithmetic mean of the net coal thickness in holes penetrating the zone is an unbiased estimator of the average net coal thickness.

The precision of an estimate of the volume of in-situ coal is a function of the natural variability of the zone thickness, the shape of the coal area and the distance between observations. The measure of precision of an estimate adopted in this study is defined to be two relative standard deviations expressed as a percentage of the value of the estimate:

$$P = 100*(2*S)/m \quad (5.1)$$

where S^2 is the estimation variance and m is the value of the estimate. If the error made in estimating the true unknown M by x is normally distributed M occurs within the interval $m \pm 2S$ with confidence 0.98.

The relationship between the precision of estimation and the amount of exploration effort is not a simple one. Once known, the relationship can be used to select the drill spacing appropriate to an acceptable precision level, and the rate of improvement in precision as a function of exploration effort can also be studied.

A simplistic model of the relationship between the precision of the estimate (P) and the number of boreholes (N) drilled in a limited area is

$$\ln P = c - k \ln N \quad (5.2)$$

where c and k are constants. If k equals one, the model may be rewritten simply as

$$P = c/N$$

and doubling the exploration effort effectively halves the uncertainty. If k is greater than one, the return on the increased effort is magnified whereas if k is less than one, the increase in precision follows a law of diminishing returns. In practice, k may also be a function of N , increasing as the information provided by more samples has a synergistic effect. The value and behaviour of k can be examined by plotting $\ln P$ against $\ln N$ for experimental data. The slope or tangent to the curve joining the points is the value of k .

5.1 Precision of Area Estimate

On the basis of all the available information, the study area is composed of three areas (Figure 18):

1. an area in which the complete coal zone exists.
2. an area in which the upper seams of the zone have been eroded at the bedrock unconformity.
3. an area in which the zone has been eroded or was not deposited.

The narrow, irregular width of the erosional edge, posed a problem in making the distinction between the complete and incomplete sections of coal zone in boreholes spaced 400 metres or more apart. For the purpose of comparing the precision at all observation distances, a borehole intersecting any coal in the zone was considered a coal intersection and the area was divided into only two areas: coal and non-coal.

The area of non-coal was calculated as the product of the number of boreholes which did not intersect coal and the area of a square with sides the length of one observation spacing. Boreholes along the edge and at the corners of the study area contributed 0.5 and 0.25 respectively of the area of an interior borehole. The relative variance of the non-coal area estimate was calculated using Matheron's approximation formula (3.20 in chapter 3). The estimation variance and precision for the area underlain by coal was derived from the relative variance of the non-coal area

estimate.

The parameters of the formula, the resulting precision and estimation variance values for three drill spacings are listed in Table 6. The number of boreholes corresponds to the number used in a complete grid pattern which was not in fact achieved at the 200 metre spacing. The parameter N is the number of cells in which coal was not observed and was interpreted from Figure 18. It contains a decimal fraction because of the arbitrary boundaries of the area. Parameters N_1 and N_2 are one-half the estimated length of the perimeter in the directions of the grid lines and contain decimal fractions because of the corner and edge boreholes.

Matheron (1971, pp. 27-28) cautions that formula 3.20 expresses the estimation variance only if the spacing of observations is small and that it neglects a fluctuating term which may be quite significant. This fluctuating term results from the unique combination of the random location of the grid origin and the frequency of observations relative to the frequency of boundaries between coal and non-coal areas. Referring to Figure 18, it appears that an 800 metre grid spacing is larger than the average diameter of the non-coal areas. Because an assumption basic to the calculation is violated, the precision of the 800 metre estimate should be taken as an approximation.

By way of comparison, the precision of the area

Table 6

Precision of area estimation using Matheron's approximation
formula for relative estimation variance.

Drill spacing (metres)	800	400	200	final
Number of holes	21	65	225	
N ₁	1.75	7	17	
N ₂	1.75	7	14	
N	1.75	9.25	32.75	
area of coal (sq. miles)	2.56	2.42	2.48	2.51
variance (ft ²)	.0256	.0064	.0009	
precision	25%	6.5%	2.4%	
precision (binomial)	19%	11%	5.9%	

estimate may also be calculated based on an assumption that areal proportion estimates are distributed as the binomial distribution. These precision estimates are included in Table 6. The precision data in Table 6 have been plotted against the number of observations on full logarithmic axes in Figure 40.

According to Matheron's approximation formula, the uncertainty decreases more rapidly than the grid spacing but that it does not decrease as rapidly as the number of observations increases. The slope of the line segment between 200 m and 400 m is about -0.8 which is an improvement over the constant slope of -0.5 for the binomial model. The slope of the curve for the approximation formula can be expected to be close to unity but will vary since the relationship also depends on the parameters N_1 and N_2 which express the complexity of the coal zone boundary apparent at various sample spacings.

5.2 Structural Analysis of Exploration Data

Precision estimates for the average net coal thickness are based on the model fitted to experimental variograms. The accuracy of the precision estimates depends upon the recovery of the underlying variogram model from the sample data. If the raw sample data contain more than one population, the natural variability of the net coal thickness may be obscured by the effect anomalous outlying

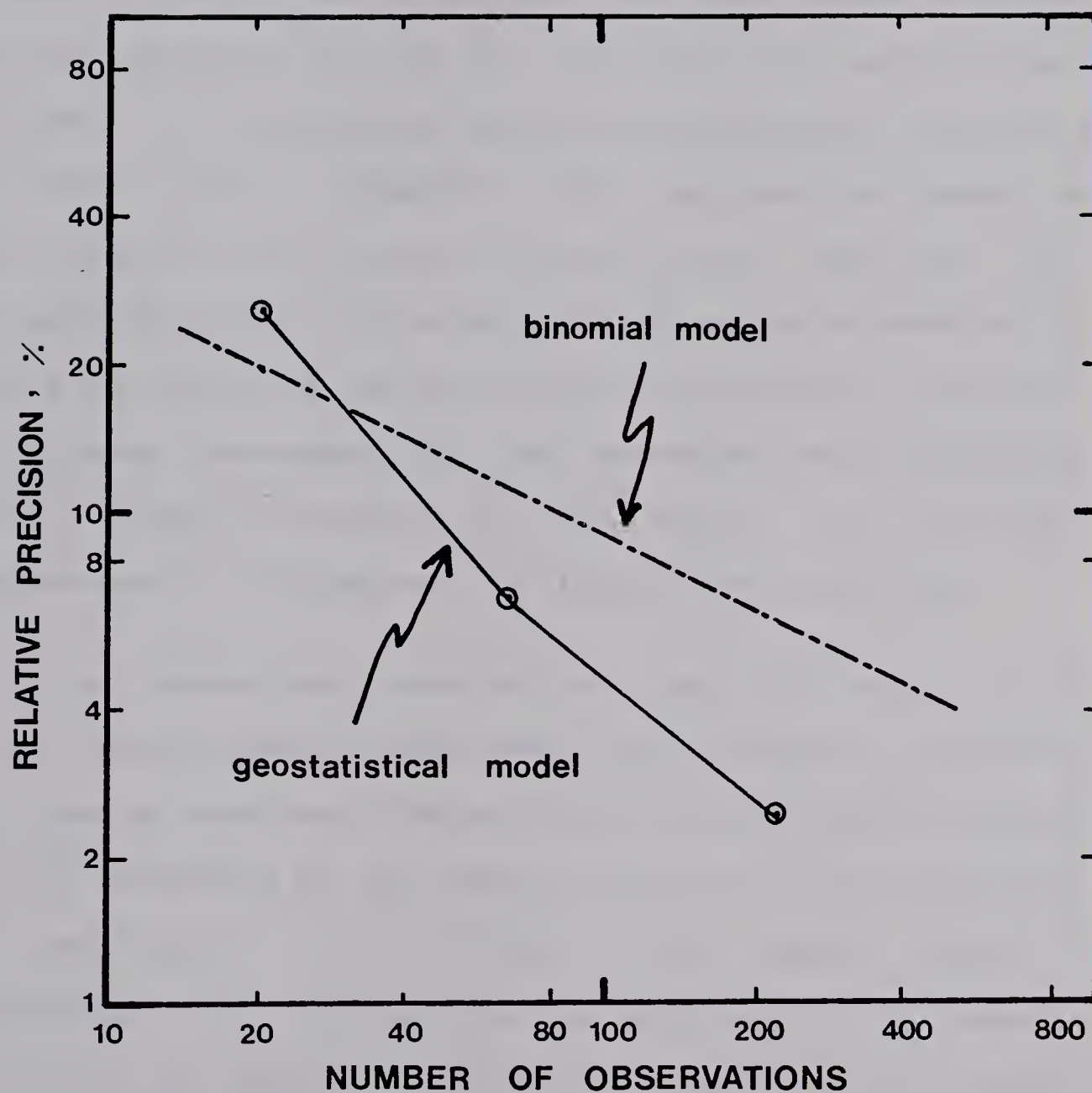


FIGURE 40—RELATIVE PRECISION OF THE AREA ESTIMATE AS A FUNCTION OF THE NUMBER OF OBSERVATIONS, SMALL SCALE AREA.

values have on the experimental variogram. That small samples often do not provide stable estimates of the population mean, variance and variogram is borne out by Table 7 in which the sample mean variance and precision for net coal thickness are calculated for three sample spacings using the available data in the study area. The calculations were made for all boreholes together and also for boreholes which show only a complete zone section. The number of observations in the truncated areas is also tabulated. The mean appears to be a relatively stable estimate whereas the variance decreases as the number of observations increases. The variance increases for all boreholes at all spacings (Table 7, column 4) because of the effect of additional holes penetrating incomplete sections of the coal zone.

As a homogeneous population, the variance for the complete zone is smaller than that for the mixed populations at all sample spacings. The precision of estimated average net coal thickness of the complete zone is about 75% of the mixed population and the mean is 5% higher. Table 8 demonstrates that similar results hold for all the samples collected in the small scale area. With an increased number of samples, the precision values for the entire small scale area are lower than for the study area although the mean and variance are comparable.

The sample variance perceived at low information levels is higher than the real population variance and leads to

Table 7

Sample mean and variance of net coal thickness observations at three drill spacings. Data are for three sections only.

Drill spacing, (metres)	800	400	200	All
* Complete Zone *				
Number of observations	18	44	157	173
Mean (ft)	12.7	12.6	12.6	12.6
Variance (ft ²)	9.3	5.0	4.25	4.16
Precision (%)	11.3	5.35	2.60	2.46
* Incomplete Zone *				
Number of observations	3	7	22	4+
* All Boreholes *				
Number of observations	21	51	179	217
Mean (ft)	12.1	12.0	12.0	11.65
Variance (ft ²)	14.9	8.4	7.47	8.55
Precision (%)	13.9	6.8	3.4	3.4

Table 8

Sample mean and variance of net coal thickness observations at three spacings. All observations in the small scale area.

Drill spacing (metres)	800	400	200	All
* Complete Zone *				
Number of observations	62	168	344	360
Mean (ft)	11.6	12.0	12.2	12.2
Variance (ft ²)	7.9	4.76	4.23	4.18
Precision (%)	6.1	2.8	1.8	1.8
* Incomplete Zone *				
Number of observations	7	12	28	50
Mean (ft)				7.47
Variance (ft ²)				9.7
Precision (%)				11.8
* All Coal *				
Number of observations	69	180	372	410
Mean (ft)	12.0	11.6	11.78	11.63
Variance (ft ²)	12.3	7.4	6.64	7.25
Precision (%)	7.0	3.5	2.3	2.3

precision estimates which are higher than those based on the population variance. Precision estimates made with only a few samples provide conservative confidence limits for resource estimates.

Experimental variograms were constructed using data from boreholes selected with complete sections of the coal zone and using data from all boreholes. The data available at the end of each year of drilling were used to illustrate the effect of the grid spacing on perception of the underlying variogram. Variograms of the selected samples represent the natural variability of the coal zone whereas variograms for all samples contain a large variance component for the small number of samples from areas where the coal was truncated by erosion.

Variograms for the first year (Figures 41 and 42) do not show any significant spatial structure and would be interpreted as the random type (Figure 21). Variograms calculated after the second year (Figure 43 and 44) indicate some spatial structure and a level of variance considerably reduced from the previous year. The variogram of the selected samples (Figure 43) has a possible short range structure which rises to a sill of 3.75 ft^2 at about 600 to 800 metres. The directional variogram for an azimuth of 45° rises above the sample variance beyond 2500 metres in response to a thinning of net coal to the southwest (Figure 19). Variograms based on all the samples (Figure 44)

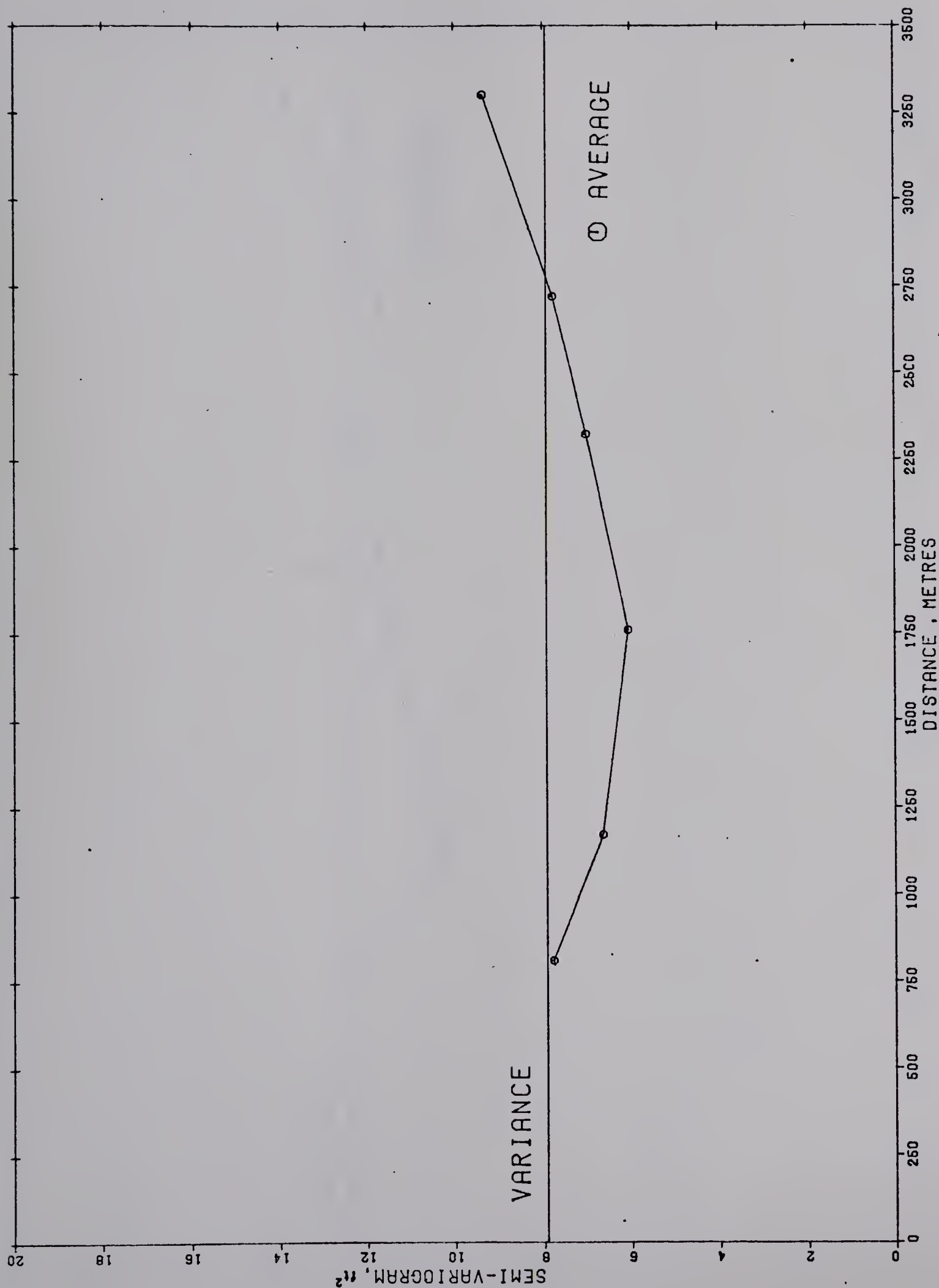


FIGURE 41. AVERAGE VARIOGRAM OF NET COAL THICKNESS, SELECTED SAMPLES - YEAR 1

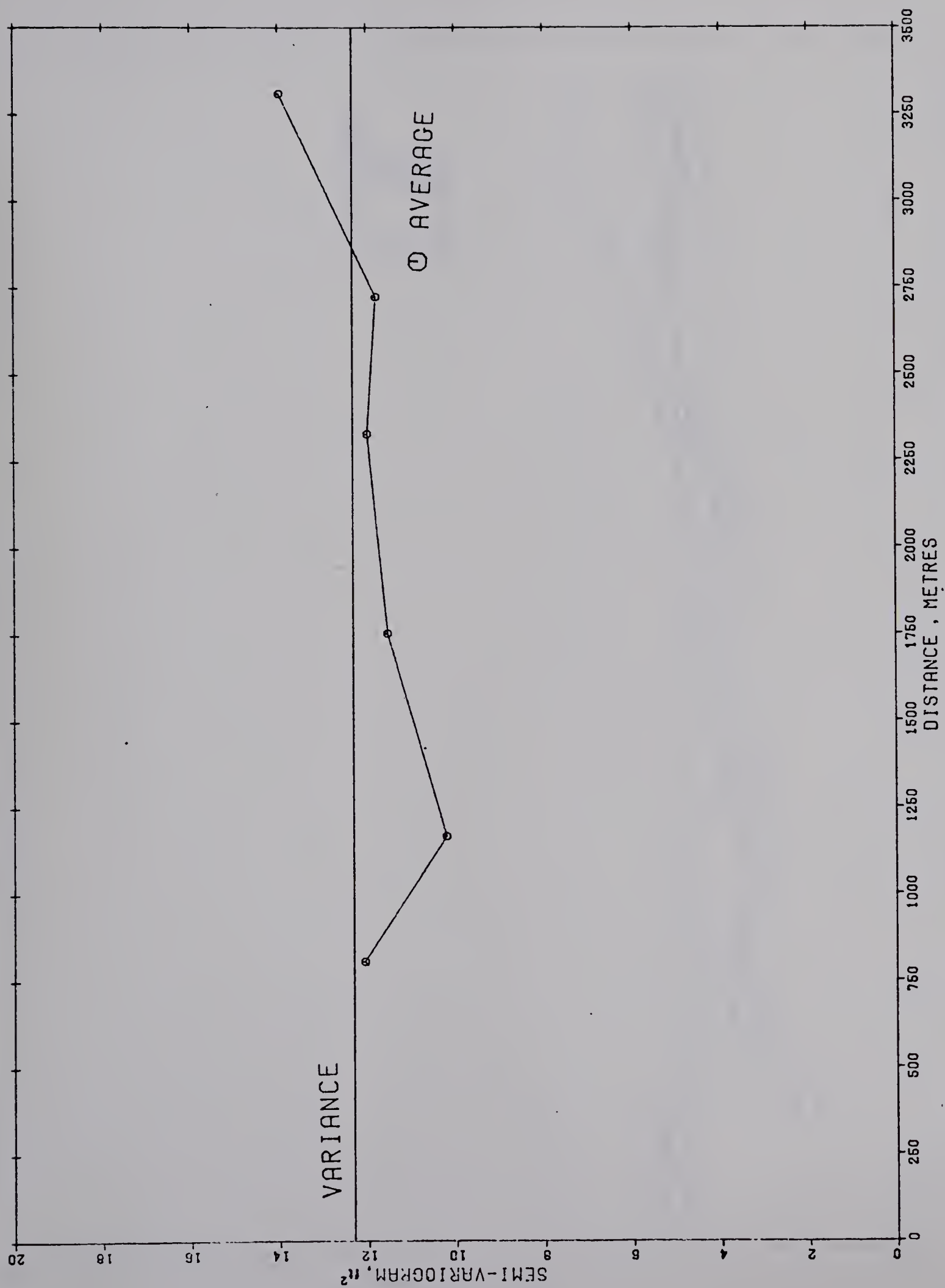


FIGURE 42. AVERAGE VARIOGRAM OF NET COAL THICKNESS, ALL SAMPLES - YEAR 1

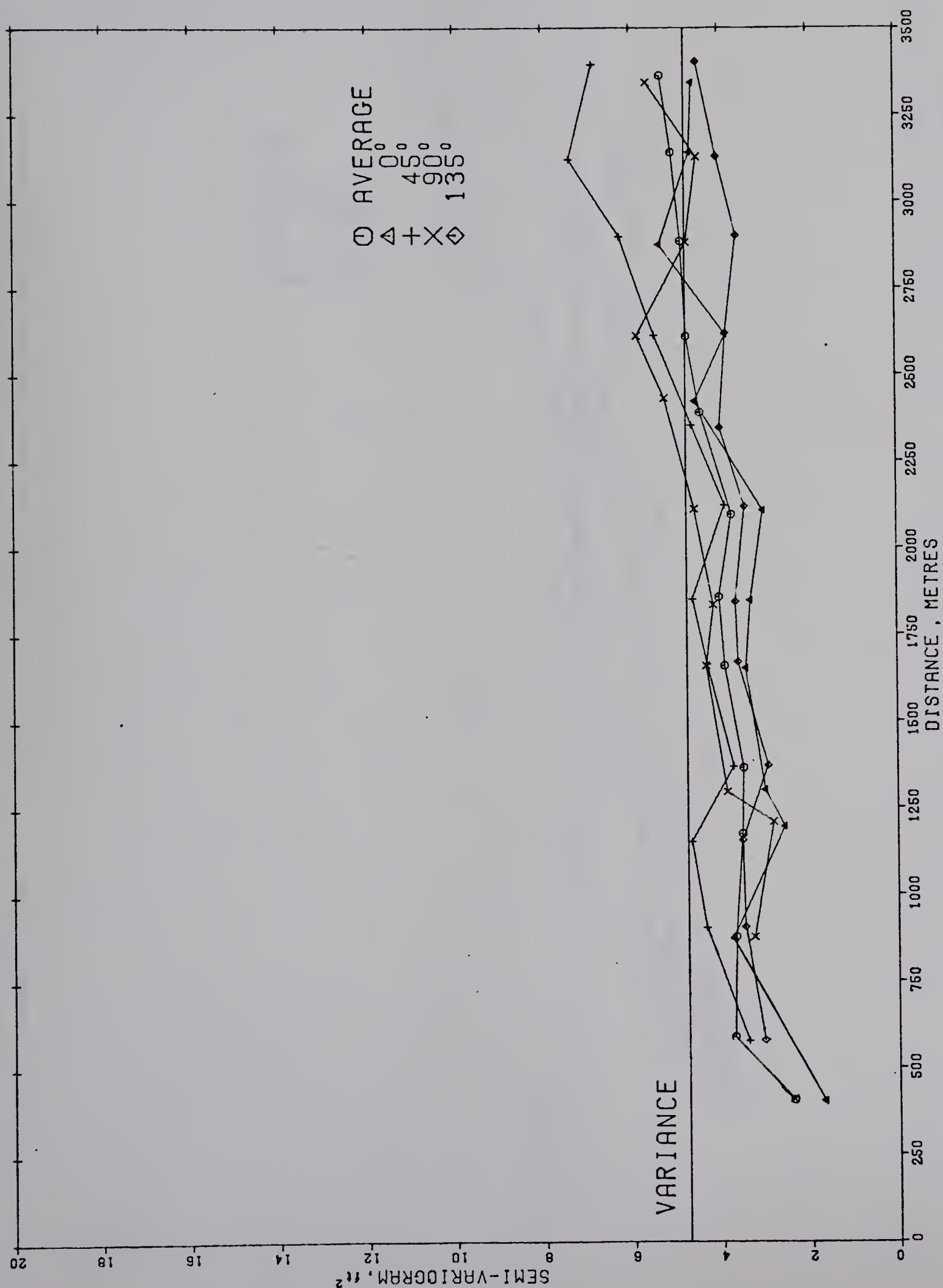


FIGURE 43. VARIOGRAMS OF NET COAL THICKNESS, SELECTED SAMPLES - YEAR 2

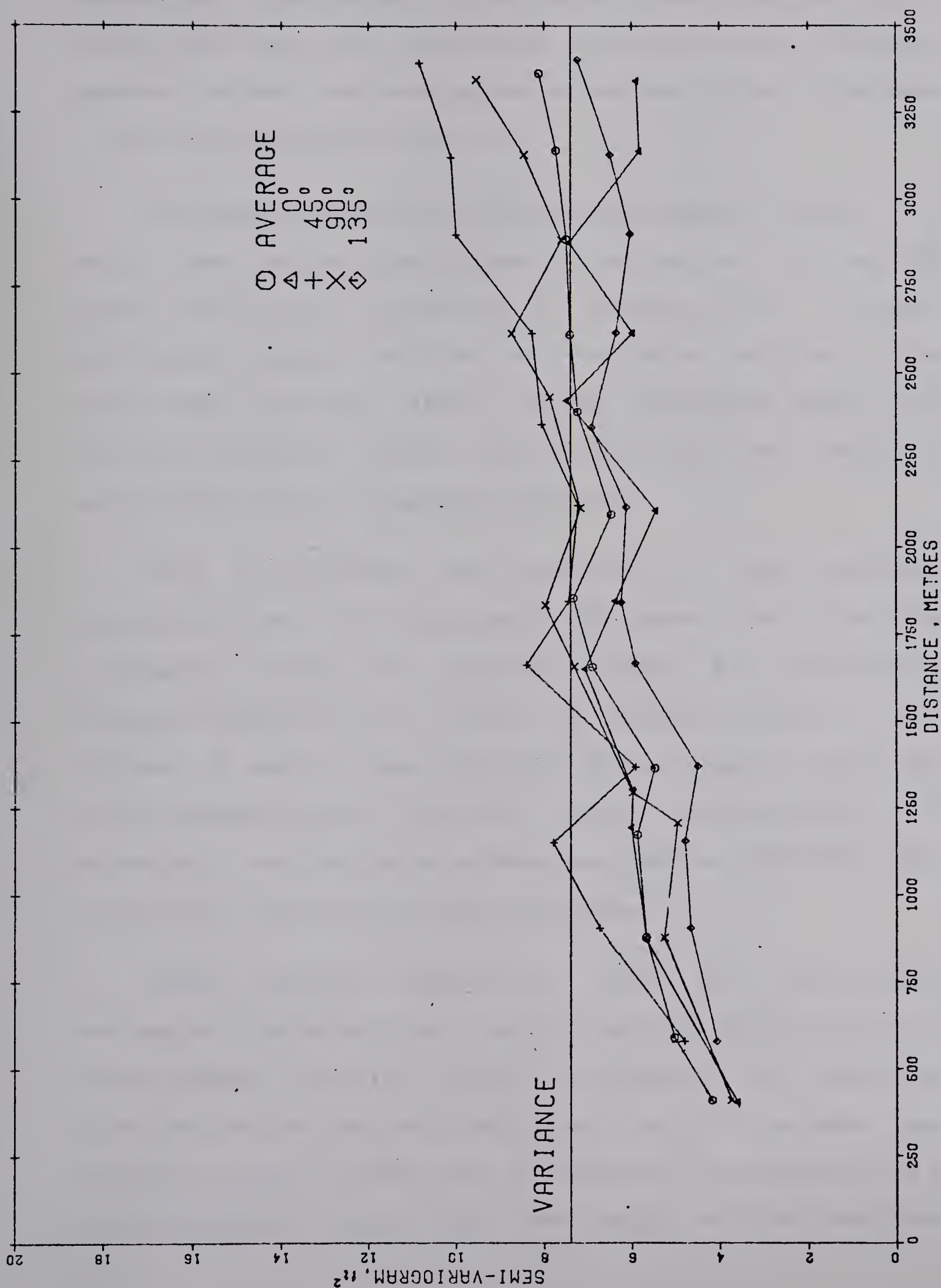


FIGURE 44. VARIOGRAMS OF NET COAL THICKNESS, ALL SAMPLES - YEAR 2

demonstrate the effect of outlying values from the partly eroded coal zone. The directional variograms show a greater scatter around the average variogram and a linear increase in the variogram with distance.

Variograms calculated from selected samples after the third year of drilling (Figure 45) are almost flat and the drift in the 45^0 direction is defined more clearly. Additional samples drilled at 100 metre spacing in the fourth year add very little to the variogram model for selected samples (Figure 46). A structure with a range of about 800 metres is suggested in both.

When all samples are considered in the variogram calculation after the third year, the shape of the resulting variograms (Figure 47) parallels those for the selected samples (Figure 45) at a level of variance about 2 ft² higher. A short range structure with a range of about 800 metres appears to be the most likely interpretation. As expected, the variogram of samples from the erosional edge (Figure 48) shows no spatial structure.

These results demonstrate that an experimental variogram calculated from a small number of samples taken at widely-spaced locations rarely indicates the underlying structure of the net coal thickness. A stable estimate was obtained with no fewer than 50 observations located with a minimum spacing of one-half the range of the smallest

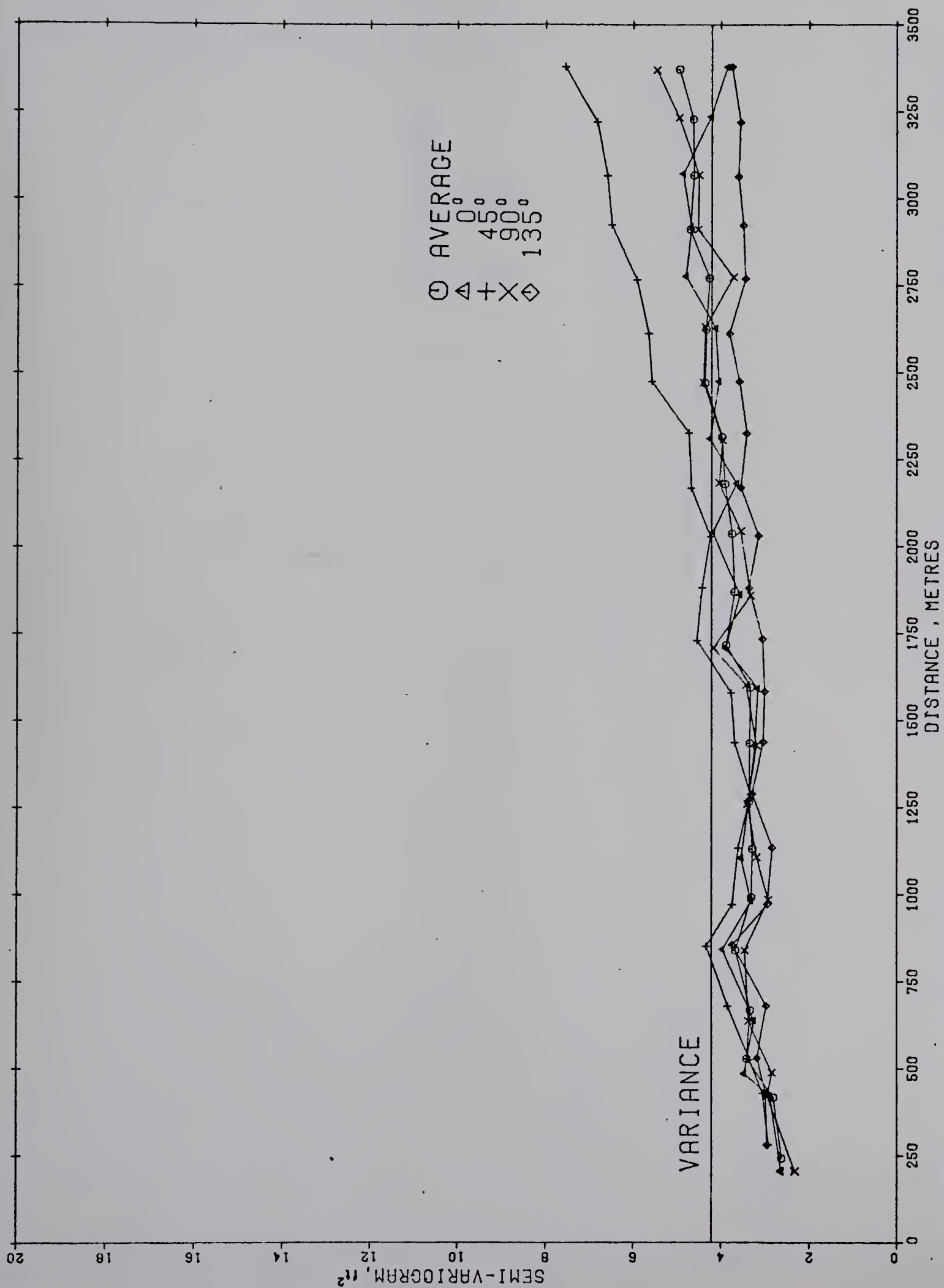


FIGURE 45. VARIOGRAMS OF NET COAL THICKNESS, SELECTED SAMPLES - YEAR 3

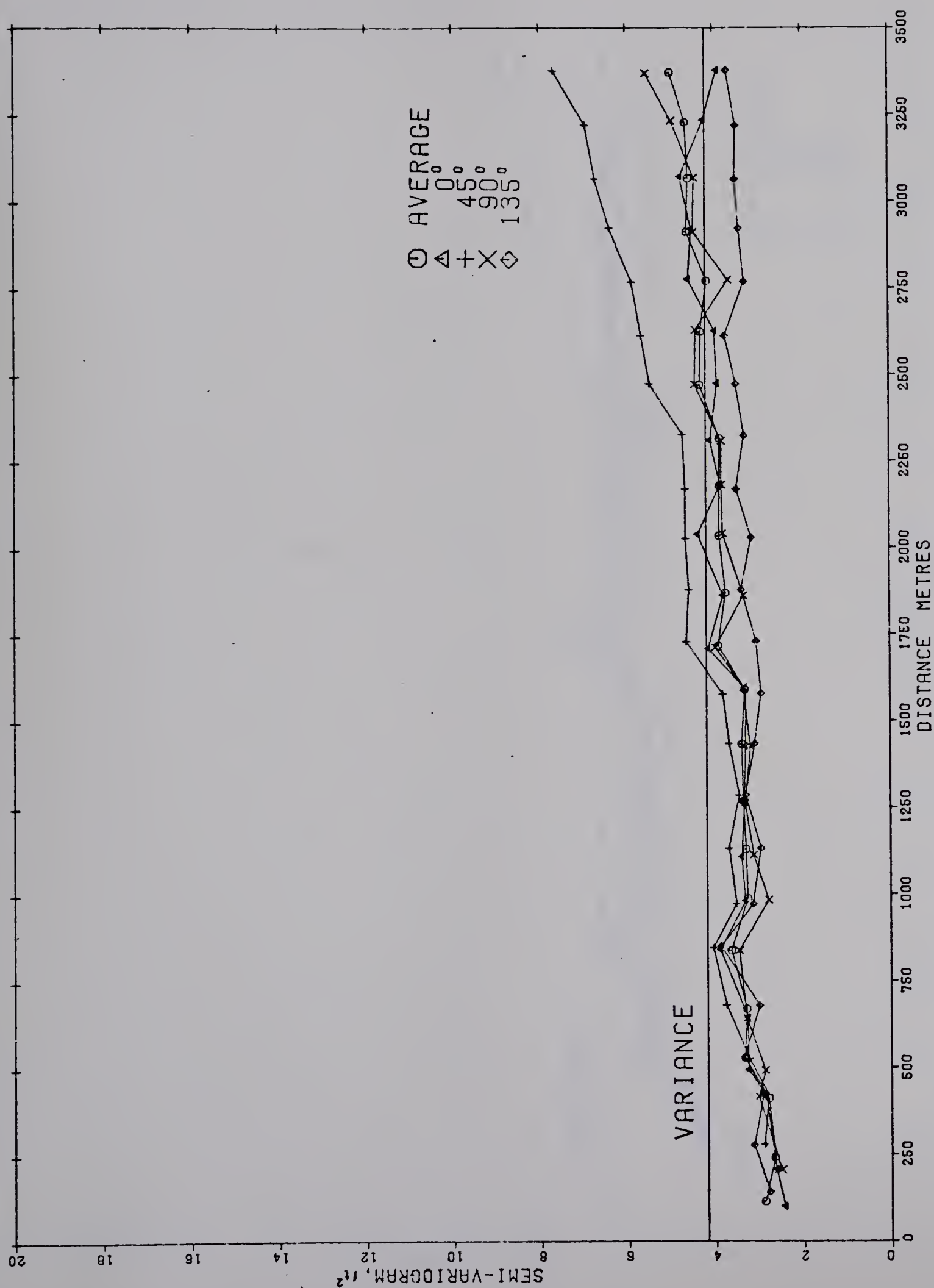


FIGURE 46. VARIOGRAMS OF NET COAL THICKNESS, SELECTED SAMPLES - YEAR 4

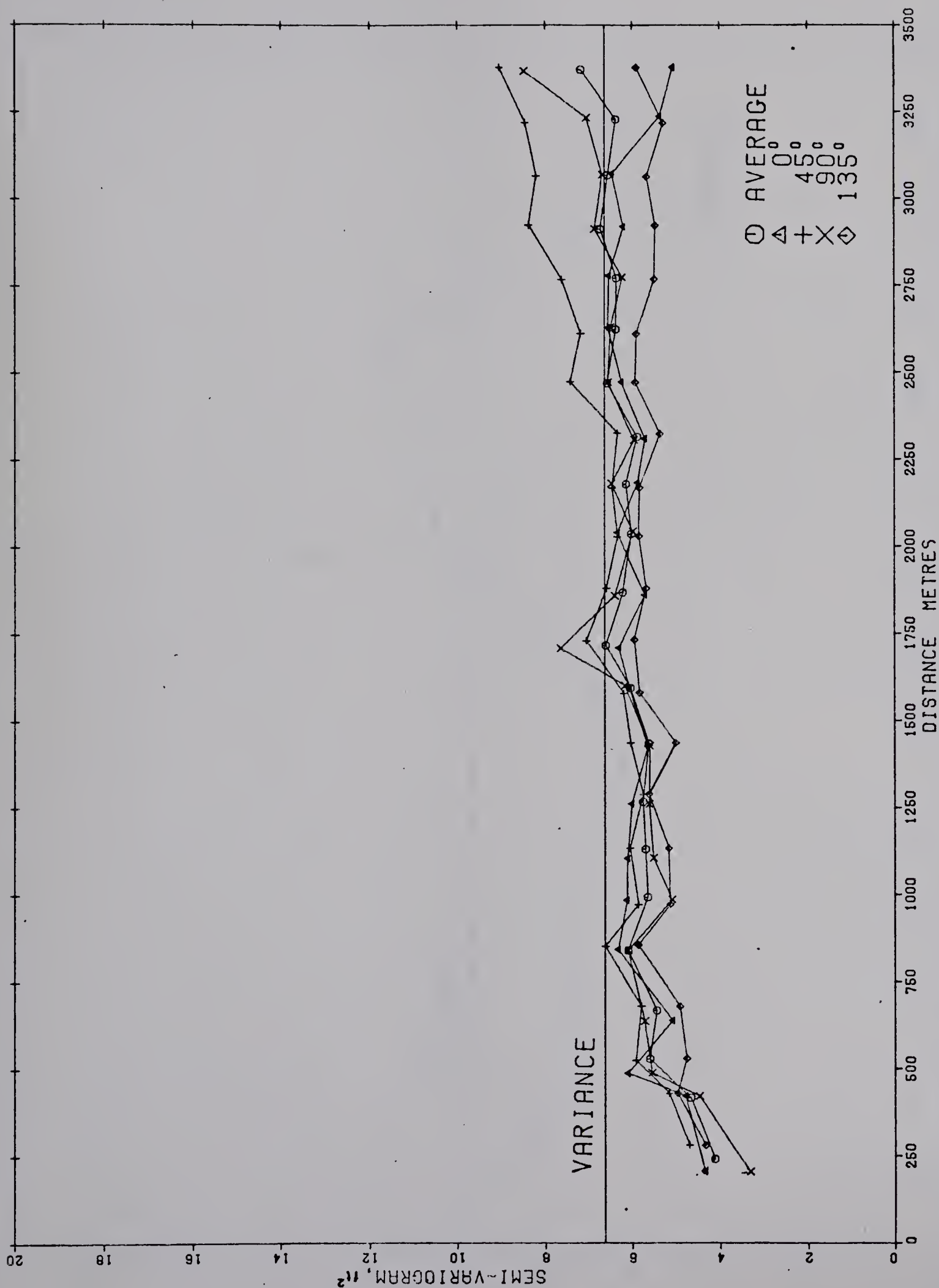


FIGURE 47. VARIOGRAMS OF NET COAL THICKNESS, ALL SAMPLES - YEAR 3

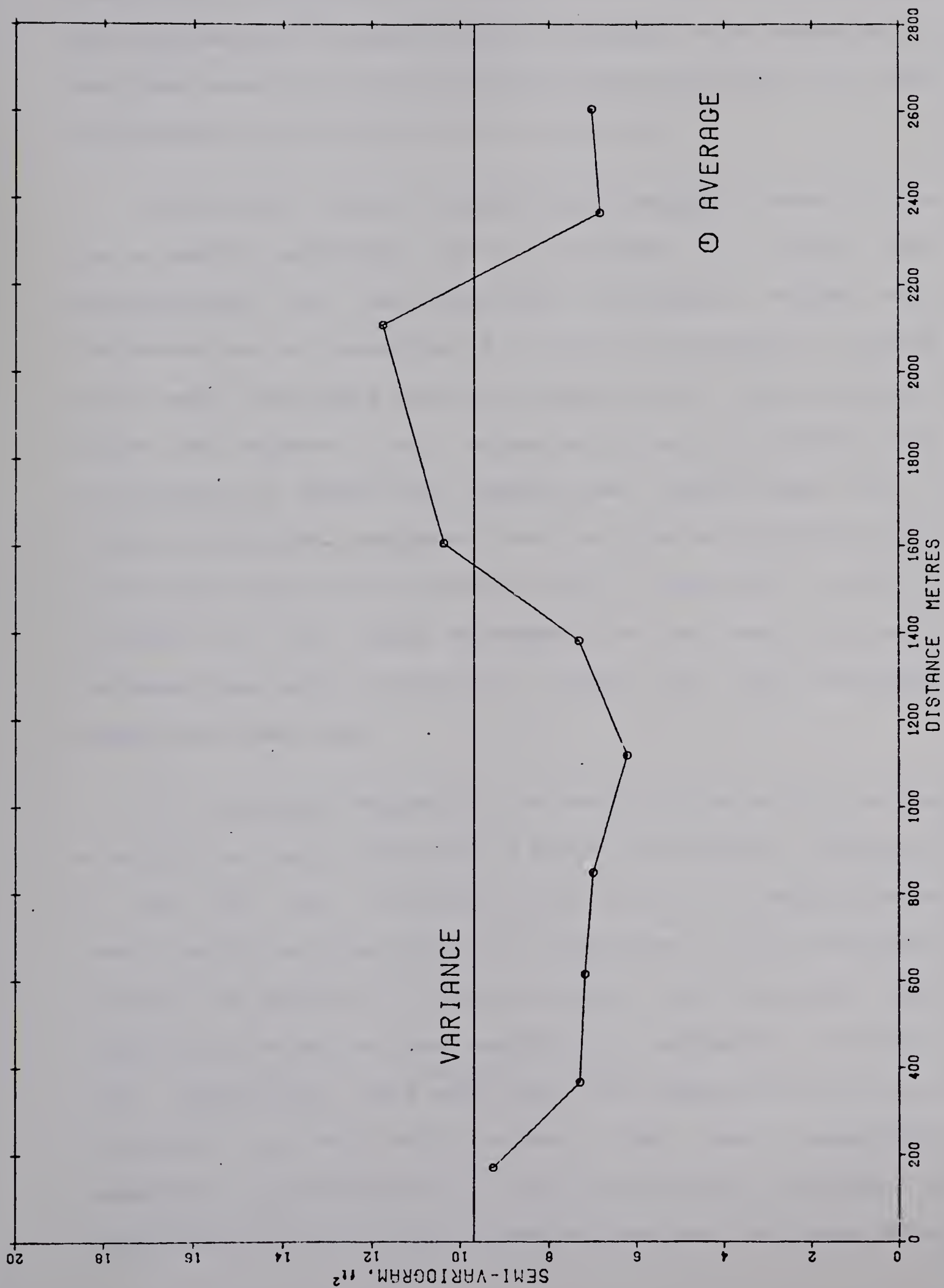


FIGURE 48. AVERAGE VARIOGRAM OF NET COAL THICKNESS, SAMPLES FROM ERODED AREAS

significant structure. If observations from two populations are intermixed, the experimental variogram will overestimate the uncertainty in the individual populations and the range of the major phenomenon will be obscured.

Techniques which optimize the spacing of observations for a desired precision of the estimate are based upon foreknowledge of the underlying variogram. Unless this variogram can be identified from outcrop exposures or mining data, such techniques are of no value in the reconnaissance stage of regional coal resource evaluation programs. The requirement in number and spacing of observations for a stable variogram estimate may not be met until the pre-production stage of exploration. This limitation could be overcome if the known variogram of an analogous well-explored coal zone is used as a model for the relatively unexplored coal zone.

The smallest separation of sample pairs which provides a stable variogram estimate is about 200 metres. Structures in the net coal thickness which have an average diameter less than 200 metres cannot be identified on the variograms. Because the behaviour of the variogram near the origin has a significant effect on the calculated estimation variance, some assumptions were made about the behaviour of net coal thickness in very local areas. The most reasonable assumption geologically is that net coal thickness is continuous and that there exists a structure (or structures)

with a range(s) shorter than 200 metres. The implications of the choice of a range for the short scale structure to the precision of estimates will be discussed in the next section.

The interpretation of net coal thickness as a continuous phenomenon is illustrated for the average variogram of all samples after the third year of drilling (Figure 49). The parameters of this model are:

$$C_1 = 3 \text{ ft}^2 \quad a_1 = 200 \text{ metres}$$

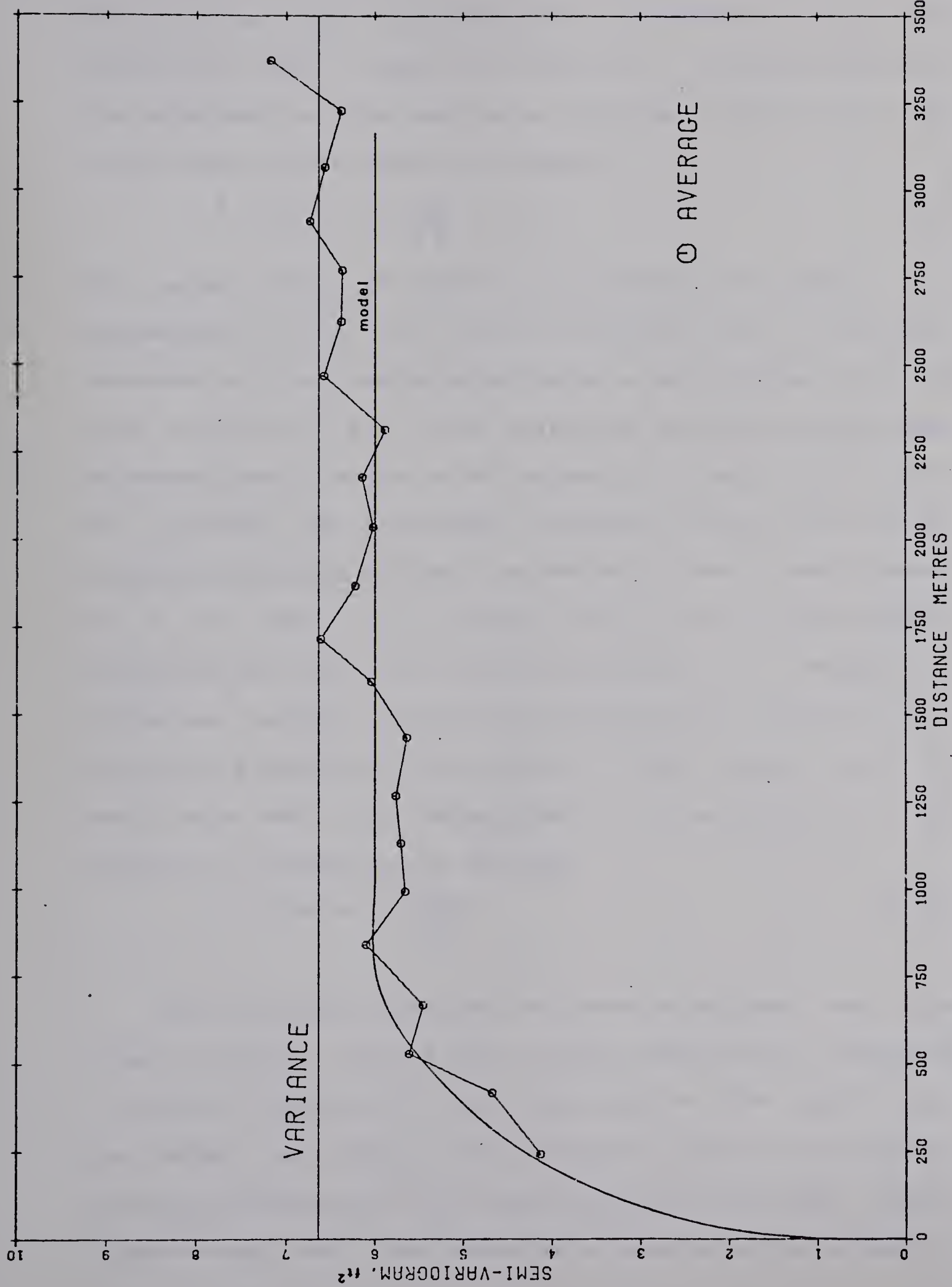
$$C_2 = 3 \text{ ft}^2 \quad a_2 = 800 \text{ metres}$$

The choice of the model for all samples after the third year for subsequent precision estimates was guided by two considerations:

1. The precision estimates for the average net coal thickness must be directly comparable to results derived for the area estimates. Thus all samples representative of the coal zone had to be included.
2. This model was more efficient computationally than the alternative of modelling the selected coal zone samples and samples from the erosional areas separately and combining the variances.

5.3 Precision of the Thickness Estimates

The precision of the average net coal thickness was calculated for nine sample grids using two different assumptions. The first is based on the assumption that



observations are statistically independent and the population has a mean of 12 feet and a variance of 6 ft². The precision in this case is an inverse function of the square root of the number of samples:

$$P = 100 * 2 * \sqrt{\frac{6}{N}} \quad (5.3)$$

The second type of precision calculation was based on the assumption that the net coal thickness has a variogram composed of a two nested structures; a short range structure with a sill of 3 ft² at 200 metres or less and a long range structure with a range of 800 metres and a sill of 3 ft². The variance of this model is the sum of the sills of the component models 6 ft² and the population mean was assumed to be 12 feet. The variance (S^2) of the error made in extending the value of a central borehole to a square of influence the size of the grid spacing was calculated using auxiliary functions (Clark, 1976). If the errors made in each grid cell are independent, the precision of the estimate is calculated as follows:

$$P = 100 * 2 * \sqrt{\frac{S^2}{N}} \quad (5.4)$$

The extension variances (S^2) were calculated for five ranges assumed for the short range structure are tabulated in Table 9. Varying the range from zero to 200 metres has the effect of reducing the estimation variance. The effect is most pronounced at grid spacings shorter than 400 metres illustrating that the choice of a model near the origin is

Table 9

Variance (ft^2) of the error made in extending the value of a central borehole to a square L metres by L metres. Calculations were performed for various assumed values for the range of the variogram short range structure.

Range of Variogram (m)	0	10	50	100	200
L (m)					
50	3.069	2.985	1.290	0.633	0.345
100	3.137	3.118	2.549	1.359	0.702
200	3.276	3.271	3.143	2.688	1.498
300	3.418	3.416	3.361	3.173	2.356
400	3.564	3.563	3.533	3.431	2.976
600	3.876	3.875	3.862	3.819	3.631
800	4.222	4.221	4.214	4.190	4.089
1200	4.938	4.938	4.935	4.925	4.881
1600	5.412	5.412	5.410	5.404	5.380

significant in the calculation of precision and particularly the improvement of precision with increased exploration effort. The precision of the average thickness estimate was calculated for three error variance models: statistical independence, the 0 metre range and the 200 metre range variogram models (Table 10). Precision values for variogram models with ranges between 0 m and 200 m fell between the values tabulated for 0 and 200 metres.

The logarithm of precision was plotted against the logarithm of the number of observations from Table 10 in Figure 50. The relationship between precision and the number of observations in the case of statistical independence is strictly linear with a slope of -0.5 . The variogram with the nugget effect represents improved precision but also displays a linear relationship with slope -0.5 . The most continuous variogram of net coal thickness (200 metre range) results in precision which is not a linear function of N but improves at grid spacings of 400 metres and less. The value of k at 200 metres is about -0.8 indicating a substantial improvement on the precision with each additional grid drilled at 200 metre spacing and less.

The curves plotted in Figure 50 are applicable only to the study area of three sections. They are specific to the ratio of population variance to the population mean and the relationship of the range of variogram model(s) to the grid sample spacings.

Table 10

Precision (%) of average net coal thickness estimates in the small scale area. Precision has been calculated at drill spacings for three variance models.

-----Variance Model-----				
Drill spacing	Number of samples	Statistical Independence	Nugget	Nested
50	3201	.79	.53	.19
100	833	1.54	1.11	.53
200	225	2.96	2.19	1.48
300	106	4.30	3.25	2.70
400	65	5.50	4.24	3.88
600	31	8.01	6.44	6.23
800	21	9.62	8.07	7.94
1200	8	16.67	15.12	15.03
1600	3	28.87	27.42	27.34

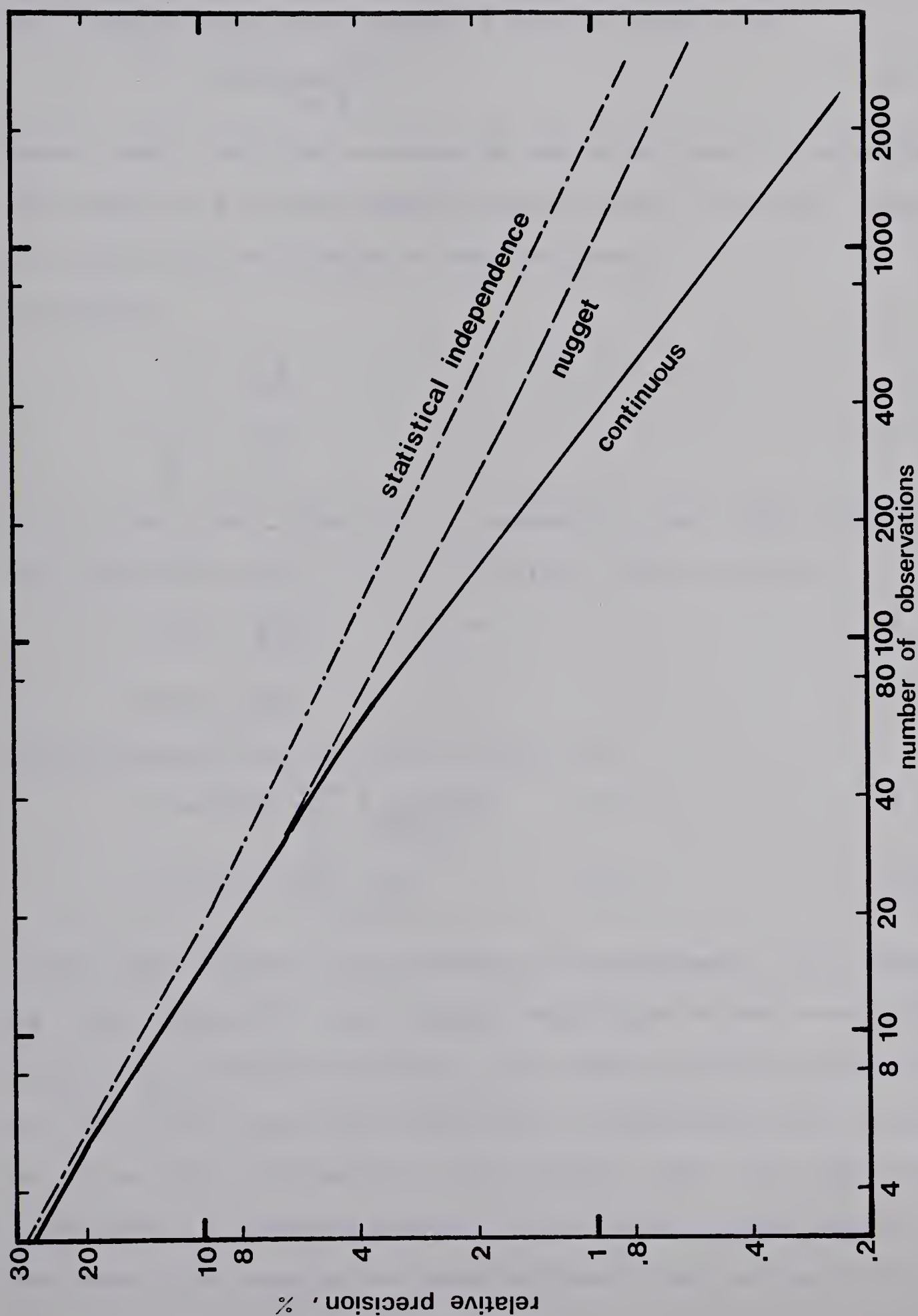


Figure 50 - Relative precision of the average net coal thickness as a function of the number of observations in the small scale area.

The equation for the relative precision of the arithmetic mean of net coal thickness observations (m) taken on a square grid with spacing d over an area A is:

$$P = 200 * \frac{S(d)}{m} * \sqrt{\frac{1}{N}} \quad (5.5)$$

where $S(d)$ is the variance of the error made in extending the value of a central observation to the enclosing square cell and N is the number of observations.

Generally,

$$N = \frac{A}{d^2}$$

so $\frac{1}{N} = \frac{d^2}{A}$ (5.6)

Let a be the range of a spherical net coal thickness variogram with sill C . The following relations hold:

$$S(d) = \sqrt{\frac{Cd}{a}} \quad d \leq a \quad (5.7)$$

$$S(d) = \sqrt{C} \quad d > a$$

Substituting (5.6) and (5.7) into (5.5)

$$P = 200 * \frac{\sqrt{C}}{m} * \frac{1}{\sqrt{A}} * \sqrt{\frac{d^3}{a}} \quad d \leq a \quad (5.8)$$

$$P = 200 * \frac{\sqrt{C}}{m} * \frac{d}{\sqrt{A}} \quad d > a \quad (5.9)$$

Three terms affect the precision of an estimate. The first is the ratio of the standard deviation to the mean. This term is characteristic of the coal zone and varies from 0.2 to 0.6 for examples considered in the thesis. The second term is the inverse of the square root of the area estimated. If the area studied is expanded by four times (at the same grid spacing for observations) then the uncertainty

is effectively halved. Finally the precision of the estimate is a function of the square root of the grid spacing cubed. Equation (5.8) may be rewritten in three ways to illustrate these relationships:

$$P = C_1 \sqrt{\frac{C}{m}} \quad C_1 = \text{constant}$$

$$\text{or} \quad \ln P = C_2 - 0.5 \ln A \quad C_2 = \text{constant}$$

$$\text{or} \quad \ln P = C_3 + 1.5 \ln d \quad C_3 = \text{constant}$$

Where a coal basin has been explored on a square grid, each coal zone will be proved to a greater or lesser degree of precision because each zone will have a characteristic ratio of standard deviation to the mean and a unique areal distribution. One uniform grid spacing does not provide consistent confidence limits for all seams, underlining the fallibility of arbitrary classification schemes based upon observation spacing. A quoted precision is also dependent upon the area estimated and cannot be applied to a smaller area because, for the same sample grid, the precision of a smaller area is higher. Finally, it must be noted that these conclusions apply when the grid spacing is less than or equal to the range of the major variogram structure which is assumed to have a spherical form. If observations are spaced farther apart than the range of the variogram structure, the precision does not depend upon the distance and area but only upon the number of observations in the area (formula 5.9).

5.4 Precision of Volume Estimates

Analytical expressions described by David (1970) were used to calculate the precision of the estimated coal volume. The relative variance of the volume estimate is the sum of the relative variance of the average net coal thickness, the relative variance of the area estimate and a supplementary term. The latter term is the product of the relative variance of the area estimate and the relative variance of net coal thickness observations and compensates for the effect the uncertainty in the area has on the average thickness estimate. The precision of the volume estimates are tabulated in Table 11. The precision of the average net coal thickness is based on a variogram model with a range of 200 metres (the nested structures model of Table 10). Table 11 also shows the percentage contribution of the component variable in the volume equation to the relative variance of the volume estimate.

The precision of the volume estimate was plotted against the number of observations on full logarithmic axes (Figure 51). The area and average thickness precision curves were plotted for comparison. The volume curve parallels the area curve very closely since the uncertainty in the area estimate comprises over 70% of the variance for any of the volume estimates (Table 6). The supplementary term is not very significant as a component of the variance.

Table 11

Precision of the volume estimate and components of the estimation variance at three drill spacings.

drill spacing (m)	800	400	200
number of observations	21	65	225
-- precision ---			
area	25	6.5	2.4
average thickness	7.94	3.88	1.48
	-----	-----	-----
volume	26.7	7.69	2.86
- component of variance -			
area	88	71	70
average thickness	9	25	27
supplementary term	3	4	3
	-----	-----	-----
volume	100%	100%	100%

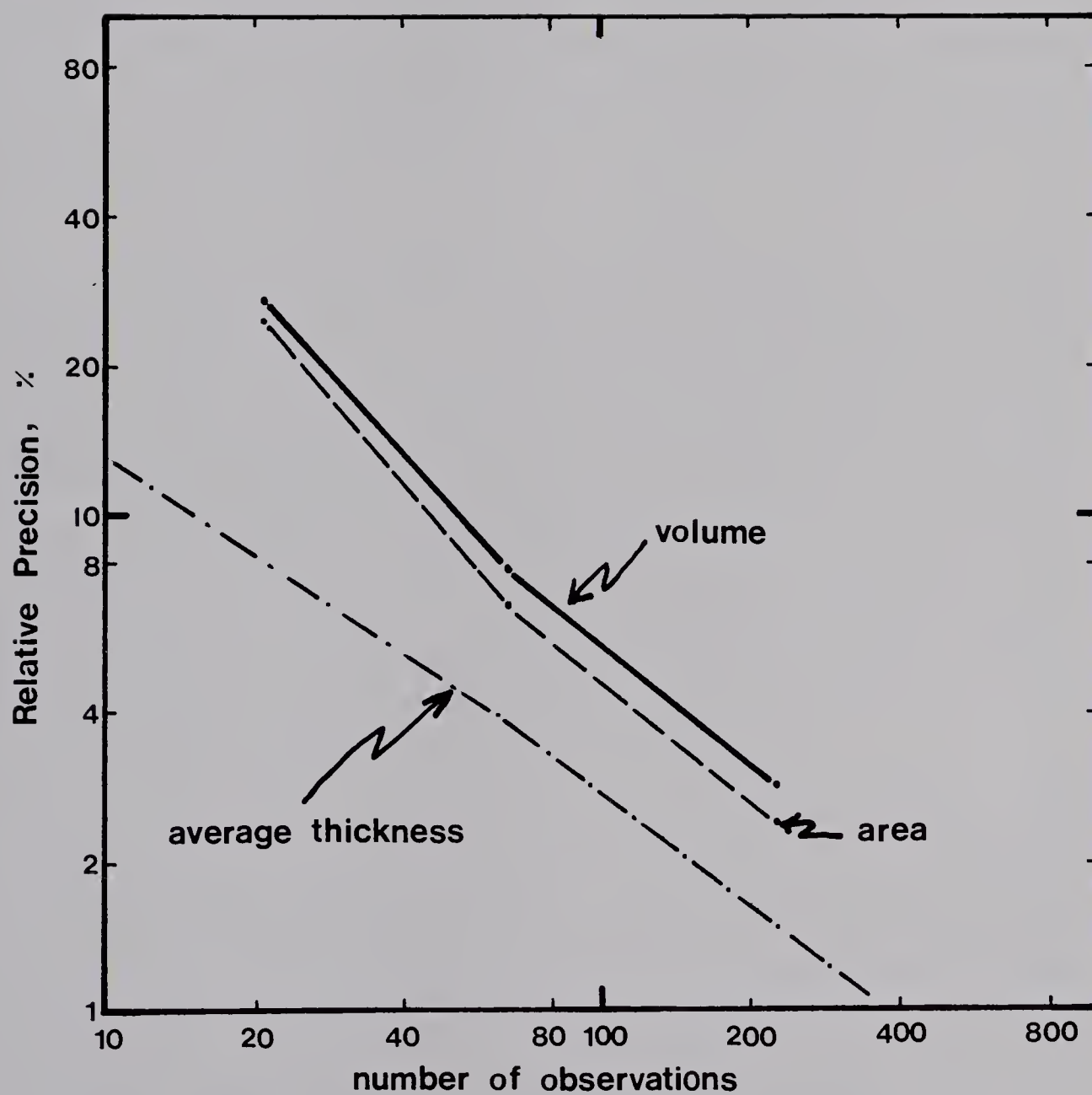


Figure 51 - Relative precision of the estimate of the volume of coal as a function of the number of observations in the small scale area.

The slope of the precision curve for volume is approximately -1 suggesting that the precision of the volume of coal in the study area is an inverse linear function of the number of observations made on a regular grid.

CHAPTER 6

Summary and Conclusions

6.1 Conclusions on the Spatial Continuity of Coal Zones

The continuity of the thickness and the structural surface of some coal zones was studied using the technique of structural analysis.

Net coal thickness appears to be wide-sense stationary and isotropic, resulting in experimental variograms which rise from the origin to a range of influence at which point the variogram is bounded forming a sill. These experimental variograms are commonly composed of two nested structures: a short range structure and a long range structure. The absolute height of the sill and the relative height of the nested structures varies from zone to zone.

The ranges of some of the net coal thickness models were: 200 m, 800 to 1000 m and 4000 to 6000 m. No attempt was made to relate the range of influence to a geological model of coal deposition which might explain the observations because the true variability of the depositional process could be masked by the size of the area, the location of the samples, seam correlation errors, the potential mining zone selection and the method of computing experimental variograms.

The elevation of the bedrock and the elevation of the

coal zone were non-stationary for distances greater than 1000 m and could be modelled with a first-order local drift component and a bounded variogram with a range of about 1000 m. The sill of the variograms varied for each individual coal zone but ranged from 400 ft² to 600 ft². The concentration of observations near the subcrop edge of the coal zone resulted in computed variograms which represent a more structurally disturbed area of the zone than the bulk of the area where the zone is undisturbed by glacial action.

Evidence from the Estevan coalfield suggests that coal zones may be disturbed structurally within the 25 foot interval below the bedrock surface and that the average width of these structures is less than 800 metres (1/2 mile). The implication for resource analysis is that in the absence of drilling at 400 m centres or less, the location of subcrop is uncertain and that boreholes which intersect the area less than 25 feet below bedrock have a limited area of influence for the purpose of estimating the area underlain by coal. Results from the small scale area confirm that zone structure may be locally complex and that the location of subcrop is not a simple contour especially where an unconformity cuts the underlying beds at a low angle.

6.2 Conclusions on Statistical Methods

Statistical methods, in combination with geological interpretation, provided quantitative statements of

geologic assurance concerning the estimated quantity of potential resource in some coal zones.

Methods of estimation based on the more appealing model of spatial correlation (particularly those derived from the Theory of Regionalized Variables) resulted in narrower confidence limits than methods that assume statistical independence of observations. The former techniques were used to estimate the average thickness of net coal in a zone over an area where sufficient data are available to obtain a stable estimate of the variogram. Kriging proved particularly valuable as an unbiased estimator of averages over irregularly sampled areas. The precision of the arithmetic mean of observations taken systematically on a square grid was obtained easily using auxiliary functions once a variogram model was identified. These techniques may be of limited use in regional coal resource evaluations because commonly the data are not sufficient to compute a stable estimate of the variogram.

The relative variance of the areal proportion of coal was calculated using an approximation formula where samples were available on a square grid and the grid cell size was smaller than the average diameter of eroded areas. The latter assumption proved difficult to verify and limits use of the method to areas where such an assumption can be made a priori. Prediction of the location of coal zone subcrop at the bedrock unconformity using kriging to estimate surfaces

and grid manipulation was not a successful application of statistical estimation methods because of structural disturbance of the seams localized within 25 feet of the bedrock surface. The size of such features was smaller than the interpolation grid spacing and smaller than the sample spacing over most of the subcrop area. Estimation of the subcrop location using these methods requires observations to be located closer than 400 m from each other and that the interpolation grid spacing is 200 m or less.

Methods of subjective probability permitted quantification of the uncertainty in estimates of the area underlain by a coal zone where methods based upon objective probability could not be used because of irregular sampling patterns or insufficient data.

6.3 Conclusions on Geologic Assurance of Coal Resource Estimates

Coal resource quantity refers here to an estimate of the volume of coal in a zone which is of sufficient thickness to be potentially mineable. Areas of low overburden thickness or greater than average net coal thickness were not selected nor were areas removed where the zone had been mined or where mining is prevented by overlying cultural or surface features.

The Estevan zone estimate was classified as a measured

resource whereas the Boundary zone estimate would be classified as an indicated resource, on the basis of a required 20% precision in the estimate. The coal quantity estimate after the first year of drilling in the small scale area was classified as an indicated resource while estimates from subsequent years were termed measured resources.

Over two-thirds of the estimation variance of the volume of coal can be attributed to uncertainty in the area estimate. In the estimates at all grid spacings for the small scale area and those for the Estevan area, the area component of uncertainty was at least twice that of the average thickness component. That these results agree, arrived at independently by methods based on subjective and objective probability, lends credence to the validity of both approaches.

The uncertainty in the area is composed of the uncertainty in the location of the subcrop perimeter and the uncertainty in the location of lithologic boundaries (both external and internal). Although coal-bearing strata of the Interior Plains are relatively undisturbed in comparison to mountain areas, structural features of small dimension in combination with a very low angle of intersection between the zone and the bedrock unconformity cause considerable uncertainty in the location of subcrop. Variations in the bedrock topography form a secondary source of uncertainty. The understanding of facies relationships in fluvial systems

has not yet reached the state where the location and size of the meander belts of an ancient river for example, can be predicted with precision given the subsurface data available in regional resource evaluation programs.

Studies have shown that a regular square grid is the most efficient sampling pattern for classification of facies and estimation of the area underlain by coal. The grid spacing would need to be 400 m or less to map precisely lithologic boundaries and the subcrop perimeter of the coal zone. Should a larger grid spacing of 800 m be chosen, the boreholes must penetrate at least to a regional marker below the interval of disturbed bedrock to facilitate zone correlation and estimation of regional trend.

The estimate of the average thickness of net coal contributes the smaller component to the uncertainty of the volume estimate. Geostatistical methods provide lower variance estimates than methods based on statistical independence but the difference is most significant when closely-spaced samples are used to form the estimate. The precision of an estimate of average thickness of net coal was seen to be a function of three factors: the natural variation in thickness of the zone, the size of the area over which thickness was averaged and the spacing of observations made on a square grid. For this reason, estimates of different sized areas from the same size observation grid results in different relative precision

values, a major shortcoming of resource classification methods based only upon distances between observations.

6.4 Recommendations for Further Study

The behavior of the variogram of net coal thickness should be investigated for observations located very close to one another, as this would contribute to the modelling of coal thickness variograms for data points from the subsurface. The observations could easily be made in outcrop or as mining progressed along a box cut in a prairie strip mine.

The development of the Theory of Regionalized Variables was sparked by problems encountered in estimating the average gold content of a volume of rock from samples of differing volumes at varied locations. The vertical and lateral variability of coal quality parameters would be an excellent study topic where samples are available from continuous outcrop or mine exposures.

SELECTED BIBLIOGRAPHY

- Agterberg, F.P. 1970: Autocorrelation functions in geology; in Geostatistics Plenum (D.F. Merriam Ed.) New York.
- Agterberg, F.P. and Chung, C.F. 1973: Geomathematical prediction of sulphur in coal, New Lignan Mine area, Sidney Coalfield; Can. Mining Met. Bull., 66, no 738, pp 85-96.
- Agterberg, F. P. 1974: Geomathematics; Elsevier, Amsterdam, 596 p.
- Berry, F.W. 1935: Floras of the Whitemud and Ravenscrag Formations, Geological Survey Canada, Mem. 182.
- Broughton, P.L. 1972: Petrology of the Estevan No. 3 lignite seam, southeastern Saskatchewan; in Proc. First Geological Conference on Western Canadian Coal. Research Council of Alberta, No. 60, pp. 185-202.
- Broughton, P.L., Irvine, J.A., Whitaker, S.H. 1974: Lignite coal resources of southern Saskatchewan; in Fuels: A Geological Appraisal, p.p. 81-94.
- Cameron, A. R. and Birmingham, T.F.: Petrographic and chemical properties of a lignite from Estevan, Saskatchewan; Geol. Surv. Canada, Paper 71-8.
- Carrigy, M. 1971: Cretaceous-Tertiary Lithostratigraphy; Res. Coun. Alberta Bull 27.
- Chiles, J.P. 1976: How to adapt kriging to non-classical problems: three case studies; in Advanced Geostatistics in the Mining Industry, Reidel, Boston.
- Christiansen, E.A. 1967: Collapse structures near Saskatoon, Saskatchewan, Canada; CJES, 4, pp. 757-767.
- Christopher, J.E., Kent, D.M., Simpson, F. 1973: Saskatchewan and Manitoba; in The future petroleum provinces of Canada-their geology and potential, CSPG Memoir 1.
- Clark, I. 1976: Some auxiliary functions for the spherical model of geostatistics; Computers & Geosciences, VI, no 4, pp. 255-273.
- Cliff, A.D. and Ord, J.K. 1973: Spatial Autocorrelation; Pion, London, 178 p.

- David, M. 1970: Geostatistical ore reserve calculation, a step by step case study in C.I.M.M. Special Volume no 12, Montreal, pp. 185-191.
- David, M. 1974: A Course in Geostatistical Reserve Estimation; unpub. ms., Dept de Genie Mineral, Ecole Polytechnique, Montreal.
- Davis, N.B. 1918: Report on the clay resources of southern Saskatchewan; Mines Branch, Dept. of Mines, Canada, no 468.
- Delfiner, P. and Delhomme, J.P. 1975: Optimum interpolation by kriging; in Display & Analysis of Spatial Data, Wiley, New York.
- Delfiner, P. 1976: Linear estimation of non-stationary spatial phenomena; in Advanced Geostatistics in the Mining Industry, Reidel, Boston.
- DeMille, G., Shouldice, J.R., Nelson, H.W. 1964: Collapse structures related to evaporites of the Prairie Formation, Saskatchewan; Geol. Soc. America Bull. 75, pp. 307-316.
- Dowling, D.B. 1904: Coal field of The Scuris River; Geol. Surv. Canada, Ann. Report, Vol XV, part F.
- Dowling, D.B. 1913: The coal fields and coal resources of Canada; 12th International Coal Congress, Canada, pp. 439-523.
- Dutta, I. and Rao, S.V.L.N. 1977: Variograms and their role in interpretatin of soft ore types; Math. Geol., 9, 1, pp. 99-111.
- EMR, 1977: Oil and natural gas resources of Canada 1976; Report EP77-1, Energy, Mines and Resources Canada.
- Fraser, F.J. et al. 1935: Geology of Southern Saskatchewan; Geol. Surv. Canada, Mem. 176.
- Furnival, G.M. 1946: Cypress Lake Map-Area, Saskatchewan; Geol. Surv. Canada, Mem 242.
- Hacquebard, P.A. and Donaldson, J.R. 1964: Carboniferous coal deposition associated with flood-plain and limnic environments in Nova Scotia; in Environments of Coal Depositon, Geol. Soc. America Special Paper 114.
- Haun, J.D. 1975: Methods of estimating the volume of undiscovered oil and gas resources; AAPG Studies in Geology, no. 1.

- Holter, M.E. 1972: Coal seams of the Estevan area, southeastern Saskatchewan; in Proc. First Geological Conference in Western Canadian Coal, Research Council of Alberta, Inf. Series no. 60, pp. 173-184.
- Jowett, G.H. 1955: Sampling properties of local statistics in stationary stochastic series; *Biometrika*, 42, pp. 160-169.
- Kent, D.M. and Simpson, F. 1973: Outline of the geology of Southern Saskatchewan; in An Excursion Guide to the Geology of Saskatchewan. Sask Geol. Soc., Spec. Pub. Number 1, pp. 103-125.
- Koch, C.S. Jr and Gomez, M. 1965: Delineation of Texas lignite beds by statistical techniques; US Bu. Mines Report of Investigation, 6833, 253.
- Krige, D.G., Watson, M.I., Oberholzer, W.J., Dutoit, S.R. 1969: The use of contour surfaces as predictive models for ore values; in A Decade of Digital Computing in the Mineral Industry.
- Latour, B.A. and Christmas, L.P. 1970: Preliminary estimate of measure of coal resources including reassessment of indicated and inferred resources of Western Canada; Geol. Surv. Canada, Paper 70-58.
- Lemke, R.W. 1960: Geology of the Souris River Area North Dakota; USGS Prof. Paper 325.
- McCammon, R.B. 1975: On the efficiency of systematic point sampling in facies; *J. Sed. Pet.* 45, pp. 217-229.
- MacKay, B.R. 1974: Coal reserves of Canada; Report of the Royal Commission on Coal, 1946.
- MacLean, A. 1918: Lignite area of southern Saskatchewan; Geol. Surv. Canada, Sum. Report. 1917, part C, pp. 35-41.
- Matern, B. 1960: Spatial Variation; Meddelanden Fran Statens Skogsforskningsinstitut, Band 49, No 5, 144 p.
- Matheron, G. 1963: Principles of geostatistics; *Economic Geology*, 58, pp. 1246-1256.
- Matheron, G. 1967: Kriging or polynomial interpolation procedures; *Bull C.I.M.*, 60, 665, pp. 1041-1045.
- Matheron, G. 1971: The theory of regionalized variables and its application; Cahier No. 5, Ecole Nationale Supérieure des Mines de Paris, 211 p.

- Matheron, G. 1973: The intrinsic random functions and their applications; Adv. in Appl. Prob. 5, pp. 439-468.
- McKelvey, V.E. 1976: Principles of the mineral resource classification system of the U.S. Bureau of Mines and the U.S. Geological Survey; Geol. Surv. Bull. 1450-A.
- Meneley, W.A., Christiansen, E.A., Kupsch, W.O. 1957: Preglacial Missouri River in Saskatchewan; Jour. Geology 65 p. 441-447.
- Newendorp, P.D. 1975: Decision analysis for petroleum exploration; Petroleum, Tulsa.
- Parsley, A.J. 1971: Application of autocorrelation criteria to the analysis of mapped geologic data from the coal measures of central England; Math. Geol., 3, no 3, pp. 281-295.
- Popoff, C.C. 1966: Computing reserves of mineral deposits - principles and conventional methods; U.S. Bu. Mines Information Circular 8283, 113 p.
- Rahmani, R.A. and Lerbekmo, J.F. 1975: Heavy-mineral analysis of Upper Cretaceous and Paleocene sandstones in Alberta and adjacent areas of Saskatchewan; in The Cretaceous System of the Western Interior of North America, Geol. Assn. Canada, Spec. Pub. No. 13.
- Roy, K.J. 1975: Hydrocarbon assessment using subjective probability and Monte Carlo methods; preprint of paper given May 21, 1975 Intern. Inst. of App. Systems Analysis, Conference on Energy Supply, Laxenburg, Austria.
- Sabourin, R. 1976: Application of two methods for the interpretation of the underlying variogram; in Advanced Geostatistics in the Mining Industry, Reidel, Boston, pp.
- Serra, J. 1968: Les structures gigonges: morphologie mathematique et interpretation metallogenique; Mineralium Deposita, 3 p. 135-154.
- Switzer, P. 1976: Applications of random process models to the description of spatial distributions of qualitative geologic variables, in Random Processes in Geology, (D.F. Merriam Ed), Springer-Verlog.
- Taylor, R.S., Mathews, H.W., Kupsch, W.O. 1964: Tertiary; in McCrossan, R.G., Glaister, R.P. editors, Geological History of Western Canada.

- Tibbetts, T.E., 1975: Quality evaluation of Saskatchewan lignite resources; Bull. C.I.M., 68, pp. 85-90.
- Webb, J.B. 1964: Historical Summary; in McCrossan, R.G., Glaister, R.P., Editors, Geological History of Western Canada.
- Whitaker, S.H. 1967: Geology and Groundwater Resources of the Wood Mountain Area (72-G); Sask. Research Council, Geology Division, Map No. 5.
- Whitaker, S.H. 1972: Lignite Exploration in the Ravenscrag Formation of Southern Saskatchewan; in Proc. First Geological Conference in Western Canadian Coal. Research Council of Alberta, No. 60, pp. 25-30.
- Whitaker, S.H. 1974a: Geology and Groundwater Resources of the Weyburn Area (62-E,F); Saskatchewan Research Council, Geology Division Map No. 21.
- Whitaker, S.H. 1974b: Geology and Groundwater Resources of the Willow Bunch Area (72-H); Saskatchewan Research Council, Geology Division Map No. 20.
- Whitaker, S.H. and Christiansen, E.A. 1972: The Empress Group in Southern Saskatchewan; CJES 9 pp. 353-360.
- Whitten, E.H.T. 1975: The practical use of trend-surface analyses in the geological sciences, in Display and Analysis of Spatial Data, Wiley, New York, pp. 282-298.

B30200